Appendix A
ACCELERATION TIME HISTORIES

Characteristics of the seismic environment of the site to be considered in selecting time-histories include: tectonic environment (e.g., subduction zone; shallow crustal faults in western United States or similar crustal environment; eastern United States or similar crustal environment); earthquake magnitude; type of faulting (e.g., strike-slip; reverse; normal); seismic-source-to-site distance; local site conditions; and design or expected ground-motion characteristics (e.g., design response spectrum; duration of strong shaking; and special ground-motion characteristics such as near-fault characteristics). Dominant earthquake magnitudes and distances, which contribute principally to the probabilistic design response spectra at a site, as determined from national ground motion maps, can be obtained from deaggregation information on the U.S. Geological Survey website.

It is desirable to select time-histories that have been recorded under conditions similar to the seismic conditions at the site listed above, but compromises are usually required because of the multiple attributes of the seismic environment and the limited data bank of recorded time-histories. Selection of time-histories having similar earthquake magnitudes and distances, within reasonable ranges, are especially important parameters because they have a strong influence on response spectral content, response spectral shape, duration of strong shaking, and near-source ground-motion characteristics. It is desirable that selected recorded motions be somewhat similar in overall ground motion level and spectral shape to the design spectrum to avoid using very large scaling factors with recorded motions and very large changes in spectral content in the spectrum-matching approach. If the site is located within 6 miles of an active fault, then intermediate-to-long-period ground-motion pulses that are characteristic of near-source time-histories should be included if these types of ground motion characteristics could significantly influence structural response. Similarly, the high short-period spectral content of near-source vertical ground motions should be considered.

Ground-motion modeling methods of strong-motion seismology are being increasingly used to supplement the recorded ground-motion database. These methods are especially useful for seismic settings for which relatively few actual strong-motion recordings are available, such as in the central and eastern United States. Through analytical simulation of the earthquake rupture and wave-propagation process, these methods can produce seismologically reasonable time series.

Response-spectrum-matching approaches include methods in which time series adjustments are made in the time domain (Lilhanand and Tseng, 1988; Abrahamson, 1992) and those in which the adjustments are made in the frequency domain (Gasparini and Vanmarcke, 1976; Silva and Lee, 1987; Bolt and Gregor, 1993). Both of these approaches can be used to modify existing time-histories to achieve a close match to the design response spectrum while maintaining fairly well the basic time-domain character of the recorded or simulated time-histories. To minimize changes to the time-domain characteristics, it is desirable that the overall shape of the spectrum of the recorded or simulated time-history not be greatly different from the shape of the design response spectrum and that the time-history initially be scaled so that its spectrum is at the approximate level of the design spectrum before spectrum matching.

When developing three-component sets of time histories by simple scaling rather than spectrum matching, it is difficult to achieve a comparable aggregate match to the design spectra for each component of motion when using a single scaling factor for each time-history set. It is desirable, however, to use a single scaling factor to preserve the relationship between the components. Approaches for dealing with this scaling issue include: (1) use of a higher scaling factor to meet the minimum aggregate match requirement for one component while exceeding it for the other two; (2) use of a scaling factor to meet the aggregate match for the most critical component with the match somewhat deficient for other components; (3) compromising on the scaling by using different

factors as required for different components of a time-history set. While the second approach is acceptable, it requires careful examination and interpretation of the results and possibly dual analyses for application of the horizontal higher horizontal component in each principal horizontal direction.

The requirements for the number of time histories to be used in nonlinear inelastic dynamic analysis and for the interpretation of the results shall take into account the dependence of response on the time domain character of the time histories (duration, pulse shape, pulse sequencing) in addition to their response spectral content.

Additional guidance on developing acceleration time histories for dynamic analysis may be found in publications by the Caltrans Seismic Advisory Board Adhoc Committee (CSABAC) on Soil-Foundation-Structure Interaction (1999) and the U.S. Army Corps of Engineers (2000). CSABAC (1999) also provides detailed guidance on modeling the spatial variation of ground motion between bridge piers and the conduct of seismic soil-foundation-structure interaction (SFSI) analyses. Both spatial variations of ground motion and SFSI may significantly affect bridge response. Spatial variations include differences between seismic wave arrival times at bridge piers (wave passage effect), ground motion incoherence due to seismic wave scattering, and differential site response due to different soil profiles at different bridge piers. For long bridges, all forms of spatial variations may be important. For short bridges, limited information appears to indicate that wave passage effects and incoherence are, in general, relatively unimportant in comparison to effects of differential site response (Shinozuka et al., 1999; Martin, 1998). Somerville et al. (1999) provide guidance on the characteristics of pulses of ground motion that occur in time histories in the near-fault region.

Appendix B
PROVISIONS FOR SITE CHARACTERIZATION

B.1 GENERAL

Site characterization shall be performed for each substructure element, as appropriate, to provide the necessary information for the design and construction of foundations. The type and extent of site characterization shall be based on subsurface conditions, structure type, and project requirements. The site characterization program shall be extensive enough to reveal the nature and types of soil deposits and/or rock formations encountered, the engineering properties of the soils and/or rocks, the potential for liquefaction, and the groundwater conditions.

B.2 SUBSURFACE EXPLORATIONS

Subsurface explorations shall be made to competent material of suitable bearing capacity or to a depth where added stresses due to the estimated footing load is less than 10% of the existing effective soil overburden stress, whichever is the greater. If bedrock is encountered at shallow depths, the exploration shall advance a minimum of 3 m into the bedrock or to 1 m beyond the proposed foundation depth, whichever is greater.

C.B.1 GENERAL

Site characterization normally includes subsurface explorations and laboratory testing of samples of soil/rock recovered during the exploration work. Subsurface exploration can include drilling and sampling of the soil or rock, as well as in situ testing.

C.B.2 SUBSURFACE EXPLORATIONS

As a minimum, the subsurface exploration and testing program should obtain information to analyze foundation stability and settlement with respect to:

- Geological formation(s);
- Location and thickness of soil and rock units;
- Engineering properties of soil and rock units, including density, shear strength and compressibility;
- Groundwater conditions;
- Ground surface topography;
- Local considerations, such as expansive or dispersive soil deposits, collapse potential of soil in arid regions, underground voids from solution weathering or mining activity, or slope instability potential; and
- Behavior under seismic loading, including liquefaction, seismic-induced ground settlement, lateral flow and spreading (e.g., sloping ground underlain by very loose saturated soil and the presence of a free face), and ground motion amplification or attenuation.

Issues related to the constructibility of the foundation system should also be identified during the subsurface investigation process. These issues can include the drivability of piles, the excavatibility/stability of holes for drilled shafts and similar bored systems (e.g., Cast-in-Drill Hole (CIDH) piles), occurrence of boulders and rocks that could affect pile or retaining wall construction, need for and ability to de-water soils or control groundwater flow.

B.2.1 In Situ Tests

In situ tests may be performed to obtain deformation and strength parameters of foundation soils or rock for the purposes of design and/or analysis. The tests shall be performed in accordance with the appropriate standards recommended by ASTM or AASHTO and may include the following in-situ soil tests and in-situ rock tests:

In Situ Soil Tests

- Standard Penetration Test - AASHTO T 206 (ASTM D 1586)
- Static Cone Test - ASTM D 3441
- Field Vane Test - AASHTO T 223 (ASTM D 2573)
- Pressuremeter Test - ASTM D 4719
- Plate Bearing Test - AASHTO T 235 (ASTM D 1194)
- Well Test (Permeability) - ASTM D 4750

In Situ Rock Tests

- Deformability and Strength of Weak Rock by an In-Situ Uniaxial Compressive Test - ASTM D 4555
- Determination of Direct Shear Strength of Rock Discontinuities - ASTM D 4554
- Modulus of Deformation of Rock Mass Using the Flexible Plate Loading Method - ASTM D 4395
- Modulus of Deformation of Rock Mass Using a Radial Jacking Test - ASTM D 4506
- Modulus of Deformation of Rock Mass Using the Rigid Plate Loading Method - ASTM D 4394

C.B.2.1 In Situ Tests

The most suitable type of exploration method will depend on the type of soil/rock encountered, the type and size of the foundation, and the requirements of design. Often a combination of one or more methods is required. In nearly every situation at least one boring with soil/rock sampling should be planned. Results of other soil exploration methods, such as the cone penetrometer or field vane, should be compared to information recovered in the soil boring. Table B-1 provides a summary of the suitability and information that can be obtained from different in situ testing methods.

Parameters derived from field tests, such as standard penetration, cone penetrometer, dynamic penetrometer, and pressuremeter tests, can often be used directly in design calculations based on empirical relationships. These are sometimes found to be more reliable than analytical calculations, especially in familiar ground conditions for which the empirical relationships are well established.

- Stress and Modulus of Deformation Determination Using the Flatjack Method - ASTM D 4729
- Stress in Rock Using the Hydraulic Fracturing Method - ASTM D 4645

If so requested by the owner or required by permitting agencies, boring and penetration test holes shall be plugged to prevent water contamination.

Table B-1 In-Situ Tests

Type of Test	Best Suited To	Not Applicable To	Properties That Can Be Determined
Standard Penetration Test (SPT)	Sand	Coarse Gravel	Qualitative evaluation of compactness. Qualitative comparison of subsoil stratification.
Dynamic Cone Test	Sand and Gravel	Clay	Qualitative evaluation of compactness. Qualitative comparison of subsoil stratification.
Static Cone Test	Sand, Silt, and Clay	Coarse Gravel, Cemented Soil, Rock	Continuous evaluation of density and strength of sands. Continuous evaluation of undrained shear strength in clays.
Field Vane Test	Clay	All Other Soils	Undrained shear strength.
Pressuremeter Test	Soft Rock, Sand, Gravel, and Till	Soft Sensitive Clays	Bearing capacity and compressibility.
Plate Bearing Test and Screw Plate Test	Sand and Clay	-	Deformation modulus. Modulus of subgrade reaction. Bearing capacity.
Flat Plate Dilatometer Test	Sand and Clay	Gravel	Empirical correlation for soil type, K_e, overconsolidation ratio, undrained shear strength, and modulus.
Permeability Test	Sand and Gravel	-	Evaluation of coefficient of permeability.

B.2.2 Explorations for Seismic Studies

In areas of high seismic activity (e.g., Seismic Detailing Requirement (SDR) 3 and above), spe-

C.B.2.2 Explorations for Seismic Studies

Subsurface exploration methods in areas of high seismicity are generally the same as those

cial consideration shall be given to the seismic response of the site during the planning of field explorations. The planning process shall consider the potential for liquefaction and the requirement to determine the Site Class Definition, as required for establishing the Seismic Hazard Level and SDR. Article 3.7 provides definitions Seismic Hazards Level (SHL), SDAP and SDR.

B.2.2.1 Liquefaction Potential

Field explorations shall be performed to evaluate the potential for liquefaction in SDR 3, 4, 5, and 6 at those sites potentially susceptible to liquefaction. For sites that are potentially liquefiable, it is important to obtain an accurate determination of soil stratigraphy, the groundwater location, and the density of cohesionless soil. Of particular importance is the identification of thin layers that, if liquefied, could result in lateral flows or spreading of the soil above the liquefied layers.

used for standard subsurface explorations. However, the empirical correlations used to estimate the potential for liquefaction or the shear wave velocity of the soil normally require use of equipment that has been calibrated according to certain standards. The geotechnical engineer or engineering geologist responsible for having the subsurface explorations carried out should become familiar with these methods and confirm during the exploration program that correct methods and calibrated equipment are being used. If incorrect methods or un-calibrated equipment are used, it is possible to predict overly conservative or unconservative ground response for a design seismic event.

C.B.2.2.1 Liquefaction Potential

A potential for liquefaction exists if the following conditions are present: (1) the peak horizontal acceleration at the ground surface is predicted to be greater than 0.15g (g = acceleration of gravity); (2) the soil consists of loose to medium dense non-plastic silts, sands, and in some cases gravels; and (3) the permanent groundwater location is near the ground surface. Appendix D provides specific guidance on the determination and evaluation of liquefaction.

Depth of Exploration

The potential depth of liquefaction is an important decision. Normally, liquefaction is assumed to be limited to the upper 15 to 20 m of soil profile. However, it appears that this limiting depth is based on the observed depth of liquefaction rather than the maximum depth of liquefaction that is physically possible. For this reason an exploration program should extend at least to 25 m or until a competent bearing layer (with no underlying loose layers) is encountered, whichever occurs first.

Methods of Exploration

Several different exploration methods can be used to identify soils that could be susceptible to liquefaction. These include the Standard Penetration Test (SPT), the cone penetration test (CPT), and certain types of shear wave velocity measurements (e.g., crosshole, downhole, and Spectral Analysis of Surface Wave methods). ASTM standards exist for conducting SPTs, CPTs (see Article B.2.1), and certain types of shear wave velocity measurement. These methods should be followed. If standards are not available, then it is essential to have testing completed by experienced individuals, who understand the limitations of the test

methods and who understand the level of accuracy needed by the designer for Site Class Definition or liquefaction determination.

Standard Penetration Test (SPT) Method: The SPT is currently the most common field exploration method for liquefaction studies. It is critical that if SPTs are conducted to obtain information for liquefaction assessments, procedures follow those recommended by Youd and Idriss (1997). These procedures have strict requirements for hammer energy, sampler size, and drilling method. If these methods are not followed, the value of the blow count determined from the SPT can vary by 100%, resulting in great uncertainty in any liquefaction assessment based on the SPT results. Recommended SPT procedures are summarized in Table B-2.

Table B-2 Recommended SPT Procedure

Borehole size	66 mm < Diameter < 115 mm
Borehole support	Casing for full length and/or drilling mud
Drilling	Wash boring; side discharge bit Rotary boring; side or upward discharge bit Clean bottom of borehole*
Drill rods	A or AW for depths of less than 15 m N or NW for greater depths
Sampler	Standard 51 mm Outer Diameter +/- 1 mm 35 mm Inner Diameter +/- 1 mm >457 mm length
Penetration resistance	Record number of blows for each 150 mm; N = number of blows from 150 to 450 mm penetration
Blow count rate	30 to 40 blows per minute

* Maximum soil heave within casing <70 mm

An automatic trip hammer should be used wherever possible; hammer energy calibrations should be obtained for the hammer, whether it is a donut hammer or an automatic hammer. Records should also be available that indicate whether the SPT sampler used liners or not, and the type of drilling method that was used. It will usually be necessary to conduct the SPTs at close depth intervals, rather than the conventional 1.5-m interval, because thin liquefiable layers could be important in design.

Sites with gravel deposits require special consideration when performing SPTs. Because of the coarse size of gravel particles, relative to the size of the sampler, these deposits can result in mis-

leadingly high blow counts. Three procedures can be considered for these sites:

- If a site has only a few gravel layers or if the gravel is not particularly abundant or large, it may be possible to obtain an equivalent SPT blow count if "incremental" blow counts are measured. To perform "incremental" blow count measurements, the number of blows for each 25 mm of penetration is recorded, rather than the blows for 150 mm. By plotting the blow counts per 25 mm versus depth, it is sometimes possible to distinguish between the blow count obtained in the matrix material and blow counts affected by large gravel particles. The equivalent blow count for 150 mm can then be estimated by summing and extrapolating the number of blows for the representative 25 mm penetrations that appear to be uninfluenced by coarse gravel particles. This procedure is described in Vallee and Skryness (1980).
- Andrus and Youd (1987) describe an alternate procedure for determining blow counts in gravel deposits. They suggest that the penetration per blow be determined and the cumulative penetration versus blow count be plotted. With this procedure, changes in slope can be identified when gravel particles interfere with penetration. From the slope of the cumulative penetration, estimates of the penetration resistance can be made where the gravel particles did or did not influence the penetration resistance.
- An alternative in gravel deposits is to obtain Becker Hammer blow counts, which have been correlated to the standard penetration test blow count (Youd and Idriss, 1997).

Cone Penetrometer Test (CPT) Method: For many locations the CPT is the preferred method of determining liquefaction potential. This method is preferred because it is able to provide an essentially continuous indication of soil consistency and type with depth. It is also less susceptible to operator-related differences in measurements. The CPT method may not be applicable at sites where cobbles and gravels overlie looser sandy soils. At these sites it may be impossible to push the CPT rod and sensor through the gravel. For these sites it is sometimes possible to auger through the gravel materials to provide access for the cone penetrometer rod and sensor.

Most CPT equipment are not capable of ob-

taining soil samples. Empirical correlations can, however, be used to estimate soil type and grain size. Although these correlations often provide very good indirect estimations of soil type and grain size, it is generally desirable to perform a limited number of SPTs at the site to obtain soil samples for laboratory determination of grain size, to confirm soil descriptions, and to provide a comparison to SPT blow counts.

Procedures for interpreting liquefaction resistance from the CPT measurement are given in Youd and Idriss (1997).

Shear Wave Velocity Methods: Shear wave velocity can also be used for both liquefaction evaluations and the determination of soil shear modulus, which is required when establishing spring constants for spread footing foundations. The shear wave velocity of the soil is also fundamental to the determination of Site Class Definition, as discussed in Article 3.4.2.1.

A variety of methods are available for making shear wave velocity measurements. They include downhole and crosshole methods, which are performed in boreholes, seismic-cone methods, which are conducted in conjunction with a CPT, and Spectral Analysis of Surface Wave (SASW) methods, which are conducted from the ground surface without a borehole. Experienced individuals should perform these methods, as the collection and interpretation of results requires considerable skill. In the absence of this experience, it is possible to obtain misleading results. Surface wave refraction procedures should not be used, as they are generally not able to obtain information in low-velocity layers. Additional information about the shear wave velocity can be found in Kramer (1996).

Procedures for interpreting liquefaction resistance from shear wave velocity data are discussed in Youd and Idriss (1997).

B.2.2.2 Site Response Determination

The field exploration shall provide sufficient information to determine the Site Class Definition (see Article 3.4.2.1), which is used to determine the Seismic Hazard Level.

C.B.2.2.2 Site Response Determination

The Site Class Definition is used to determine whether amplification or de-amplification of ground motions occurs as earthquake-induced motions propagate from depth to the ground surface. Five general site classes have been defined (Article 3.4.2.1) for seismic studies. These categories generally require determination of soil properties in the upper 30 m of soil profile. Procedures for establishing the soil properties include the SPT, the shear wave velocity, and the strength of the material. It is important when planning the field

explorations to recognize that this information could be important to a site and make explorations plans accordingly.

B.3 LABORATORY TESTING

Laboratory tests shall be performed to determine the strength, deformation, and flow characteristics of soils and/or rocks and their suitability for the foundation selected. In areas of higher seismicity (e.g., SDR 3, 4, 5, and 6), it may be appropriate to conduct special dynamic or cyclic tests to establish the liquefaction potential or stiffness and material damping properties of the soil at some sites if unusual soils exist or if the foundation is supporting a critical bridge.

C.B.3 LABORATORY TESTING

An understanding of the engineering properties of soils is essential to the use of current methods for the design of foundations and earth structures. The purpose of laboratory testing is to provide the basic data with which to classify soils and to measure their engineering properties. The design values selected from the laboratory tests should be appropriate to the particular limit state and its corresponding calculation model under consideration.

For the value of each parameter, relevant published data together with local and general experience should be considered. Published correlations between parameters should also be considered when relevant.

B.3.1 Standard Laboratory Tests

Laboratory soil tests may include:

- Water Content - ASTM D 4643
- Specific Gravity - AASHTO T 100 (ASTM D 854)
- Grain Size Distribution - AASHTO T 88 (ASTM D 422)
- Soil Compaction Testing – ASTM D 698 or D 1557
- Liquid Limit and Plastic Limit - AASHTO T 90 (ASTM D 4318)
- Direct Shear Test - AASHTO T 236 (ASTM D 3080)
- Unconfined Compression Test - AASHTO T 208 (ASTM D 2166)
- Unconsolidated-Undrained Triaxial Test - ASTM D 2850
- Consolidated-Undrained Triaxial Test - AASHTO T 297 (ASTM D 4767)
- Consolidation Test - AASHTO T 216 (ASTM D 2435 or D 4186)
- Permeability Test - AASHTO T 215 (ASTM D 2434)

CB.3.1 Standard Laboratory Tests

Standard laboratory tests of soils may be grouped broadly into two general classes:

- Classification tests. These can be performed on either disturbed or undisturbed samples.
- Quantitative tests for permeability, compressibility, and shear strength. These tests are generally performed on undisturbed samples, except for materials to be placed as controlled fill or materials that do not have an unstable soil structure. In these cases, tests should be performed on specimens prepared in the laboratory.

A certain number of classification tests should be conducted at every bridge site; the number of quantitative tests will depend on the types of soils encountered. In many cases disturbance associated with the soil sampling process can limit the usefulness of quantitative test results. This is particularly the case for cohesionless soil. It can also occur for cohesive soil if high quality Shelby tube samples are not obtained. High quality sampling also requires careful sampling and careful soil setup once the sample is retrieved from the ground.

B.3.2 Special Testing for Seismic Studies

For some important projects it may be necessary or desirable to conduct special soil laboratory tests to establish the liquefaction strength or stiffness and material damping properties of the soil. These tests can include resonant column, cyclic triaxial, and cyclic simple shear tests. Only a limited number of academic and consulting organizations are currently conducting these types of tests; therefore, special care is required when selecting a testing laboratory for these tests. Kramer (1996) provides a summary of the laboratory testing for determination of dynamic properties of soil.

B.3.3 Rock Testing

Laboratory rock tests may include:

- Determination of Elastic Moduli - ASTM D 3148
- Triaxial Compression Test - AASHTO T 266 (ASTM D 2664)
- Unconfined Compression Test - ASTM D 2938
- Splitting Tensile Strength Test - ASTM D 3967

C.B.3.2 Special Testing for Seismic Studies

For liquefaction assessments it is generally preferable to rely on in situ methods for determining the liquefaction strength of the soil, because of difficulties associated with sample disturbance. The exception to this general rule is for non-plastic silty soil, where the database for in situ-based correlations is not as well established. For these soils cyclic laboratory test may be necessary to estimate liquefaction strengths.

Empirical correlations have also been developed to define the effects of shearing strain amplitude and confining pressure on shear modulus and material damping of cohesionless and cohesive soils. Laboratory determination of these properties may be warranted where special soil conditions exist or where the stress state on the soil could change. Kramer (1996) provides a summary of the available methods for estimating shear modulus and material damping as a function of shearing strain amplitude and confining pressure.

C.B.3.3 Rock Testing

Laboratory testing of rock has very limited applicability for measuring significant rock properties, such as:

- Compressive strength,
- Shear strength,
- Hardness,
- Compressibility, and
- Permeability.

Rock samples small enough to be tested in the laboratory are usually not representative of the entire rock mass. Laboratory testing of rock is used primarily for classification of intact rock samples, and, if performed properly, serves a useful function in this regard.

Laboratory tests on intact samples provide upper bounds on strength and lower bounds on compressibility. Frequently, laboratory tests can be used in conjunction with field tests to give reasonable estimates of rock mass behavioral characteristics.

Appendix C
GUIDELINES FOR MODELING OF FOOTINGS

C.1 Spring Constants for Footings

A Winkler spring model is normally used to represent the vertical stiffness and moment-rotation relationship in the analysis. A uniformly distributed rotational stiffness can be calculated by dividing the total rotational stiffness of the footing by the moment of inertia of the footing in the direction of loading. Similar methods are used for vertical stiffness.

Strain and Liftoff Adjustment Factors

Equations given in Tables C-1 and C-2 are based on elastic halfspace theory. These equations were originally developed for low levels of dynamic loading associated with machine foundations. For these levels of loading, it is possible to use the low-strain shear modulus (G_{max}) of the soil, and the footing remains in full contact with the soil. During seismic loading, at least two different phenomena occur which are inconsistent with the assumptions used in the original development of these equations. These differences involve (1) the nonlinear response of the soil from both free-field earthquake wave propagation and from local strain amplitude effects and (2) the liftoff of the footing.

- *Strain Amplitude Effects:* The strain amplitude effects reflect the inherent nonlinearity of soil, even at low shear strain amplitudes. As the seismic wave propagates through the soil, the soil softens, resulting in a reduced shear modulus. Both field measurements and numerical modeling have shown this softening, as discussed by Kramer (1996). A second source of soil nonlinearity also must be considered. As the footing responds to inertial loading from the bridge column, local soil nonlinearities occur around the footing as the soil is subjected to stress from the shear forces and overturning moments. While various procedures exist for estimating the free-field effects of wave propagation, simple methods for estimating the local strain effects have yet to be developed. Nonlinear finite-element or finite-difference methods can be used to evaluate these ef-

fects; however, for most bridge studies such modeling cannot be justified. In recognition of the need for simple guidelines, G/G_{max} adjustment factors were estimated. This approach for dealing with soil nonlinearity involves considerable judgment, which may warrant modification on a case-by-case basis.

- *Liftoff Effects:* The consequence of uplift during seismic loading will be that the effective area of the footing will be less than if full contact were to occur. The amount of uplift is expected to be larger in a higher seismic zone and during an event with a long return period. The area adjustments for liftoff were made by recognizing that the maximum liftoff allowed under the extreme loading condition will usually be one-half uplift of the footing. It was also recognized that the maximum uplift would only occur for a short period of time, and that during most of the earthquake, the maximum loading might be from 50 to 70% of the peak value. For this reason the effective uplift would not be as much as the peak uplift. Values shown were selected after discussing the potential values of effective area that might occur and then applying considerable engineering judgment.

Uncertainty in Spring Constant Determination

Stiffness constants developed in the manner described in this Article involve uncertainty. A prudent design will account for this uncertainty by evaluating stiffness for upper and lower-bound modulus values, in addition to the best-estimate shear modulus. The upper and lower-bound values are used to account for (1) the variability of shear modulus that is likely to occur in the field, (2) the uncertainty in adjustments being used for shearing strain and geometric nonlinearities, and (3) limitations in the equation for determining stiffness.

The range of modulus variation used in a sensitivity evaluation is expected to change, depending on the characteristics of the site, the details of the site characterization process, and the type of analysis. Common practice is often to assume that the lower bound shear modulus is approximately 50% of the best estimate and the upper bound is approximately 100% greater than the best estimate. If the resulting upper and lower-bound values of stiffness are such that

significant differences in bridge response are possible, then consideration should be given to either (1) evaluating bridge response for the range of stiffness values or (2) performing additional site characterization studies to reduce the range used in defining the upper and lower bound.

Geometric or Radiation Damping

The conventional approach during the use of elastic halfspace methods accounts for energy loss within the foundation system through a spectral damping factor. The spectral damping factor is typically defined as 5%, and is intended to represent the damping of the structure-foundation system. This damping differs from the geometric or radiation damping of a foundation. For translational modes of loading, the foundation damping can be in excess of 20%. The 5% spectral damping used in the modal analysis procedures is intended to account for the geometric damping within the foundation system, as well as damping in the bridge structure. While it may be possible to increase the spectral damping of the overall system to a higher level to account for the high geometric damping within the foundation, in view of the liftoff that is allowed to occur during the design earthquake, it is generally not prudent to count on the high levels of foundation damping, at least without special studies that properly account for the liftoff of the foundation.

Table C-1 Surface Stiffnesses for a Rigid Plate on a Semi-Infinite Homogeneous Elastic Half-Space (Adapted from Gazetas, 1991)[1]

Stiffness Parameter	Rigid Plate Stiffness at Surface, Ki'
Vertical Translation, K_z'	$\frac{GL}{1-\nu}\left[0.73+1.54\left(\frac{B}{L}\right)^{0.75}\right]$
Horizontal Translation, K_y' (toward long side)	$\frac{GL}{2-\nu}\left[2+2.5\left(\frac{B}{L}\right)^{0.85}\right]$
Horizontal Translation, K_x' (toward short side)	$\frac{GL}{2-\nu}\left[2+2.5\left(\frac{B}{L}\right)^{0.85}\right]-\frac{GL}{0.75-\nu}\left[0.1\left(1-\frac{B}{L}\right)\right]$
Rotation, $K_{\theta x}'$ (about x axis)	$\frac{G}{1-\nu}\ I_x^{0.75}\ \left(\frac{L}{B}\right)^{0.25}\left(2.4+0.5\frac{B}{L}\right)$
Rotation, $K_{\theta y}'$ (about y axis)	$\frac{G}{1-\nu}\ I_y^{0.75}\ \left[3\left(\frac{L}{B}\right)^{0.15}\right]$

Table note:

1. See FigureC-1** for definitions of terms

Table C-2 Stiffness Embedment Factors for a Rigid Plate on a Semi-Infinite Homogeneous Elastic Half-Space (Adapted from Gazetas, 1991)[1]

Stiffness Parameter	Embedment Factors, ei
Vertical Translation, e_Z	$\left[1+0.095\frac{D}{B}\left(1+1.3\frac{B}{L}\right)\right]\left[1+0.2\left(\frac{(2L+2B)}{LB}d\right)^{0.67}\right]$
Horizontal Translation, e_Y (toward long side)	$\left[1+0.15\left(\frac{2D}{B}\right)^{0.5}\right]\left\{1+0.52\left[\frac{\left(D-\frac{d}{2}\right)16\,(L+B)\,d}{BL^2}\right]^{0.4}\right\}$
Horizontal Translation, e_X (toward short side)	$\left[1+0.15\left(\frac{2D}{L}\right)^{0.5}\right]\left\{1+0.52\left[\frac{\left(D-\frac{d}{2}\right)16\,(L+B)\,d}{LB^2}\right]^{0.4}\right\}$
Rotation, $e_{\theta X}$ (about x axis)	$1+2.52\frac{d}{B}\left(1+\frac{2d}{B}\left(\frac{d}{D}\right)^{-0.20}\left(\frac{B}{L}\right)^{0.50}\right)$
Rotation, $e_{\theta Y}$ (about y axis)	$1+0.92\left(\frac{2d}{L}\right)^{0.60}\left(1.5+\left(\frac{2d}{L}\right)^{1.9}\left(\frac{d}{D}\right)^{-0.60}\right)$

Table note: Embedment factors multiplied by spring

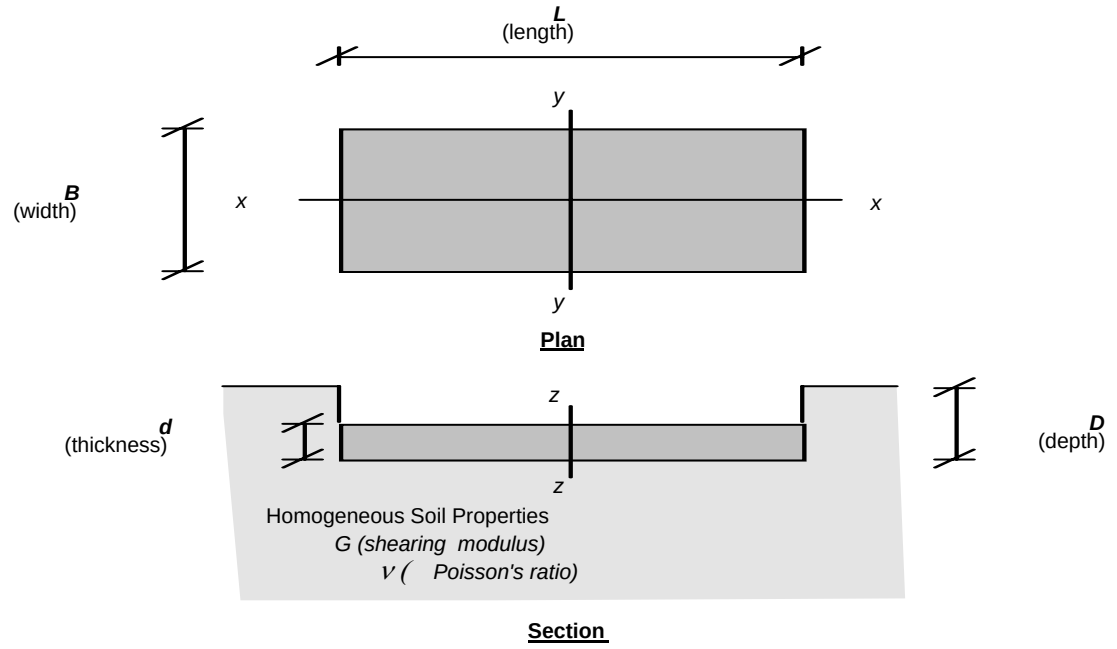

Figure C-1 Properties of a Rigid Plate on a Semi-Infinite Homogeneous Elastic Half-Space for Stiffness Calculations

C.2 Axial and Rocking Stiffness for Driven Pile/Pile Cap Foundations (Nonliquefiable Sites)

The axial stiffness of the driven pile foundations shall be determined for design cases in which foundation flexibility is included. For many applications, the axial stiffness of a group of piles can be estimated within sufficient accuracy using the following equation:

$$K_{sv} = \Sigma\ 1.25AE/L \qquad \text{(C-1)}$$

where

A = cross-sectional area of the pile
E = modulus of elasticity of the piles
L = length of the piles
N = number of piles in group and is represented by the summation symbol in the above equations.

The rocking spring stiffness values about each horizontal pile cap axis can be computed assuming each axial pile spring acts as a discrete Winkler spring. The rotational spring constant (i.e., moment per unit rotation) is then given by

$$K_{srv} = \Sigma\ k_{vn}\ S_n^2 \qquad \text{(C-2)}$$

where

k_{vn} = axial stiffness of the nth pile

S_n = distance between the nth pile and the axis of rotation

The effects of group action on the determination of stiffness shall be considered if the center-to-center spacing of piles for the group in the direction of loading is closer than 3 pile diameters.

C.3 Lateral Stiffness Parameters for Driven Pile/Pile Cap Foundations (Nonliquefiable Sites)

The lateral stiffness parameters of driven pile foundations shall be estimated for design cases in which foundation flexibility is included. Lateral response of a pile foundation system depends on the stiffness of the piles and, very often, the stiffness of the pile cap. Procedures for defining the stiffness of the pile component of the foundation system are covered in this article. Methods for introducing the pile cap stiffness are addressed in Article C.4.

For preliminary analyses involving an estimate of the elastic displacements of the bridge, pile stiffness values can be obtained by using a series of charts

prepared by Lam and Martin (1986). These charts are reproduced in Figures C-2 through C-7. The charts are applicable for mildly nonlinear response, where the elastic response of the pile dominates the nonlinear soil stiffness.

For push-over analyses the lateral load displacement relationship must be extended into the nonlinear range of response. It is usually necessary to use computer methods to develop the load-displacement relationship in this range, as both the nonlinearity of the pile and the soil must be considered. Programs such as LPILE (Reese and Wang, 1997), COM 624 (Wang and Reese, 1991), and FLPIER (Hoit and McVay, 1996) are used for this purpose. These programs use nonlinear "p-y" curves to represent the load-displacement response of the soil; they also can accommodate different types of pile-head fixity. Procedures for determining the "p-y" curves are discussed by Lam and Martin (1986) and more recently by Reese et al. (1997).

The effects of group action on lateral stiffness shall be considered if the center-to-center spacing of the piles is closer than 3 pile diameters.

C.4 Pile Cap Stiffness and Capacity

The stiffness and capacity of the pile cap shall be considered in the design of the pile foundation. The pile cap provides horizontal resistance to the shear loading in the column. Procedures for evaluating the stiffness and the capacity of the footing in shear shall follow procedures given in Article C.5 for spread footings, except that the base shear resistance of the cap shall be neglected.

When considering a system comprised of a pile and pile cap, the stiffness of each shall be considered as two springs in parallel. The composite spring shall be developed by adding the reaction for each spring at equal displacements.

C.5 Moment-Rotation and Shear-Displacement Relationships for Footings

The foundation capacity requires an evaluation of the soil to resist the overturning moment and the shear force from the column. Vertical loading to the footing will also change during seismic loading, and this change also needs to be considered.

The initial slope of the moment-rotation curve should be established using the best-estimate rotational spring constant defined in the previous article. Checks can be performed for the upper and lower bound of the initial slope; however, these variations will not normally be important to design.

It is critical, during determination of the moment capacity, for the moment-rotation curve to use the ultimate bearing capacity for the footing without use of a resistance factor (i.e., use $\phi = 1.0$). The determination of ultimate bearing capacity should not be limited by settlement of the footing, as is often done for static bearing capacity determination. The ultimate capacity for the moment-rotation relationship should be defined for the best-estimate soil conditions.

For important bridges, the design should consider use of upper and lower bounds for bearing capacity to account for uncertainties. The range for the upper and lower bound will depend on the variability of soils at the site and the extent of field explorations and laboratory testing. Common practice is often to assume that the lower bound capacity is approximately 50% of the best estimate and the upper bound is approximately 100% greater than the best estimate.

Shear-Displacement

During horizontal shear loading, the resisting force comprises the resistance developed along the base and the sides of the footing and from the passive pressure at the face of the footing. The passive pressure will often provide most of the reaction during a seismic event. For simplicity it can be assumed that the maximum resistance (passive + base + two sides) is developed at a deformation equal to 2% of the footing thickness.

The shear resistance on the base and side of the footing should be determined using an interface shear strength. For most cast-in-place concrete foundations, a value of interface friction of 0.8 times the friction angle of the soil will be appropriate. Displacements to mobilize this resistance will normally be less than 10 to 20 mm. The passive pressure at the face of the footing should be computed assuming an interface friction angle equal to 50% of the friction angle of the backfill material. The log spiral or Caquot-Kerisel (1948) methods should be used for determining the ultimate passive pressure. If the backfill material changes within twice the height

of the footing, the effects of the second material should be included in the computation of the passive pressure. A method of slices similar to a slope stability analysis offers one method of accomplishing this computation.

Deformations needed to mobilize the ultimate passive resistance of the face of a footing could easily exceed 25 mm for a typical footing thickness. The potential consequences of this movement relative to column behavior will usually be evaluated during the soil-structure interaction analysis. The uncertainty in computing deformations associated with ultimate passive resistance determination is such that a variation of –50% and +100% would not be unusual. If this variation has a significant effect on, say, the push-over-analysis, the designer may want to modify the foundation or the soil conditions to reduce the uncertainty or limit the deformations.

As discussed by Kramer (1996), evidence exists that the available ultimate passive resistance during seismic loading could be reduced by the seismic response of the ground. This condition occurs if the direction of loading from the inertial response of the bridge structure is the same as the motions in the ground. These two loadings normally occur at different frequencies, and therefore, the coincidence of the directions of loading is usually for only a moment in time. When the movements are out of phase, the loading increases. It was felt that reducing the passive ultimate resistance for the short periods of coincidence would underestimate the effective passive capacity of the foundation (i.e., low ultimate resistance), and therefore the approach taken in these *Specifications* is to ignore this potential effect. This approach clearly involves considerable judgment, and therefore, an alternative approach that includes the reduction in passive resistance could be used, subject to the Owner's approval.

Vertical Load Capacity

For most designs it is unnecessary to consider increases in vertical forces on the footing during seismic loading, as these forces will normally be a fraction of the gravity load. However, if the bridge site is located in proximity to an active fault, vertical accelerations could become important, as discussed in Article 4.7.2. For these situations the potential displacement should be checked using the spring constants given in Table C-1 together with the increase in

vertical column load. The potential consequences of reduction in vertical loads through inertial response should also be considered. This effect could temporarily decrease lateral resistance and moment capacity

Liquefaction below a spread footing foundation located in SDC D and above could be significant because of the combination of higher ground accelerations and larger earthquake magnitudes. As the potential for liquefaction increases, the potential for damage or failure of a bridge from loss in bearing support, lateral flow or lateral spreading of the soil, or settlements of the soil as porewater pressures in the liquefied layers dissipate also increases.

Additional discussion of the consequences of liquefaction is provided in Appendix E.

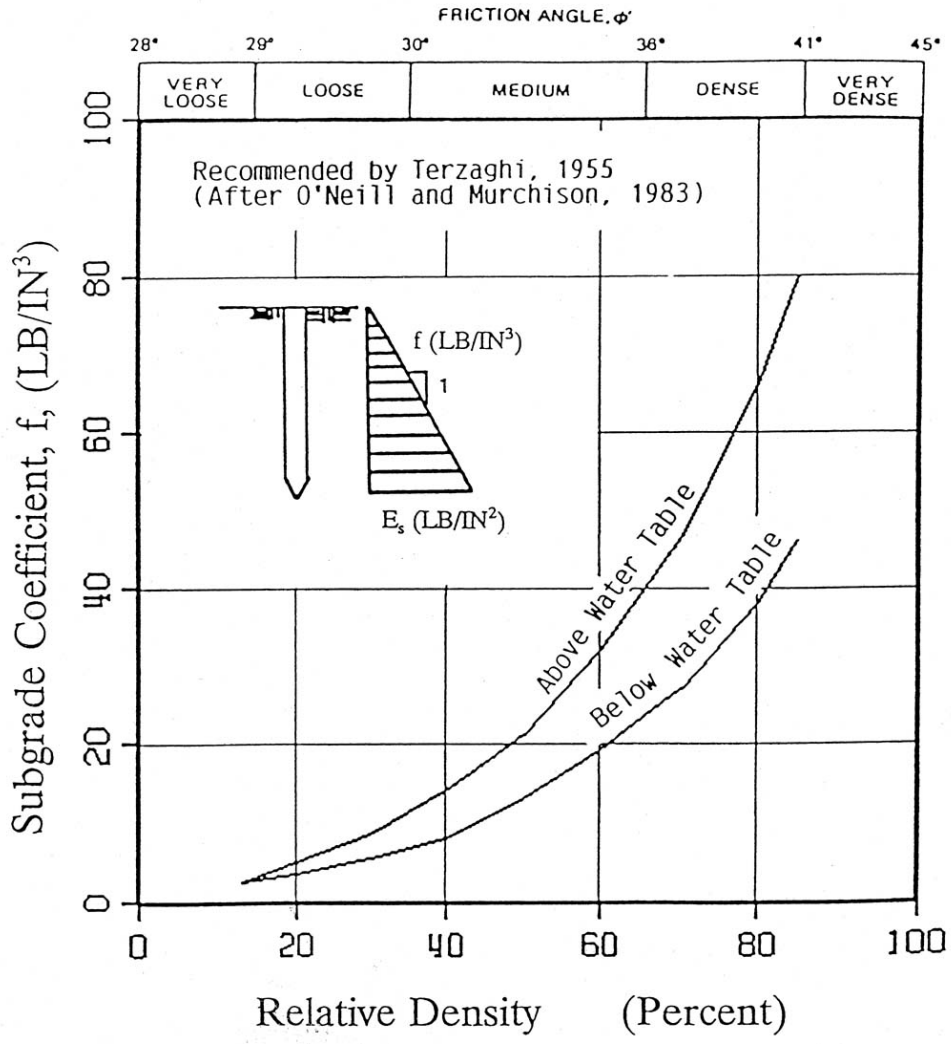

Figure C-2 **Recommendations for Coefficient of Variation in Subgrade Modulus with Depth for Sand (ATC, 1996)**

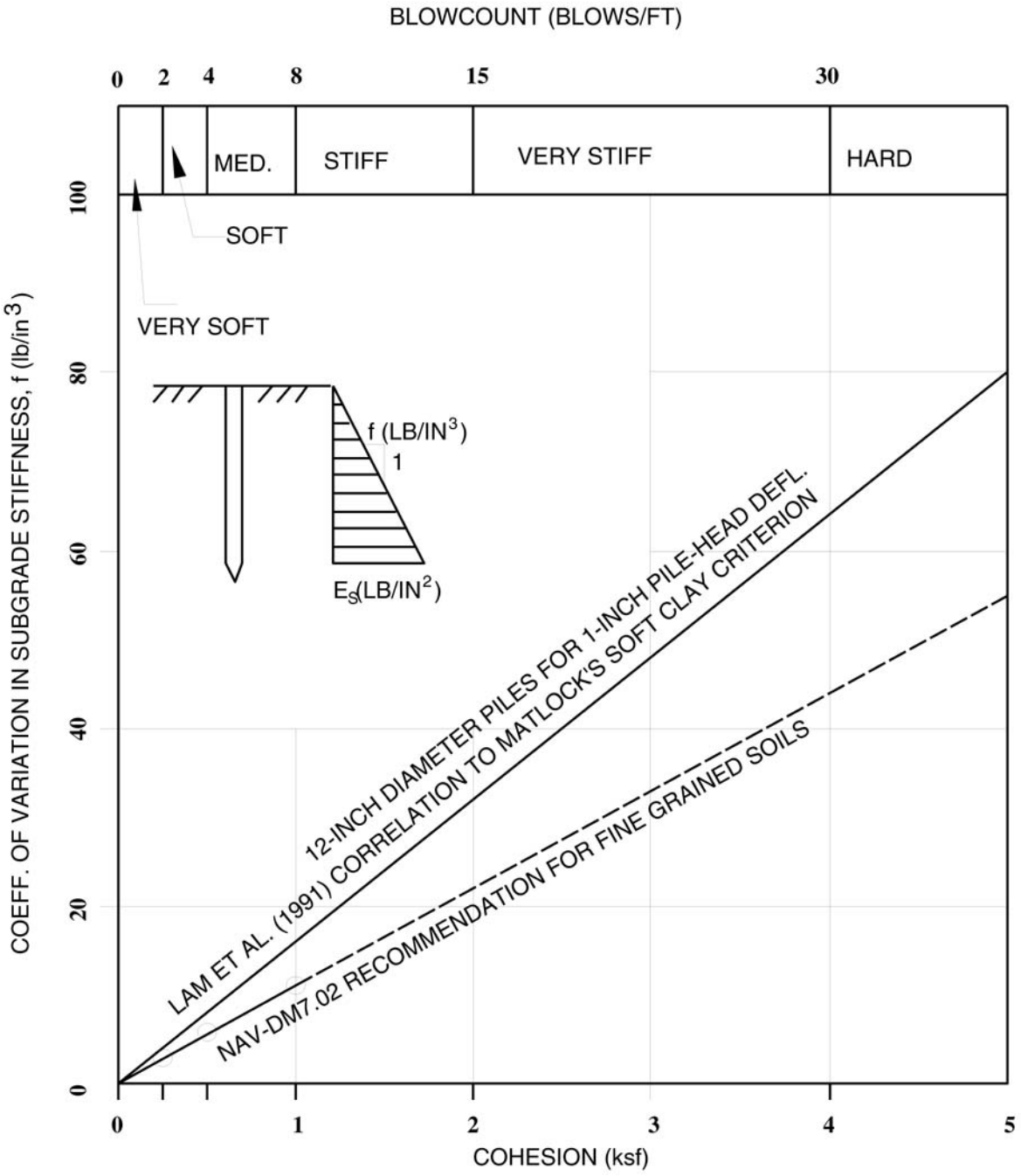

Figure C-3 **Recommendations for Coefficient of Variation in Subgrade Modulus with Depth for Clay (ATC, 1996)**

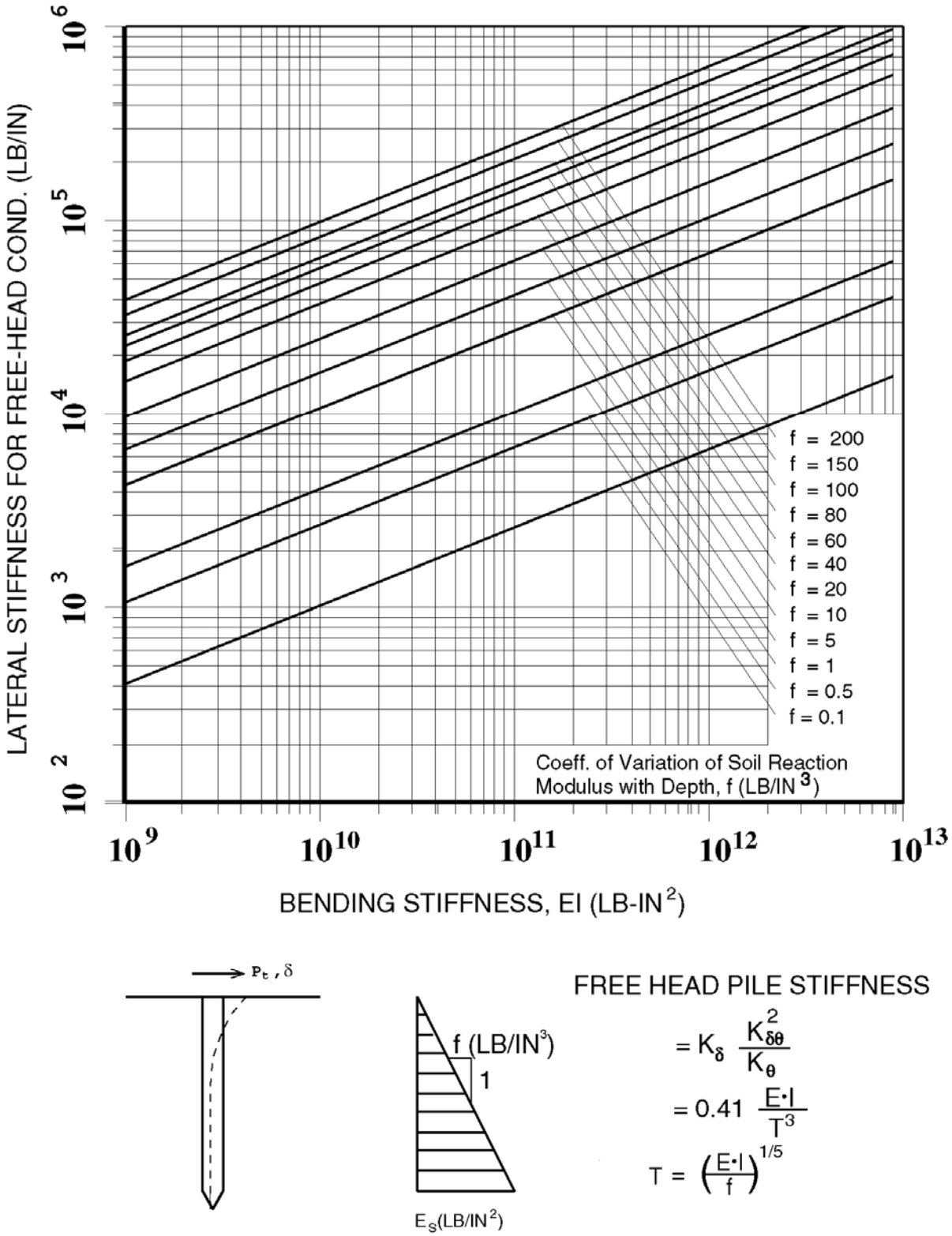

Figure C-4 **Coefficient of Lateral Pile Head Stiffness for Free-Head Pile Lateral Stiffness (ATC, 1996)**

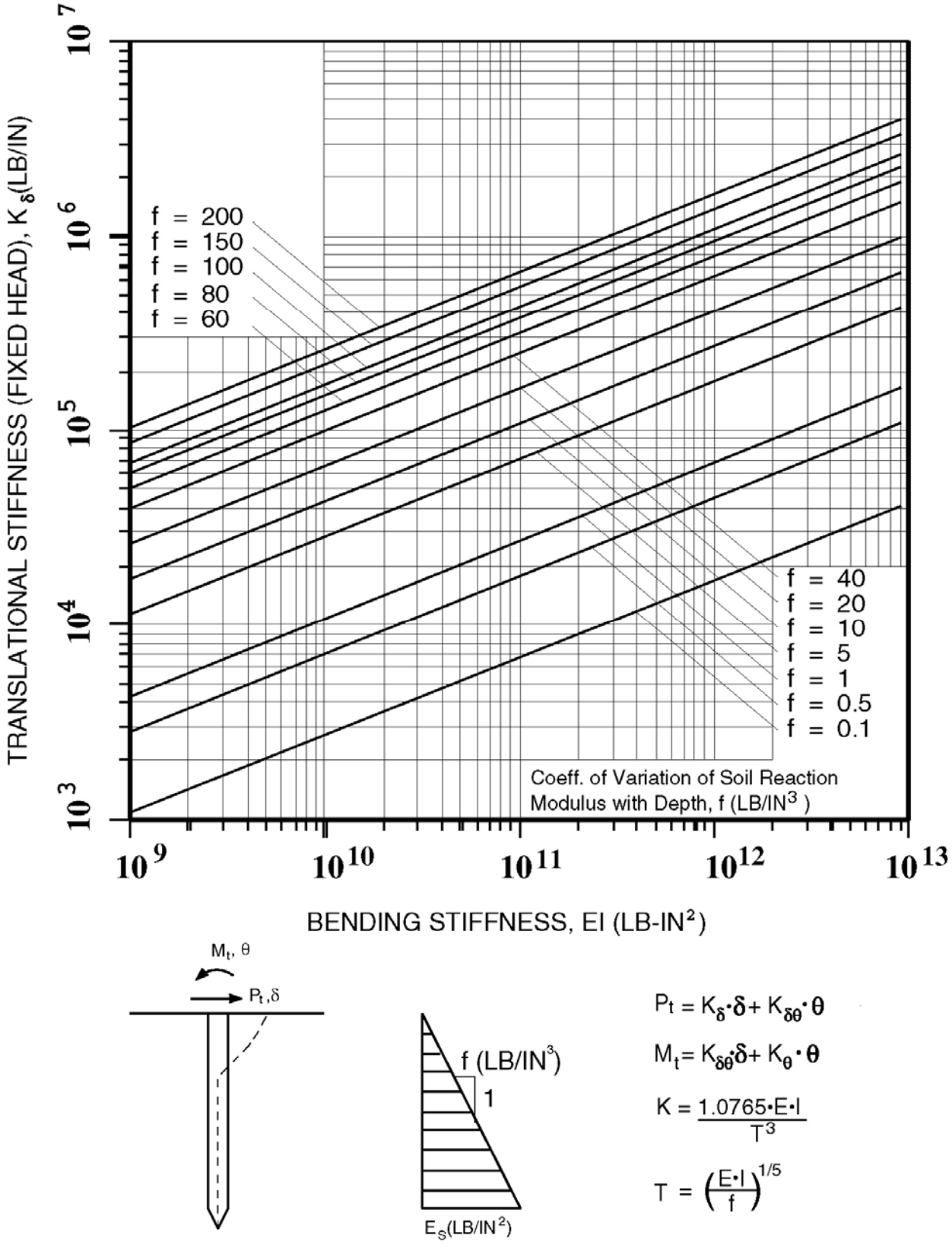

Figure C-5 **Coefficient for Lateral Pile-Head Stiffness for Fixed-Head Pile Lateral Stiffness (ATC, 1996)**

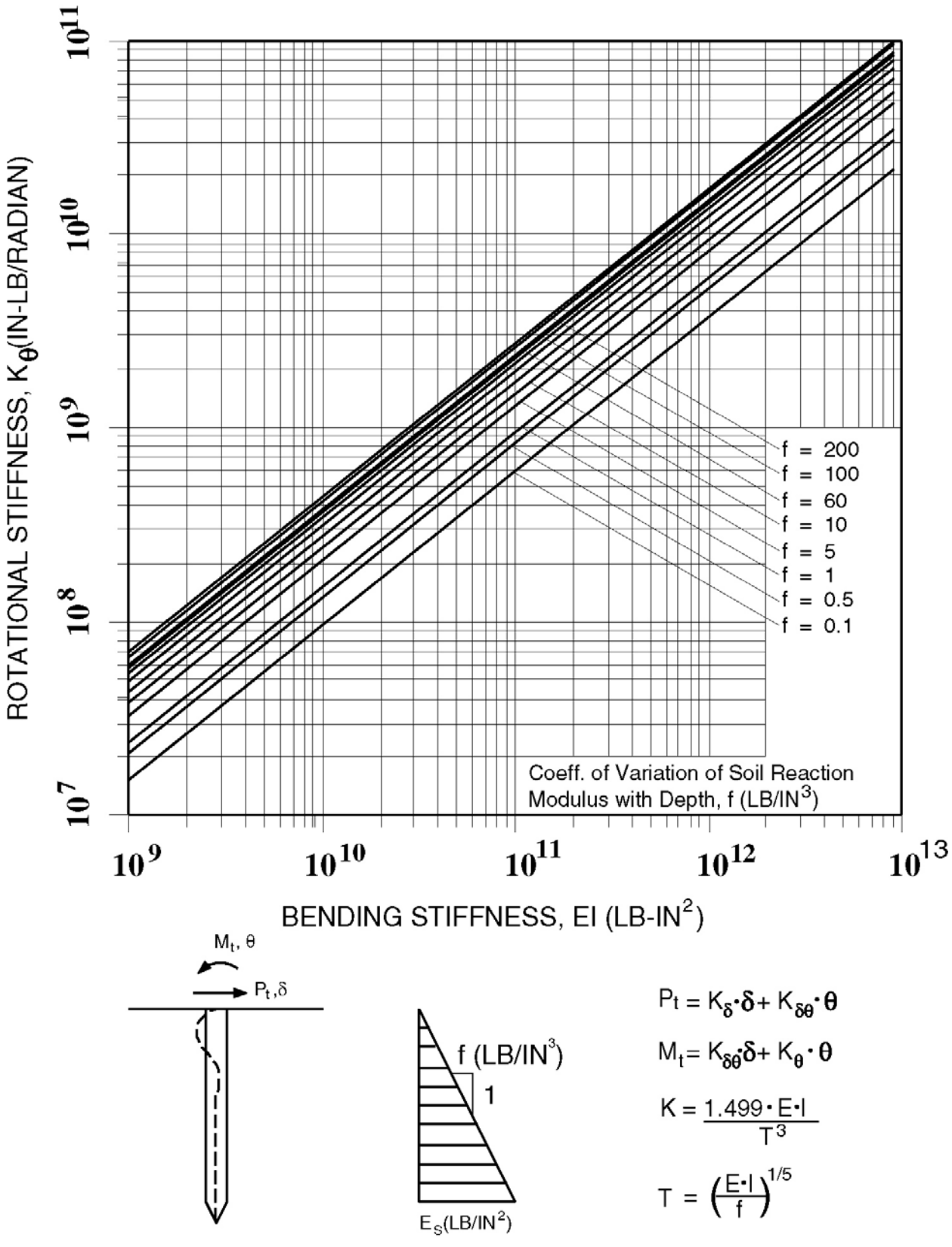

Figure C-6 Coefficient for Pile Head Rotation (ATC, 1996)

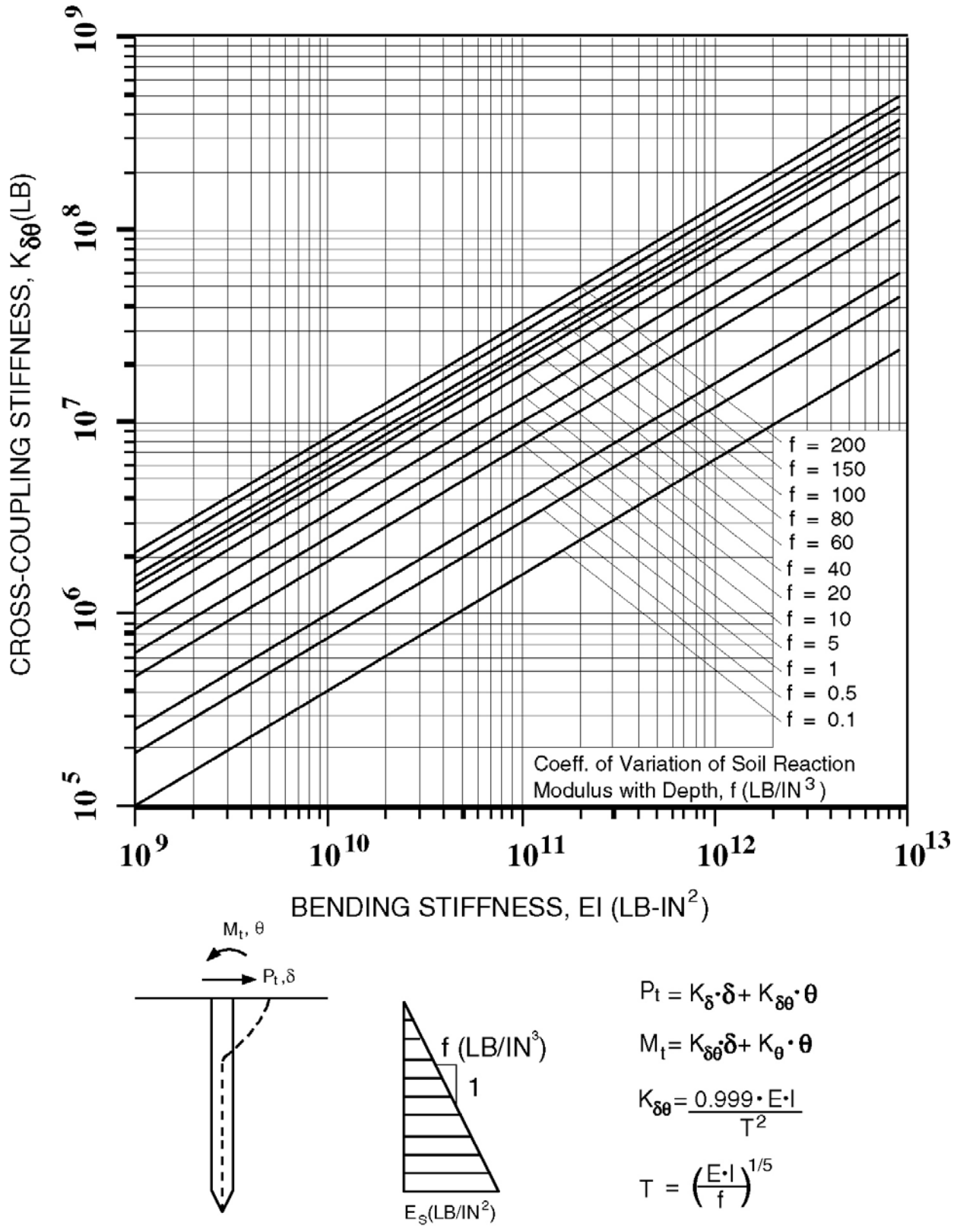

Figure C-7 **Coefficient for Cross-Coupling Stiffness Term (ATC, 1996)**

Appendix D
PROVISIONS FOR COLLATERAL SEISMIC HAZARDS

COLLATERAL SEISMIC HAZARDS

The term collateral seismic hazards refers to earthquake-caused movement of the earth that either results in loads being imposed on a bridge foundation system or causes changes in the resistance of the earth that affects the response of a bridge-foundation system. These effects can be either dynamic or static in form. Liquefaction is one of the most well-known examples of a collateral hazard. This Appendix provides an overview of methods used to evaluate and design for these collateral hazards. This overview includes

- a general discussion of the term collateral hazards and the implication of these hazards on design of bridge foundations (Article D.1)
- a summary of methods used to screen for and evaluate liquefaction and associated hazards, such as lateral flows, lateral spreading, settlement, and differential settlement (Article D.2)
- an overview of other collateral hazards such as faulting, landsliding, differential compaction, and flooding and inundation (Article D.3), and
- a review of methods for designing spread footings and deep foundations for the most common collateral hazards, liquefaction (Article D.4)

The design of a bridge structure should consider the potential for these collateral hazards during the initial type, size, and location (TS&L) phase of the project, as significant cost can be incurred to design for, mitigate, or avoid these hazards.

D.1 GENERAL

The most common of the collateral hazards is liquefaction. During liquefaction, saturated granular soil loses stiffness and strength, which can affect the vertical or lateral bearing support of a foundation. Under normal circumstances, these losses in support can be handled during design. The more serious consequences of liquefaction are permanent lateral ground movements and settlement of the soil, both of which can damage a bridge foundation system.

Several other types of hazards associated with seismic-related ground behavior also can lead to damage of a bridge. These hazards include ground faulting, landsliding, differential compaction, and inundation and flooding resulting from earthquake-induced failures of dams or reservoirs, and tsunami..

CD.1 GENERAL

The term collateral hazards has been selected to differentiate loads that are imposed on a structure by displacement of soil from loads developed within a structure due to the inertial response of the bridge deck and abutments. These hazards are also called geologic or geotechnical hazards by those practicing in the areas of geology and geotechnical engineering. In this Appendix the terms geologic hazards and collateral hazards are used interchangeably.

Displacement associated with these collateral hazards can be very large, often being on the order of a meter and sometimes being as large as several meters. In some cases such as liquefaction-induced flow failures or landsliding, it will be difficult to prevent or limit displacement without significant expenditure of project funds. In the case of faulting the displacement cannot be prevented; all that can be done is to design the structure to withstand or avoid the movement.

D.1.1 Evaluation of Collateral Hazards

Various procedures have been developed over

C.D.1.1 Evaluation of Collateral Hazards

As time passes and more is learned about seis-

the past 20 years for quantifying the potential for and the consequences of these geologic hazards. The discussions in this Appendix summarize procedures and approaches commonly employed within the profession. The applicability of these procedures will depend on the soil conditions at the site, the complexity of the structure, and the risk that the owner is prepared to assume.

mic response of soil, methods for identifying and dealing with collateral seismic hazards will likely change. For this reason this Appendix is intended to provide guidance and not be prescriptive.

Much of the following discussion will focus on the evaluation of liquefaction and its related hazards. Procedures given in this Appendix for the assessment of liquefaction are based on a consensus document prepared after a workshop sponsored by the National Center for Earthquake Engineering Research (NCEER) in 1996 (Youd and Idriss, 1997). The workshop was attended by a group of leading professionals working or conducting research in the area of liquefaction. The NCEER Workshop participants were not always in complete agreement in all areas dealing with liquefaction or design for liquefaction; however, the participants did agree that the NCEER Workshop report would form a minimum basis for conducting liquefaction evaluations. It was expected that the profession would build on these methods as more information became available.

The dilemma that an owner will face is deciding when methods advocated by an individual or group of individuals should be used to upgrade the procedures developed during the consensus NCEER Workshop. There is no simple process of making these decisions, a situation that is common to any evolving technology.

D.1.2 Designing for Collateral Hazards

The design of bridge structures for collateral hazards must consider the movement of the earth and the changes in soil properties resulting from this movement. In the case of liquefaction both effects must be considered in design. The first is that the bridge must perform adequately with just the liquefaction-induced soil changes alone. This means that the mechanical properties of the soil that liquefy are changed to reflect their post-liquefaction values (e.g., properties such as "p-y curves" and modulus of subgrade reaction values used to evaluate the lateral stiffness of a pile foundation are reduced). The second component of the design is the consideration of liquefaction-related ground movements. These can take several forms: lateral spreading, lateral flow, and ground settlement.

- Lateral spreading is a lateral movement that is induced by the ground shaking and develops in an incremental fashion as shaking occurs.
- Lateral flow is movement that occurs due to

CD.1.2 Designing for Collateral Hazards

The focus of this Appendix is the design for liquefaction and liquefaction-related hazards, as liquefaction has been perhaps the single most significant cause of damage to bridge structures during past earthquakes. Most of the damage has been related to lateral movement of soil at the bridge abutments. However, cases involving the loss in lateral and vertical bearing support of foundations for central piers of a bridge have also occurred.

Loss in lateral support and permanent ground movement can occur simultaneously during a seismic event. Their simultaneous occurrence is a complicated process that is difficult to represent without the use of very complex computer modeling. For most bridges the complexity of the modeling does not warrant performing a combined analysis. In these cases the recommended methodology is to consider these effects independently, i.e., de-coupled. The reasoning behind this is that it is not likely that the peak vibrational response and the peak spreading or flow effect will occur simultaneously. For many earthquakes the peak vibration response occurs somewhat in advance of

the combined effects of sustained porewater pressure and gravity loads without the inertial loading from the earthquake. Flows can occur several minutes following an earthquake, when porewater pressures redistribute to form a critical combination with gravity loading.

- Dynamic settlement occurs following an earthquake as porewater pressures dissipate.

These liquefaction-related effects are normally considered separately as uncoupled events.

D.2 LIQUEFACTION[1]

The need for an evaluation of liquefaction and liquefaction-related hazards depends on the level of ground shaking and the magnitude of the earthquake that could occur at a site. In areas of very low seismicity (SDR 1 and SDR 2), no specific seismic design requirements occur. On the other hand, the potential for liquefaction at sites should be determined for sites located in SDR 3, 4, 5, and 6.

The evaluation of liquefaction potential should follow procedures given in Youd and Idriss (1997) and SCEC (1999). These procedures are summarized in Article D.2.

maximum ground movement loading. For very large earthquakes where liquefaction may occur before peak ground accelerations occur, the peak vibration response is likely to be significantly attenuated and, hence, inertial loading reduced from peak design values. In addition peak displacements demands arising from lateral ground spreading are likely to generate maximum pile moments at depths well below peak moments arising from inertial loading. Finally, the de-coupling of response allows the flexibility to use separate and different performance criteria for design to accommodate these phenomena.

Two detailed case studies on the application of the recommended design methods for both liquefaction and lateral flow design are given in the companion Liquefaction Study Report (ATC/MCEER, 2003a) and summarized in Appendix H of this document.

CD.2 LIQUEFACTION

In SDR's 1 and 2 the potential for liquefaction is generally low. In some cases the peak ground acceleration in these SDR's may exceed 0.15g. While this level of peak ground acceleration is sufficient to cause liquefaction, the magnitude of the earthquake causing liquefaction in these categories will generally be less than 6. For this earthquake magnitude liquefaction develops slowly for most soils, and results in minimal effects other than ground settlement.

The potential for liquefaction in SDR's 3, 4, 5, and 6 is much higher, and therefore careful attention to the determination of the potential for and consequences of liquefaction is needed for sites with these classifications. At some locations it may be necessary to use ground improvement methods to mitigate the potential effects of liquefaction. As these methods are often expensive, detailed consideration of the potential for liquefaction is warranted.

[1] Much of the contents of this discussion of liquefaction was taken from a report titled "*Recommended Procedures for Implementation of DMG Special Publication 117, Guideline for Analyzing and Mitigating Liquefaction in California*" and referenced as SCEC (1999). The SCEC report was prepared by a group of consultants and government agency staff led by G.R. Martin of the University of Southern California and M. Lew of Law/Crandall. Funding for the report was provided by the City of Los Angeles, the County of Los Angeles, the California Division of Mines and Geology, the Federal Emergency Management Agency, as well as the Counties of Riverside, San Bernadino, San Diego, Orange, and Ventura. The intent of the SCEC report was to provide practical guidance to design engineers in the implementation of liquefaction prediction and hazards evaluation methods. The SCEC report represented the current state-of-the-practice at the time that these Guidelines were being prepared. Where appropriate, the SCEC report recommendations have been updated or augmented in this Appendix to be more consistent with requirements for bridge design or new developments in liquefaction assessment methodologies.

D.2.1 Preliminary Screening for Liquefaction

An evaluation of liquefaction hazard potential may not be required if the following conditions occur at a site:

- The estimated maximum-past-, current-, and maximum-future-groundwater-levels (i.e., the highest groundwater level applicable for liquefaction analyses) are determined to be deeper than 15 m below the existing ground surface or proposed finished grade, whichever is deeper.
- "Bedrock" or similar lithified formational material underlies the site. In many areas glacially overridden (till) deposits fall in this classification.
- The corrected standard penetration blow count, $(N_1)_{60}$, is greater than or equal to 30 in all samples with a sufficient number of tests. If cone penetration test soundings are made, the corrected cone penetration test tip resistance, q_{c1N}, should be greater than or equal to 160 in all soundings in sand materials.
- The soil is clayey. For purposes of this screening, clayey soils are those that have a clay content (i.e., particle size <0.005 mm) greater than 15%. However, based on the so-called "Chinese Criteria," (Seed and Idriss, 1982) clayey soils having all of the following characteristics may be susceptible to severe strength loss:
  - Percent finer than 0.005 mm: less than 15 %
  - Liquid Limit: less than 35
  - Water Content: greater than 0.9 of the Liquid Limit

If the screening investigation clearly demonstrates the absence of liquefaction hazards at a project site and the owner concurs, the screening investigation will satisfy the site investigation report requirement for liquefaction hazards. If not, a quantitative evaluation will be required to assess the liquefaction hazards.

CD.2.1 Preliminary Screening for Liquefaction

Liquefaction will generally occur in loose, saturated granular materials. These granular materials can include silts, sands, and in some cases loose gravels. Liquefaction of loose gravels has been observed during several earthquakes when cohesive soils overlying the gravel prevented drainage of porewater pressures.

Geologically young cohesionless materials are more susceptible than geologically old cohesionless soils, as a result of cementation and other similar aging effects that tend to occur in geologically old materials. Common geologic settings for liquefaction-susceptible soils include unlithified sediments in coastal regions, bays, estuaries, river floodplains and basins, areas surrounding lakes and reservoirs, and wind-deposited dunes and loess. In many coastal regions, liquefiable sediments occupy back-filled river channels that were excavated during Pleistocene low stands of sea level, particularly during the most recent glacial stage. Among the most easily liquefiable deposits are beach sand, dune sand, and clean alluvium that were deposited following the rise in sea level at the start of the Holocene age, about 11,000 years ago.

Preliminary screening can often be used to eliminate a site from further liquefaction consideration. The screening investigation should include a review of relevant topographic, geologic, and soils engineering maps and reports, aerial photographs, groundwater contour maps, water well logs, agricultural soil survey maps, the history of liquefaction in the area, and other relevant published and unpublished reports. The purpose of the screening investigations for sites within zones of required study is to filter out sites that have no potential or low potential for liquefaction.

No specific limitation is placed on the depths of liquefiable soils in the screening process. As discussed in a following section of this Appendix, liquefaction can occur to depths of 25 m or more.

D.2.2 Field Explorations for Liquefaction Hazards Assessment

Two field exploration methods are normally used during the evaluation of liquefaction potential, Standard Penetration Test (SPT) methods and Cone Penetrometer Test (CPT) methods. Appendix B gives a brief discussion of these methods. Shear wave velocity methods have also been found to be advantageous for evaluating liquefaction potential at some sites. The SPT and CPT methods should be regarded as the minimum requirement for evaluating site liquefaction potential. A geologic reconnaissance and review of the available geotechnical information for the site should supplement any field investigation.

SPT Method

Procedures for evaluating liquefaction potential using SPT methods are described in detail by Youd and Idriss (1997) and by SCEC (1999). These procedures include consideration of correction factors for drilling method, hole diameter, drive-rod length, sampler type, energy delivery, and spatial frequency of tests.

Information presented in Youd and Idriss (1997) and in SCEC (1999) indicate that the results of SPT explorations are affected by small changes in measurement method; therefore, it is critical for these tests that standard procedures are followed and that all information regarding the test method and equipment used during the field work be recorded. The energy of the SPT hammer system should also be established for the equipment, as this energy directly affects the determination of liquefaction potential. The variation in hammer energy can be as much as a factor of 2, which can easily cause a liquefiable site to be identified as being nonliquefiable, if a correct hammer calibration factor is not introduced.

CPT Method

The CPT is gaining recognition as the preferred method of evaluating liquefaction potential in many locations. Methods for assessing liquefaction potential from CPT results are given in Youd and Idriss (1997). The primary advantages of the CPT method are:

- The method provides an almost continuous penetration resistance profile that can be used for stratigraphic interpretation, which is particularly important in determining the poten-

CD.2.2 Field Explorations for Liquefaction Hazards Assessment

A number of factors must be considered during the planning and conduct of the field exploration phase of the liquefaction investigation.

Location of Liquefiable Soils

During the field investigation, the limits of unconsolidated deposits with liquefaction potential should be mapped within and beyond the footprint of the bridge. Typically, this will involve investigations at each pier location and at enough locations away from the approach fill to establish the spatial variability of the material. The investigation should establish the thickness and consistency of liquefiable deposits from the ground surface to the depth at which liquefaction is not expected to occur. The "zone of influence" where liquefaction could affect a bridge approach fill will generally be located within a 2H:1V (horizontal to vertical) projection from the bottom of the approach fill.

Location of Groundwater Level

The permanent groundwater level should be established during the exploration program. Shallow groundwater may exist for a variety of reasons, of natural or man-made origin. Groundwater may be shallow because the ground surface is only slightly above the elevation of the ocean, a nearby lake or reservoir, or the sill of a basin. Another concern is man-made lakes and reservoirs that may create a shallow groundwater table in young sediments that were previously unsaturated. If uncertainty exists in the location of the groundwater level, piezometers should be installed during the exploration program. The location of the groundwater level should be monitored in the piezometers over a sufficient duration to establish seasonal fluctuations that may be due to rainfall, river runoff, or irrigation.

Usually, soils located below the groundwater level are fully saturated; however, at locations where fluctuations in groundwater occur, soil can be in a less than fully saturated condition. The liquefaction resistance of the soil is affected by the degree of saturation, with the resistance increasing significantly as the degree of saturation decreases. If the groundwater level fluctuates due to tidal action or seasonal river fluctuations, then the zone of fluctuation will often have a lower degree of saturation, making the soil more resistant to liquefac-

tial for lateral spreading, lateral flows, and significant differential post-liquefaction settlements.

- The repeatability of the test is very good.
- The test is fast and economical compared to drilling and laboratory testing of soil samples.

The limitations of the method are:

- The method does not routinely provide soil samples for laboratory tests.
- The method provides approximate, interpreted soil behavior types and *not* the actual soil types according to ASTM Test Methods D 2488 (Visual Classification) or D 2487 (USCS Classification) [ASTM, 1998].
- The test cannot be performed in gravelly soils and sometimes the presence of hard/dense crusts or layers at shallow depths makes penetration to desired depths difficult.

The CPT method should be performed in accordance with ASTM D 3441 (ASTM, 1998). Generally, it is recommended that at least one boring be drilled to confirm soil types and obtain samples for laboratory testing if the CPT method is used for evaluating liquefaction potential.

Shear Wave Velocity Method

Correlations have also been developed between liquefaction potential and shear wave velocity, as reported in Youd and Idriss (1997). The shear wave velocity method offers a rapid screening of liquefiable sites, if velocities are obtained by the Spectral Analysis of Surface Wave (SASW) procedure. Procedures involving the use of boreholes, such as downhole and crosshole methods, can be used as a comparison with liquefaction potential obtained by SPT or CPT methods. The shear wave velocity method also provides an estimate of liquefaction potential in soils where SPT and CPT methods are not usually successful, such as in gravels. Limitations of the shear wave velocity method include its limited database and its inability to measure thin layers that could serve as sliding surfaces for flow failures.

D.2.3 Ground Motions for Liquefaction Analysis

To perform an analysis of liquefaction triggering, liquefaction settlement, seismically induced tion. Unless the seasonal fluctuation is in place for an extended period of time, say weeks at a higher level, it is usually acceptable to use a long-term groundwater level as a basis for design.

Depth of Liquefaction

The field exploration should be conducted to the maximum depth of liquefiable soil. A depth of about 15 m has often been used as the depth of analysis for the evaluation of liquefaction. However, the Seed and Idriss (1982) EERI Monograph on "Ground Motions and Soil Liquefaction During Earthquakes" does not recommend a minimum depth for evaluation, but notes 12 m as a depth to which some of the numerical quantities in the "simplified procedure" can be estimated reasonably. Liquefaction has been known to occur during earthquakes at deeper depths than 15 m given the proper conditions such as low-density granular soils, presence of groundwater, and sufficient cycles of earthquake ground motion. For example, liquefaction occurred to depths in excess of 25 m during the 1964 Alaska earthquake.

For this reason it is recommended that a minimum depth of 25 m below the existing ground surface or lowest proposed finished grade (whichever is lower) be investigated for liquefaction potential. For deep foundations (e.g., shafts or piles), the depth of investigation should extend to a depth that is a minimum of 6 m below the lowest expected foundation level (e.g., shaft bottom or pile toe) or 25 m below the existing ground surface or lowest proposed finished grade, whichever is deeper.

If, during the investigation, the indices to evaluate liquefaction indicate that the liquefaction potential may extend below that depth, the exploration should be continued until a significant thickness (e.g., at least 3 m, to the extent possible) of nonliquefiable soils is encountered.

CD.2.3 Ground Motions for Liquefaction Analysis

The peak ground acceleration used in the simplified liquefaction evaluation is defined at the

settlement, and lateral spreading, a peak horizontal ground acceleration and a mean earthquake magnitude must be established for the site:

- *Peak Ground Acceleration (PGA):* The PGA may be determined from 0.40 S_{DS} as defined in Article 3.4.1 or from the seismic hazard maps described in Article 3.4 or a site-specific probabilistic seismic hazard analysis (PSHA). Appropriate adjustments must be made to correct the firm-ground motion (obtained from the map or from the PSHA) for local site effects. This adjustment is included in S_{DS}.
- *Earthquake Magnitude:* The magnitude required in the liquefaction analysis can be determined from magnitude-distance deaggregation information for PGA given in the USGS Website (http:// geohazards.cr.usgs.gov/eq/) or as part of the site-specific PSHA. The mean magnitude of the deaggregation will be applicable for most locations; however, if a single or few magnitude-distance peaks dominate the distribution (e.g., characteristic earthquake on a seismic source), the peak or the mean of the few peaks should be used to define the magnitude. In locations where bi- or tri-modal magnitude-distance distributions occur, each magnitude and an associated acceleration level should be considered.

Although for most analyses, information in the USGS Website will be sufficient for determining the PGA and the earthquake magnitude, a site-specific PSHA may provide better estimation of the ground motions at some locations. The decision to perform a PSHA should be made after detailed discussions with the owner.

D.2.4 Evaluation of Liquefaction Hazard

Two basic procedures are used to evaluate the potential for liquefaction at a site. These involve

- a simplified procedure that is based on empirical correlations to observations of liquefaction, or
- more rigorous numerical modeling.

The decision between the two procedures should be made after careful review of conditions at the site and the risks associated with liquefaction, and with the concurrence of the owner.

ground surface. Maps and most site-specific hazard evaluations also define the PGA at the ground surface; however, the soil conditions used to develop the PGA maps or the attenuation relationships in the PSHA are relatively stiff (Site Classification B/C) as defined in Article 3.4.2 of the companion *Guidelines*. It is necessary to adjust these accelerations for local site effects. This adjustment can be made by either using the factors given in Table 3.4.2.3-1 or by conducting site-specific ground response studies with a computer program such as SHAKE (Idriss and Sun, 1992) or DESRA 2 (Lee and Finn, 1978).

When Table 3.4.2.3-1 is used to estimate site factors, the amplification or attenuation factor is determined on the basis of the site class before liquefaction and the spectral acceleration at short periods (S_s), where S_s is equal to 2.5 × PGA.

CD.2.4 Evaluation of Liquefaction Hazard

For most projects the simplified procedure will be acceptable, However, for critical projects, more rigorous modeling using equivalent linear and nonlinear computer codes may be appropriate. Conditions warranting use of more rigorous methods include (1) sites where liquefiable soils extend to depths greater than 25 m, (2) sites that have significant interlayering, particularly where interlayers comprise highly permeable soils or soft clay layers, and (3) sites where the cost of ground remediation methods to mitigate liquefaction is great. Most site-specific ground response analyses result in lower estimations of ground acceleration and shearing stresses within the soil profile be-

cause the energy dissipative mechanisms occurring during liquefaction are explicitly considered in this approach.

D.2.4.1 Simplified Method

The most basic procedure used in engineering practice for assessment of site liquefaction potential is that of the "Simplified Procedure" originally developed by Seed and Idriss (1971, 1982) with subsequent refinements by Seed et al. (1983), Seed et al. (1985), Seed and De Alba(1986), and Seed and Harder (1990). The procedure essentially compares the cyclic resistance ratio (CRR) [the cyclic stress ratio required to induce liquefaction for a cohesionless soil stratum at a given depth] with the earthquake-induced cyclic stress ratio (CSR) at that depth from a specified design earthquake (defined by a peak ground surface acceleration and an associated earthquake magnitude).

Cyclic Resistance Ratio

Values of CRR for the Simplified Method were originally established from databases for sites that did or did not liquefy during past earthquakes and where values of the normalized SPT value, $(N_1)_{60}$, could be correlated with liquefied strata. The current version of the baseline chart defining values of CRR as a function of $(N_1)_{60}$ for magnitude 7.5 earthquakes is shown on Figure D.2.4-1. This chart was established by a consensus at a 1996 NCEER Workshop, which convened a group of experts to review current practice and new developments in the area of liquefaction evaluations (Youd and Idriss, 1997). Magnitude adjustment factors are presented in Figure D.2.4-2. The CRR value can also be obtained using CPT, Becker Hammer Tests (BHT), or shear wave velocity methods, as discussed by Youd and Idriss (1997). The determination of CRR must consider the fines content of the soil, the energy of the hammer for the SPT and BHT methods, the effective overburden pressure, and the magnitude of the earthquake. Figures D.2.4-3 and D.2.4-4 show the liquefaction potential (i.e., CRR values) for the CPT and shear wave velocity methods.

Cyclic Stress Ratio

For estimating values of the earthquake-induced cyclic shearing stress ratio, CSR, the NCEER Workshop recommended essentially no change to the original simplified procedure (Seed and Idriss, 1971), where the use of a mean r_d fac-

CD.2.4.1 Simplified Method

Adjustments for changes in water table and overburden condition should be made during the simplified analyses. The following guidance can be used in making these adjustments.

Overburden Corrections for Differing Water Table Conditions

To perform analyses of liquefaction triggering, liquefaction settlement, seismically induced settlement, and lateral spreading, it is necessary to develop a profile of SPT blow counts, CPT q_c-values or shear wave velocities that have been normalized using the effective overburden pressure.

This normalization should be performed using the effective stress profile that existed at the time the SPT, CPT or shear wave velocity testing was performed. Then, those normalized values are held constant throughout the remainder of the analyses, regardless of whether or not the analyses are performed using higher or lower water-table conditions. Although the possibility exists that softening effects due to soil moistening can influence CRR results if the water table fluctuates, it is commonly assumed that the only effect that changes in the water table have on the results is due to changes in the effective overburden stress.

Raw, field N-values (or q_c-values) obtained under one set of groundwater conditions should not be input into an analysis where they are then normalized using C_N correction factors based on a new (different) water table depth.

Overburden Corrections for Differing Fill Conditions

Approach fills and other increases in overburden pressure should be handled similar to that described above for changes in groundwater location. It is necessary to develop a profile of SPT blow counts or CPT q_c-values that have been normalized using the effective overburden pressure existing before the fill is placed. Then, these normalized values are held constant throughout the remainder of the analyses, regardless of whether or not the analyses are performed using a deeper fill.

Although the overburden effects of the fill will modify the effective stress condition and could change the SPT, CPT or shear wave velocity re-

tor defining the reduction in CSR with depth is usually adopted for routine engineering practice, as shown in Figure D.2.4-5. As an alternative, a site-specific response analysis of the ground motions can be performed, as mentioned in the next section.

sults, it is commonly assumed that these effects will be minor.

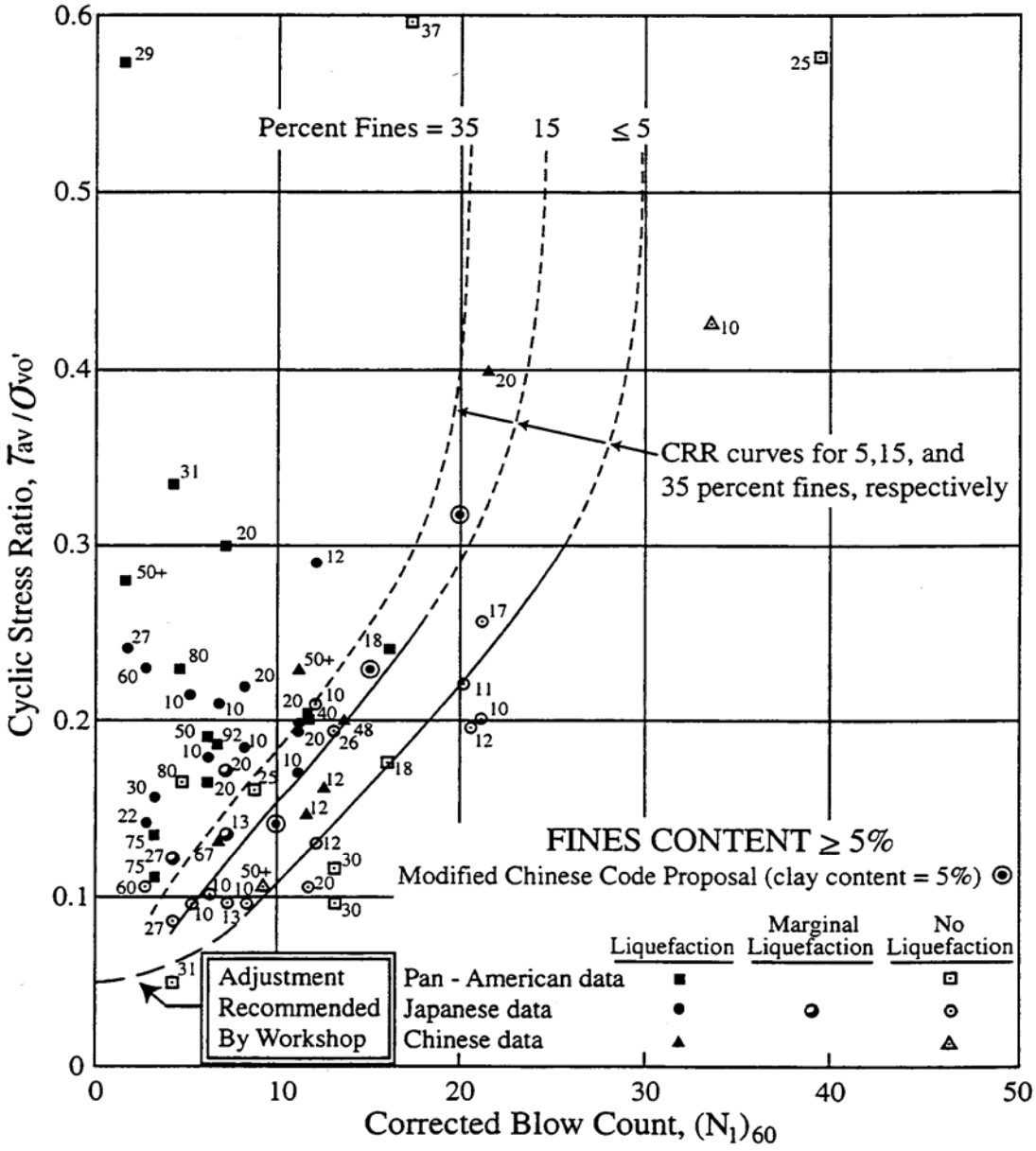

Figure D.2.4-1 Simplified Base Curve Recommended for Determination of CRR from SPT Data for Magnitude 7.5 Earthquakes, with Empirical Liquefaction Data (after Youd and Idriss, 1997)

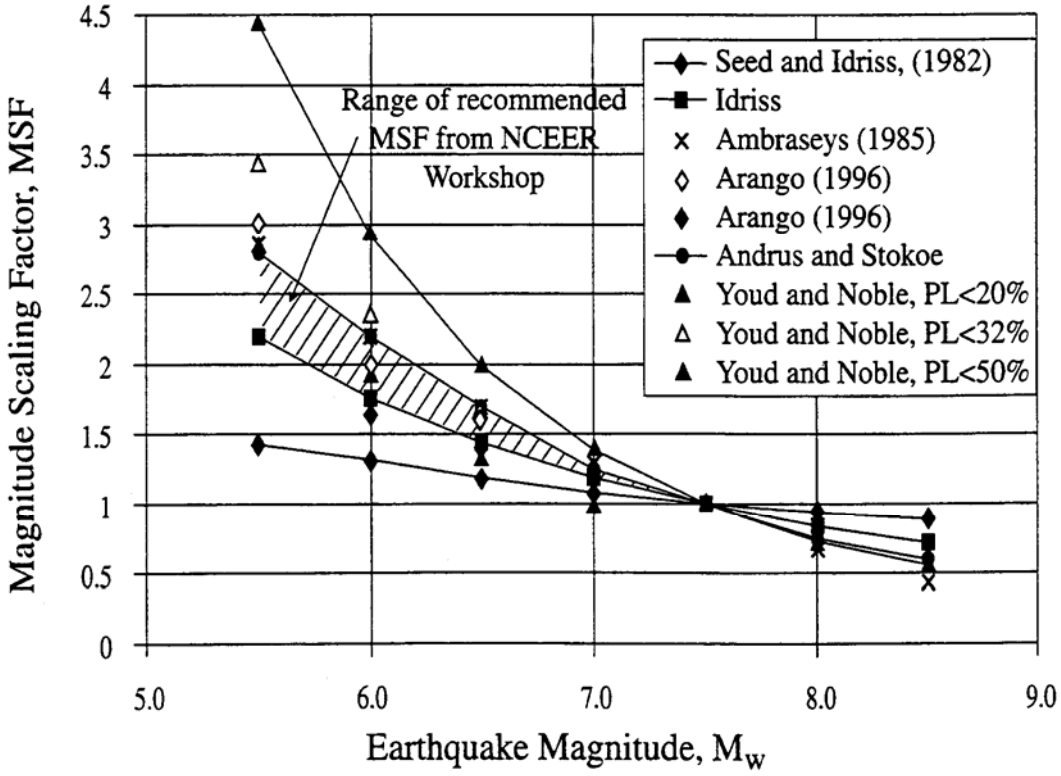

Figure D.2.4-2 Magnitude Scaling Factors derived by Various Investigators (after Youd and Idriss, 1997)

CSR is calculated using the following equation:

$$CSR = (\tau_{av}/\sigma'_{vo}) = 0.65(a_{max}/g)(\sigma_{vo}/\sigma'_{vo})r_d$$

where τ_{av}/σ'_{vo} is the earthquake-induced shearing stress, a_{max}/g is the PGA at the ground surface, σ_{vo}/σ'_{vo} is the ratio of total overburden stress to effective overburden stress, and r_d is a soil flexibility number.

Liquefaction Potential

Once values of CRR and CSR are established for a soil stratum at a given depth, the factor of safety against liquefaction (i.e., FS = CRR/CSR) can be computed. The ratio of CRR to CSR should be greater than 1.0 to preclude the development of liquefaction. As the ratio drops below 1.0, the potential for liquefaction increases. Even when the ratio of CRR to CSR is as high as 1.5, increases in porewater pressure can occur. The potential consequences of these increases should be considered during design.

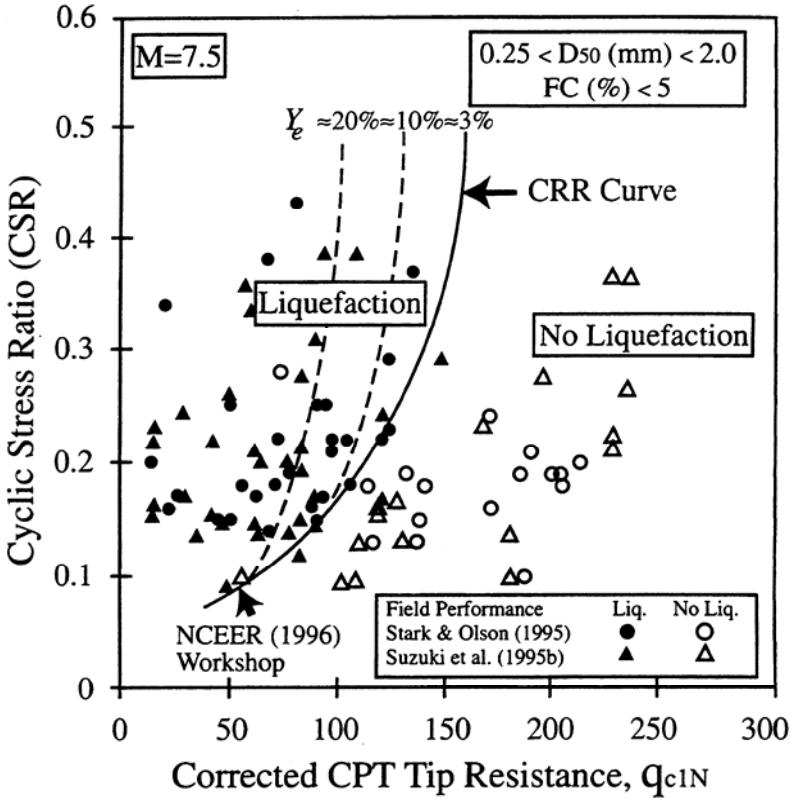

Figure D.2.4-3 Curve Recommended for Calculation of CRR from CPT Data, with Empirical Liquefaction Data

D.2.4.2 Numerical Modeling Methods

For critical projects, the use of equivalent linear or non-linear site specific, one-dimensional ground response analyses may be warranted to assess the liquefaction potential at a site. For these analyses, acceleration time histories representative of the seismic hazard at the site are used to define input ground motions at an appropriate firm-ground interface at depth.

One common approach is to use the equivalent linear total stress computer program SHAKE (Idriss and Sun, 1992) to determine maximum earthquake-induced shearing stresses at depth for use with the simplified procedure described above, in lieu of using the mean values of r_d shown in Figure D.2.4-5. Another alternative involves the use of nonlinear, effective stress methods, such as with the computer program DESRA 2 (Lee and Finn,1978) or DESRA-MUSC (Martin and Qiu, 2000), a modified version of DESRA 2.

CD.2.4.2 Numerical Modeling Methods

In general, equivalent linear analyses are considered to have reduced reliability as ground shaking levels increase to values greater than about 0.4g in the case of softer soils, or where maximum shearing strain amplitudes exceed 1 to 2%. For these cases, true non-linear site response programs should be used, where non-linear shearing stress-shearing strain models (including failure criteria) can replicate the hysteric soil response over the full time history of earthquake loading. The computer program DESRA 2, originally developed by Lee and Finn (1978), was perhaps the first of the widely recognized non-linear, one-dimensional site response program. Since the development of DESRA 2, a number of other non-linear programs have been developed, including MARDES (Chang et al., 1991), D-MOD (Matasovic, 1993) and SUMDES (Li et al., 1992), and DESRA-MUSC (Martin and Qiu, 2000).

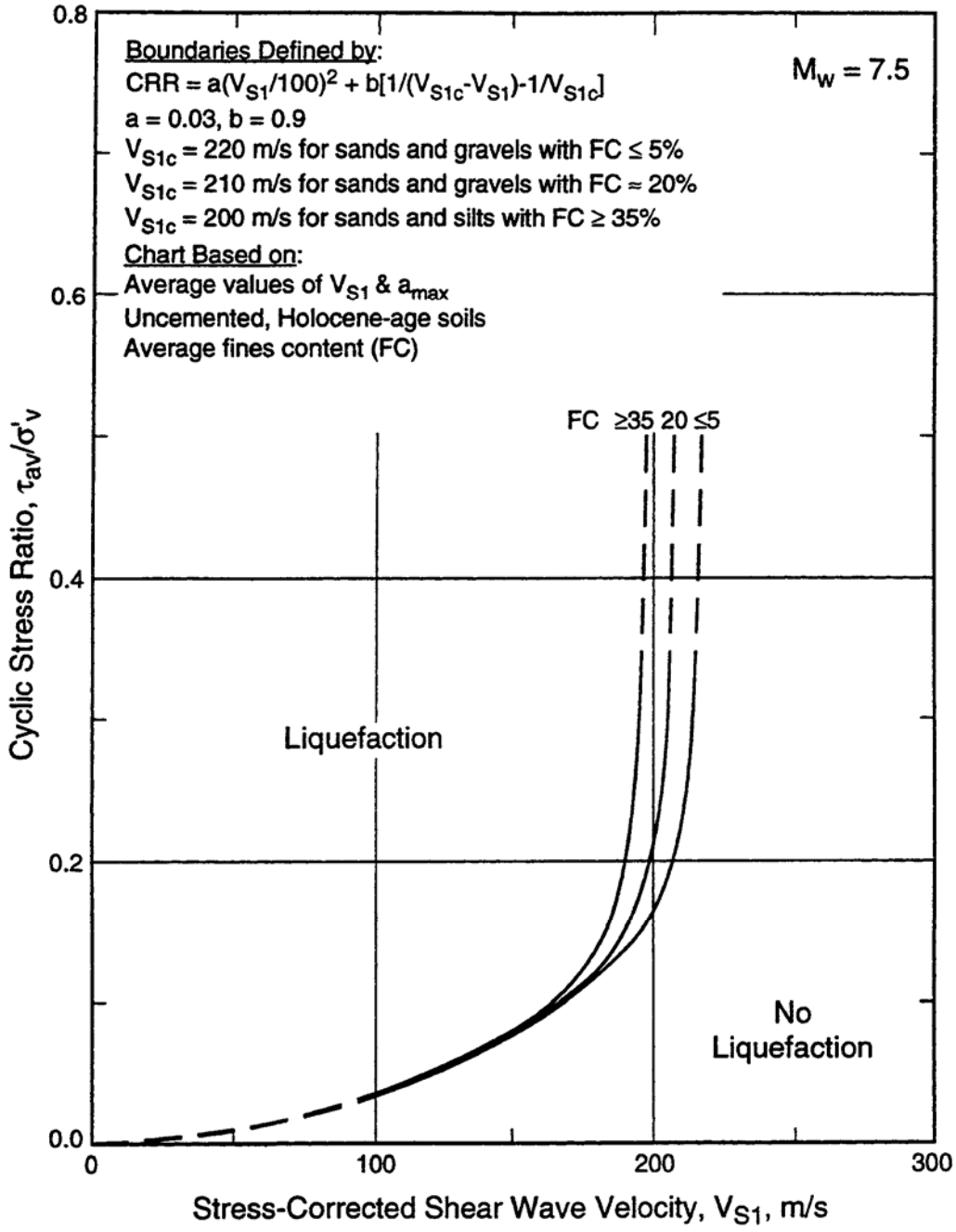

Figure D.2.4-4 Recommended Liquefaction Assessment Chart Based on V_{s1} and CSR for Magnitude 7.5 Earthquakes and Uncemented Soils of Holocene Age

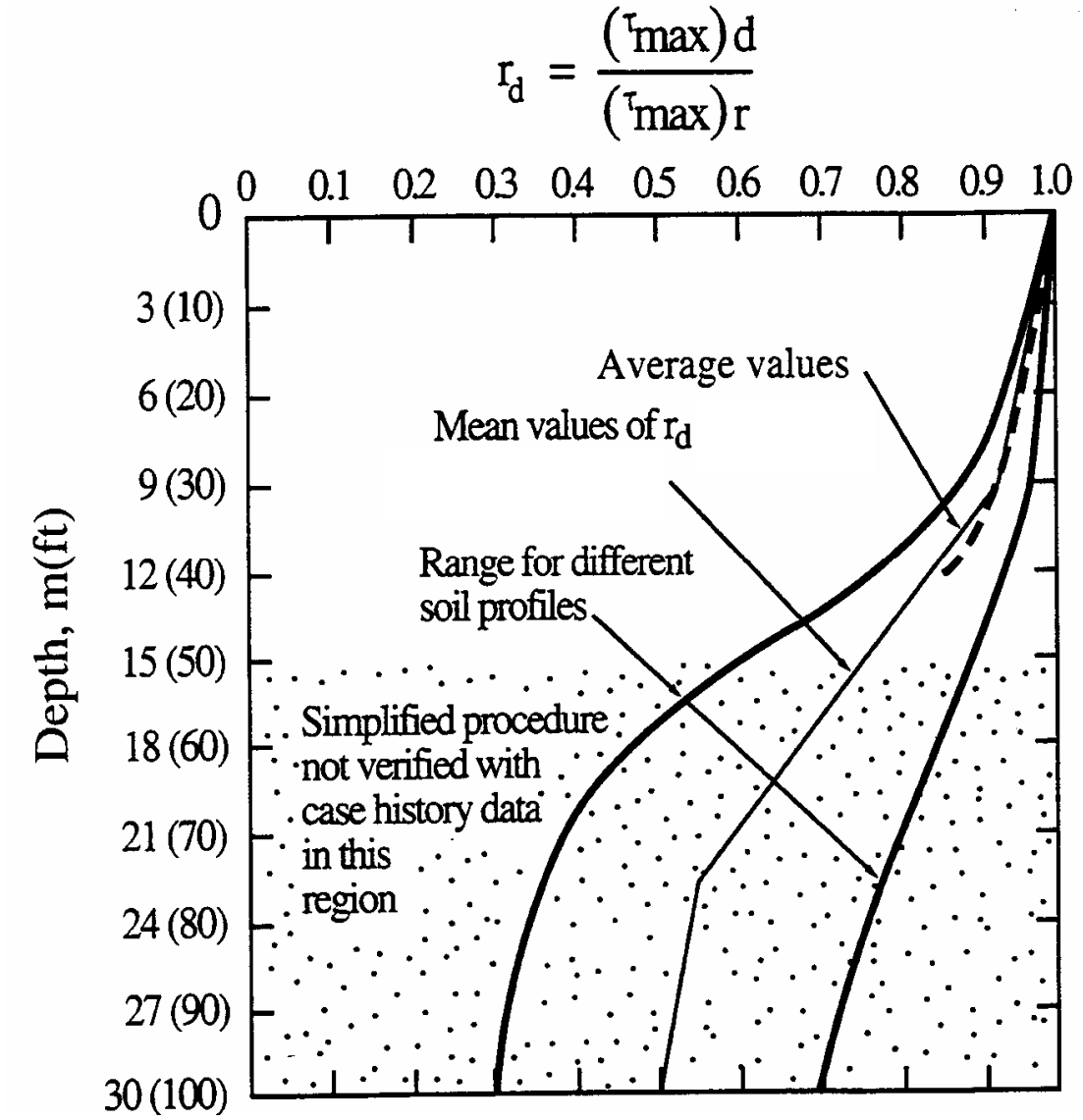

Figure D.2.4-5 Soil Flexibility Factor (rd) versus Depth Curves Developed by Seed and Idriss (1971) with Added Mean Value Lines (after Youd and Idriss, 1997)

D.2.5 Liquefaction Hazards Assessment

Results of the liquefaction assessment are used to evaluate the potential severity of three liquefaction-related hazards to the bridge:

- Flow failures that involve large translational or rotational slope failures mobilized by existing static stresses (i.e., the site static factor of safety drops below 1.0 due to low strengths of liquefied soil layers).
- Limited lateral spreads that involve a progressive accumulation of deformations during

CD.2.5 Liquefaction Hazards Assessment

The factor of safety from the liquefaction analysis can be used to determine if a more detailed evaluation of these hazards is warranted. No single factor of safety value can be cited in a guideline, as considerable judgment is needed in weighing the many factors involved in the decision. A number of those factors are noted below:

- The type of structure and its vulnerability to damage. Structural mitigation solutions may be more economical than ground remediation.

ground shaking with eventual deformations that can range from a fraction of a meter to several meters.

- Ground settlement.

The potential for these hazards can be determined initially on the basis of the factor of safety calculated from the ratio of CRR to CSR. If the ratio is less than 1.0 to 1.3, the hazard should be evaluated following the guidelines given below, unless agreed otherwise by the owner.

- Levels of risk accepted by the owner regarding design for life safety, limited structural damage, or essentially no damage.
- Damage potential associated with the particular liquefaction hazards. Flow failures or major lateral spreads pose more damage potential than differential settlement. Hence, factors of safety could be adjusted accordingly.
- Damage potential associated with design earthquake magnitude. A magnitude 7.5 event is potentially far more damaging than a 6.5 event.
- Damage potential associated with SPT values, i.e., low blow counts have a greater cyclic strain potential than higher blow counts.
- Uncertainty in SPT- or CPT- derived liquefaction strengths used for evaluations. Note that a change in silt content from 5 to 15% could change a factor of safety from say 1.0 to 1.25.
- For high levels of design ground motion, factors of safety may be indeterminate. For example, if $(N_1)_{60}$ = 20, M = 7.5 and fines content = 35% liquefaction strengths cannot be accurately defined due to the vertical asymptote on the empirical strength curve.

In addition a change in the required factor of safety from 1.0 to 1.25 often only makes minor differences in the extent of liquefiable zones, albeit it would increase the blow count requirements for ground remediation. However, for the example cited, the additional costs of remediation from $(N_1)_{60}$ = 20 to $(N_1)_{60}$ = 25 say, could be small.

The final choice of an appropriate factor of safety must reflect the particular conditions associated with a specific site and the vulnerability of site-related structures.

D.2.5.1 Lateral Flows

Flow failures are the most catastrophic form of ground failure that may be triggered when liquefaction occurs. These large translational or rotational flow failures are mobilized by existing static stresses when average shearing stresses on potential failure surfaces exceed the average residual strength developing in the liquefied soil.

To assess the potential for flow failure, the static strength properties of the soil in a liquefied layer is replaced with the residual strength determined from Figure D.2.5-1. A conventional slope stability check is then conducted. No seismic coef-

CD.2.5.1 Lateral Flows

Valuable commentary on this problem may be found, for example, in publications by NRC (1985), Seed (1987), Seed and Harder, (1990), Dobry (1995), and Kramer (1996). The topic of Post-Liquefaction Shear Strength of Granular Soils was also the subject of an NSF-sponsored NCEER Workshop at the University of Illinois in 1997, a summary of which has been published by Stark et al. (1998). The complexities of the problem have also been illustrated in centrifuge tests, as described by Arulandan and Zeng (1994) and Fiegel and Kutter (1994).

ficient is used during this evaluation, thus representing conditions after the completion of the earthquake. The resulting factor of safety defines the potential for flow failures. If the factor of safety is less than 1.0, lateral flow is predicted.

The estimation of deformation associated with lateral flow cannot be easily made. The deformations can be in excess of several meters, depending on the geometry of the flowing ground and the types and layering of soil. In the absence of reliable methods for predicting deformations, it is usually necessary to assume that the soil will undergo unlimited deformations. If the loads imposed by these movements exceed those that can be tolerated by the structure, some type of ground remediation will likely be required. This situation should be brought to the attention of the owner and a strategy for dealing with the flow problem agreed upon.

The most difficult step in the flow analysis is the determination of the residual strength of the soil. The most common procedure for evaluating the residual strength involves an empirical correlation between SPT blow counts and apparent residual strength back-calculated from observed flow slides. This relationship is shown in Figure D.2.5-1. Mean or lower-bound values in the data range shown are often adopted. Some experimental work suggests that residual strength is related to confining pressure (Stark and Mesri, 1992). Steady state undrained shear strength concepts based on laboratory tests have also been used to estimate post liquefaction residual strengths (Poulos et al., 1985; Kramer, 1996). Due to the difficulties of test interpretation and corrections for sample disturbance, empirically based correlations are normally used.

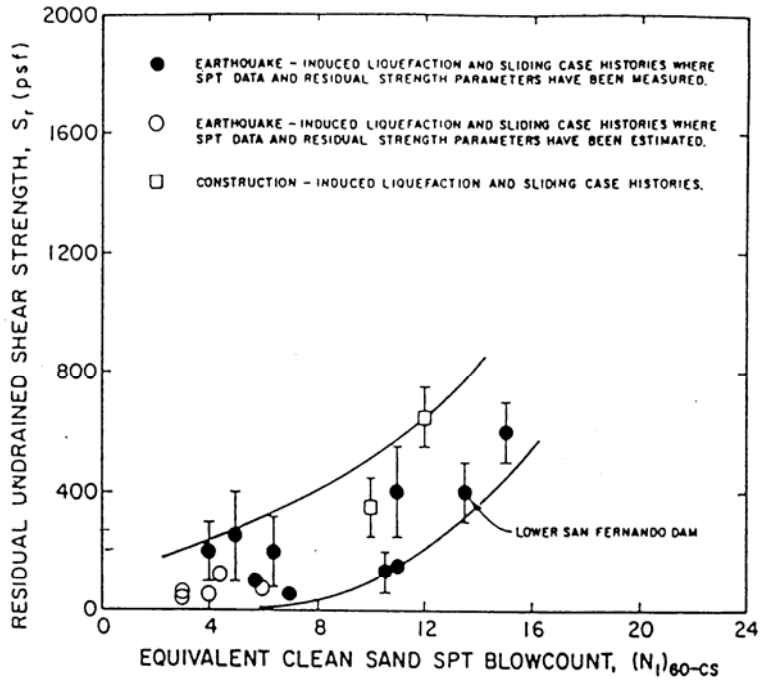

RECOMMENDED FINES CORRECTION FOR S_R EVALUATION USING SPT DATA

Percent Fines	N_{corr} (blows/ft)
10%	1
25%	2
50%	4
75%	5

Figure D.2.5-1 Relationship between Residual Strength (S_r) and Corrected "Clean Sand" SPT Blowcount $(N_1)_{60}$ from Case Histories (after Seed and Harder, 1990)

D.2.5.2 Lateral Spreading

The degradation in undrained shearing resistance arising from liquefaction can lead to limited lateral spreads induced by earthquake inertial loading. Such spreads can occur on gently sloping ground or where nearby drainage or stream channels can lead to static shearing stress biases on essentially horizontal ground (Youd, 1995).

Four general approaches can be used to assess the magnitude of the lateral spread hazard:

- *Youd Empirical Approach:* Using regression analyses and a large database of lateral spread case histories from past earthquakes, Bartlett and Youd (1992) developed empirical equations relating lateral-spread displacements to a number of site and source parameters. A refined version of this approach was recently presented by Youd et al. (1999). Generally, this approach should be used only for screening of the potential for lateral spreading, as the uncertainty associated with this method of estimating displacement is generally assumed to be too large for bridge design.
- *Newmark Time History Analyses:* The simplest of the numerical methods is the so called Newmark sliding block analysis, (Newmark, 1965; Kramer, 1996), where deformation is assumed to occur on a well-defined failure plane and the sliding mass is assumed to be a rigid block. This approach requires (1) an initial pseudo-static stability analysis to determine the critical failure surface and associated yield acceleration coefficient (k_y) corresponding to a factor of safety of 1.0, and (2) a design earthquake acceleration record at the base of the sliding mass. Cumulative displacements of the sliding mass generated when accelerations exceed the yield acceleration are computed using computer programs such as described by Houston et al. (1987). These methods are most appropriate when local site effects modify the ground motion as it propagates though the soil profile and when the database for the chart method described below is not adequate. This latter consideration generally involves sites where the source mechanism will be from a magnitude 8 or higher event.
- *Simplified Newmark Charts:* Charts have been developed by a number of individuals

CD.2.5.2 Lateral Spreading

The lateral spreading mechanism is a complex process involving the post-liquefaction strength of the soil, coupled with the additional complexities of potential porewater pressure redistribution and the nature of earthquake loading on the sliding mass. At larger cyclic shearing strains, the effects of dilation can also significantly increase post-liquefaction undrained shearing resistance of the liquefied soil. Incremental permanent deformations will still accumulate during portions of the earthquake load cycles when low residual resistance is available. Such low resistance will continue even while large permanent shearing deformations accumulate through a ratcheting effect. These effects have recently been demonstrated in centrifuge tests to study liquefaction-induced lateral spreads, as described by Balakrishnan et al. (1998). Once earthquake loading has ceased, the effects of dilation under static loading can mitigate the potential for a flow slide.

The four methods available for estimating deformations from lateral spreading account for this complex process in varying degrees.

The Youd Empirical Approach

The Youd empirical approach uses a variety of earthquake parameters, including magnitude, geometry, and soil grain size in an empirical equation to estimate displacement. Two cases, a sloping ground model and a free-face model, are used. This prediction method is the least reliable in the small displacement range with the level of accuracy probably no better than 1 m. However, it does allow a relatively straightforward screening to be accomplished to identify the potential severity of lateral spreads. Several research projects are also presently in progress to enhance these empirical prediction models by improvements in approaches used in the regression analysis and the use of a larger database.

Newmark Time History Analyses

The Newmark method has been used extensively to study earthquake-induced displacements in dams (e.g., Makdisi and Seed, 1978) and natural slopes (e.g., Jibson, 1993). This approach involves the double integration of earthquake records above the yield acceleration. The yield acceleration (k_y) is determined by finding the seismic coefficient that causes the factor of safety in a slope stability assessment to be 1.0. During the stability analyses,

(Franklin and Chang, 1977; Hynes and Franklin, 1984; Wong and Whitman, 1982; and Martin and Qiu, 1994) using large databases of earthquake records and the Newmark Time History Analysis method. These charts allow deformations during seismic loading to be estimated using relationships between the acceleration ratio (i.e., ratio of yield acceleration (k_y) to the peak ground acceleration (k_{max}) occurring at the base of the sliding mass) to ground displacement. The Martin and Qiu (1994) charts are recommended in this Appendix, as they include peak ground acceleration and peak ground velocity as additional regression parameters. This method does not include earthquake magnitude. Martin and Qiu note that magnitude was not a statistically significant parameter for the range of magnitudes (M6 to M7.5) used in their evaluation.

- *Numerical Modeling:* The most rigorous approach to assessing liquefaction-induced lateral spread or slope deformations entails the use of dynamic finite element / finite difference programs coupled with effective stress based soil constitutive models. However, the use of such programs is normally beyond the scope of routine bridge design projects. Finn (1991) gives a summary of such approaches, and a recent case history has been described by Elgamel et al. (1998).

The decision between use of the Youd empirical approach and any one of several charts or numerical models will depend on a number of factors, including the level of seismic loading and the consequences of failure. Normally, the Youd empirical approach should be used only for screening of the potential for lateral spreading, as the uncertainty associated with this method of estimating displacements is generally assumed to be large. Although charts and numerical methods offer the capability of estimating displacements more accurately, these methods are often limited by the methods of characterizing the boundary conditions for the problem and on the selection of material properties. Extreme care must be exercised when any of these methods are used.

If lateral spreading is anticipated at a site, the geotechnical engineer should meet with the owner and decide what approach offers the most appropriate method of estimating the magnitude of lateral spread.

the liquefied layer is modeled with the residual strength of the soil. Other layers with partial buildup in porewater pressure can al-so be degraded in strength during the evaluation.

The earthquake records must be selected from the available catalogue of records, such that they are representative of the source mechanism, magnitude, and distance for the site. A minimum of three records from three independent earthquakes should be selected for the Newmark analyses. Often it is necessary to modify these records for local site effects, as the ground motion propagates through soil to the base of the sliding block.

A number of uncertainties are inherent in this approach due to the assumptions involved. In particular, for liquefaction-induced lateral spreads, uncertainties include:

- The point in the time history when cyclic strength degradation or liquefaction is triggered.
- The magnitude of the apparent post-liquefaction residual resistance as discussed above.
- The influence of the thickness of liquefied soil on displacement.
- Changes in values of yield acceleration (k_y) as deformations accumulate.
- The influence of a non-rigid sliding mass.
- The influence of ground motion incoherence over the length of the sliding mass.

Simplified Newmark Charts

The simplified chart correlations were developed by conducting Newmark analyses on a large number of earthquake records and then statistically analyzing the results. Of the various chart methods, the Martin and Qiu (1994) method is recommended for use on bridge design projects. Figure D.2.5-2 and Figure D.2.5-3 show the relationships developed by Martin and Qiu (1994). A velocity-to-acceleration ratio of 60 is used if the epicentral distance is less than 15 km; a velocity-to-acceleration ratio of 30 is used for distances greater than 30 km; and values are interpolated between these distances. These figures are appropriate for magnitudes between 6 and 7.5. If magnitudes exceed 7.5, the deformation should be determined using other methods, such as by conducting Newmark time history analyses or 2-dimensional numerical modeling.

The Franklin and Chang (1977) procedure,

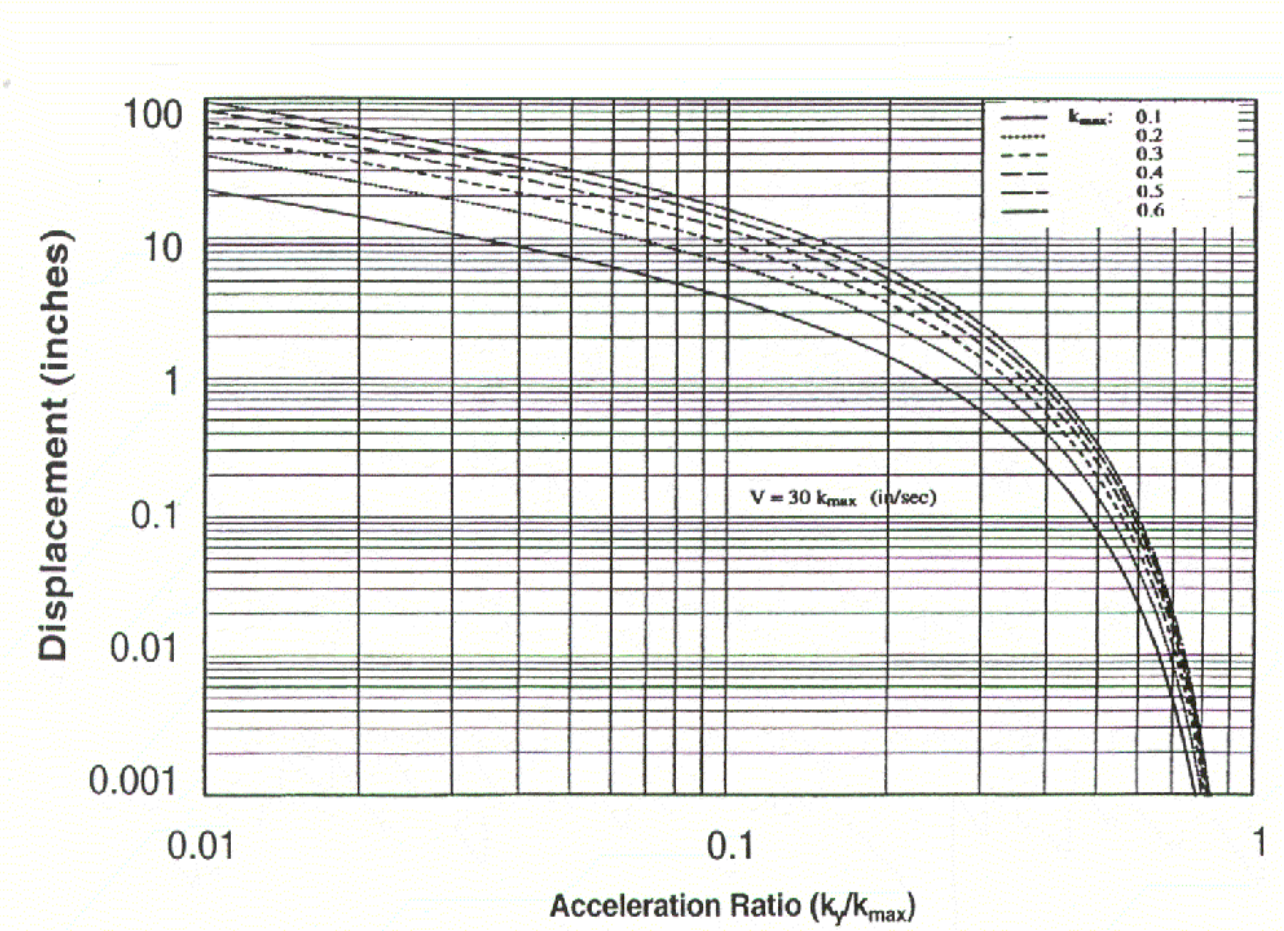

Note: **Displacements less than several inches are shown for presentation purposes only. The accuracy of the predictive method is such that predicted deformations less than several inches should not be used.**

Figure D.2.5-2 Martin and Qiu (1994) Simplified Displacement Chart for Velocity-Acceleration Ratio of 30

which was given in earlier editions of the AASHTO *Standard Specifications for Highway Bridges,* is now thought to overestimate displacements, partly because it was developed by bounding all data and partly because the database had some artificially high records. The Hynes and Franklin (1984) charts used the same database as did Martin and Qiu, and therefore the mean values from the Hynes and Franklin chart are normally similar to the values estimated by the Martin and Qiu method. Wong and Whitman (1982) provides the smallest estimate of displacements, and appears to be unconservative at times.

To use these charts, the yield acceleration is determined by finding the seismic coefficient that causes the factor of safety in a slope stability assessment to be 1.0. As noted for the Newmark Time History Analyses, the liquefied layer is modeled with the residual strength of the soil.

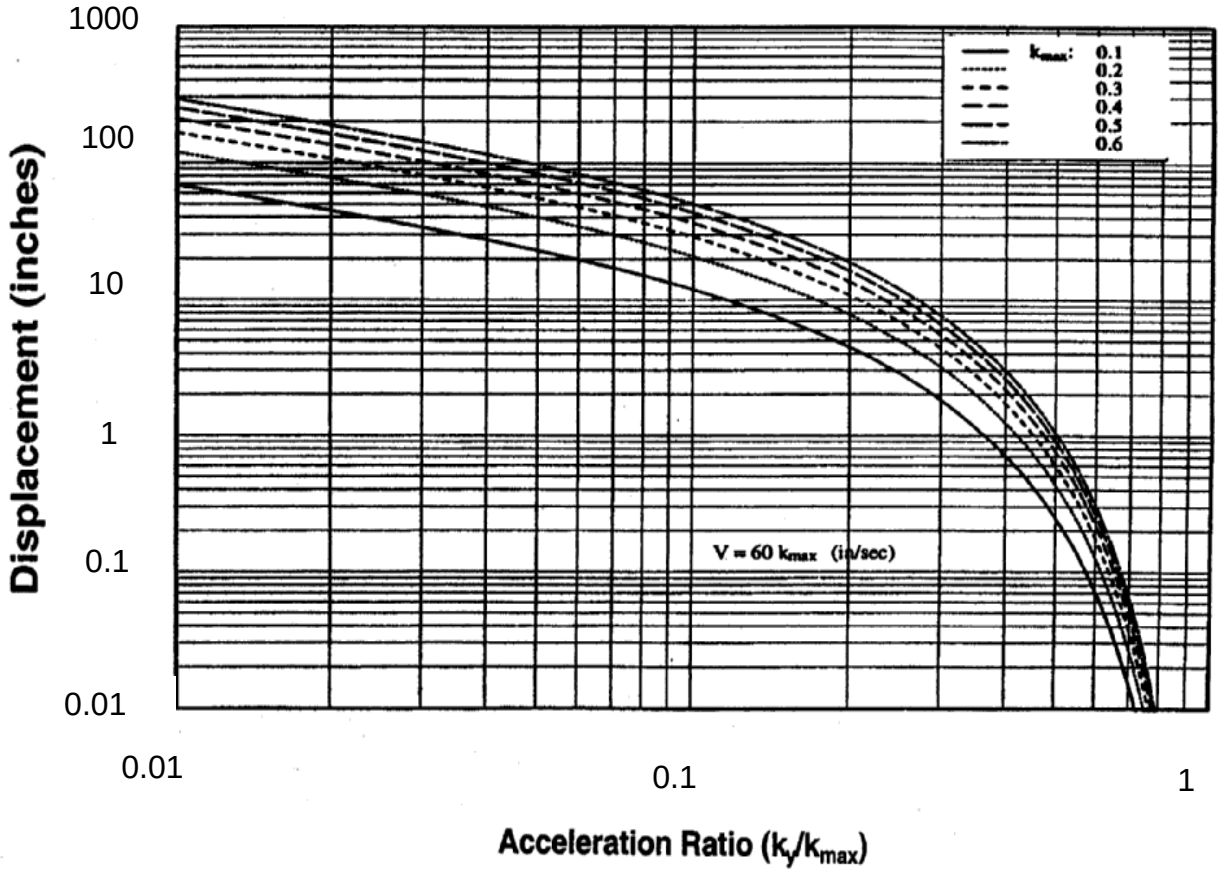

Note: **Displacements less than several inches are shown for presentation purposes only. The accuracy of the predictive method is such that predicted deformations less than several inches should not be used.**

Figure D.2.5-3 Martin and Qiu (1994) Simplified Displacement Charts for Velocity-Acceleration Ratio of 60

Other layers with partial buildup in porewater pressure can also be degraded in strength during the evaluation. With the yield acceleration and the peak ground acceleration at the base of the failure surface (k_{max}), it is a simple matter to enter the chart and determine the estimated amount of displacement.

These simplified chart methods are limited by the database used in their development. Typically few re cords greater than magnitude 7.5 were available for analysis, and therefore, use of the methods for larger magnitudes must be done with caution. Other limitations are similar to those presented for the Newmark Time History Analyses.

Numerical Modeling

Various two-dimensional, nonlinear computer programs have been used to perform these analyses.

For realistic modeling, these programs must be able to account for large displacements, nonlinear soil properties, and changes in effective stress during seismic modeling. One computer program seeing increasing use for this type of modeling is FLAC (Itasca, 1998). This program has been used on a number of bridge-related projects, including the Alaskan Way Viaduct in downtown Seattle, Washington (Kramer et al., 1995).

As with any rigorous modeling method, considerable experience and judgment are required when using a program such as FLAC to model soil-pile-structure interaction during earthquake-induced liquefaction. Good practice when using these methods is to compare the results to results of empirically-based simplified methods or to laboratory experimental data, such as produced in the centrifuge.

D.2.5.3 Settlement

Another consequence of liquefaction resulting from an earthquake is the volumetric strain caused by the excess porewater pressures generated in saturated granular soils by the cyclic ground motions. The volumetric strain, in the absence of lateral flow or spreading, results in settlement. Liquefaction-induced settlement could lead to collapse or partial collapse of a structure, especially if there is significant differential settlement between adjacent structural elements. Even without collapse, significant settlement could result in damage.

In addition to the settlement of saturated deposits, the settlement of dry and/or unsaturated granular deposits due to earthquake shaking should also be considered in estimating the total seismically induced settlements.

CD.2.5.3 Settlement

The Tokimatsu and Seed (1987) procedures for both saturated and dry (or unsaturated) sands is the most common of the procedures currently used to estimate the magnitude of settlement. Figure D.2.5-4 shows the relationship between the cyclic stress ratio (τ_{av}/σ'_o) and volumetric strain for different values of $(N_1)_{60}$. It should also be noted that the settlement estimates are valid only for level-ground sites that have no potential for lateral spreading. If lateral spreading is likely at a site and is not mitigated, the settlement estimates using the Tokimatsu and Seed method will likely be less than the actual values.

The settlement of silty sand and silt requires adjustments of the cyclic strength for fines content. Ishihara (1993) recommends increasing the cyclic shear strength of the soils if the Plasticity Index (PI) of the fines is greater than 10. This increases the factor of safety against liquefaction and decreases the seismically-induced settlement estimated using the Ishihara and Yoshimine procedure. Field data suggest that the Tokimatsu and Seed procedure without correcting the SPT values for fines content could result in overestimation of seismically-induced settlements (O'Rourke et al., 1991; Egan and Wang, 1991). The use of an appropriate fines-content correction will depend on whether the soil is dry/unsaturated or saturated and if saturated whether it is completely liquefied (i.e., post-liquefaction), on the verge of becoming liquefied (initial liquefaction), or not liquefied. SCEC (1999) suggests that for 15% fines, the SPT correction value ranges from 3 to 5 and for 35% fines

it ranges from 5 to 9.

Although the Tokimatsu and Seed procedure for estimating liquefaction- and seismically-induced settlements in saturated sand is applicable for most level-ground cases, caution is required when using this method for stratified subsurface conditions. Martin et al. (1991) demonstrated that for stratified soil systems, the SPT-based method of liquefaction evaluation outlined by Seed et al. (1983) and Seed et al. (1985) could over-predict (conservative) or under-predict (unconservative) excess porewater pressures developed in a soil layer depending on the location of the soil layer in

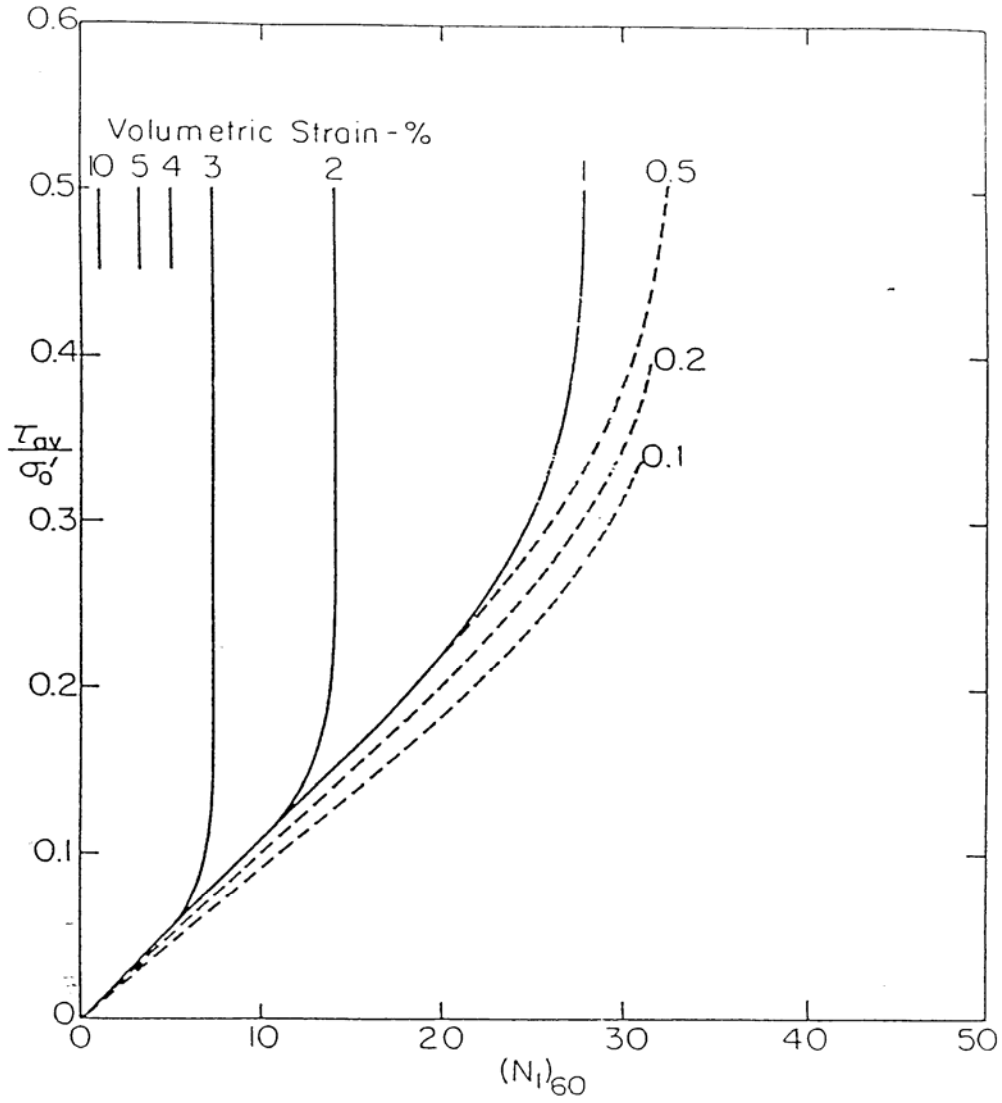

Figure D.2.5-4 Relationship Between Cyclic Stress Ratio, $(N_1)_{60}$ and Volumetric Strain for Saturated Clean Sands and Magnitude = 7.5 (after Tokimatsu and Seed, 1987)

the stratified system. Given the appropriate boundary conditions, Martin et al. (1991) shows that thin, dense layers of soils could liquefy if sandwiched between liquefiable layers. For this situation the estimated settlement using the Tokimatsu and Seed procedure (which is based on the SPT values and excess porewater pressures generated in the individual sand layers) therefore, may be over-predicted or under-predicted.

The Tokimatsu and Seed (1987) method can be used to estimate settlement in layered deposits by accounting for settlement of non-liquefiable layers. One approach to estimate the settlement of such a non-liquefiable soil layer is to use Figure D.2.5-4 in combination with Figure D.2.5-5 to determine if the layer will be affected by the layer

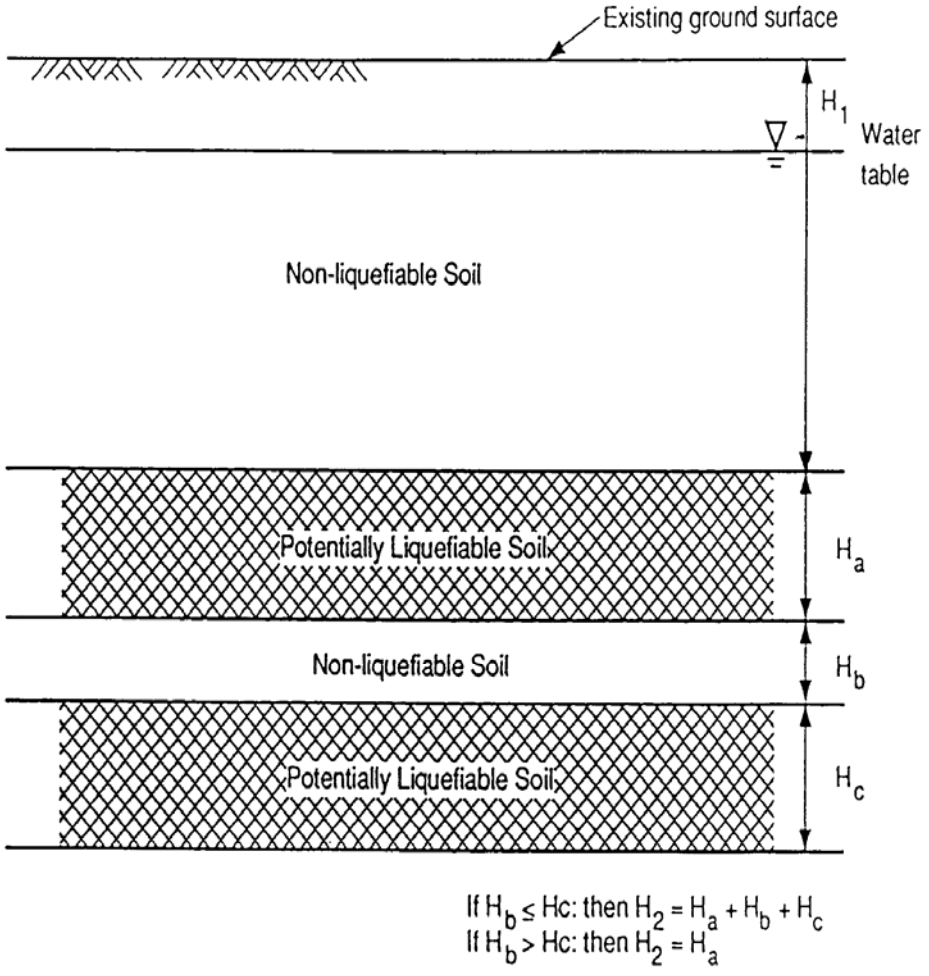

Figure D.2.5-5 Schematic Diagram for Determination of H_1 and H_2 (after Ishihara, 1985)

below. If $H_c > H_b$, then the settlement of the nonliquefied layer can be estimated by assuming that the volumetric strain in the layer will be approximately 1.0% (1.0% seems to be the volumetric strain corresponding to initial liquefaction), given that the non-liquefiable layer (H_b) meets all of the following criteria:

- Thickness of the layer is less than or equal to 1.5 m.
- Corrected SPT value $(N_1)_{60}$ less than 30 or CPT tip resistance normalized to 100 kPa (q_{c1N}) less than 160.
- Soil type is sand or silty sand with fines content less than or equal to 35%.
- Magnitude of design earthquake is greater than or equal to 7.0.

The logic for using these four criteria is that the migration of porewater pressure and subsequent settlement of the non-liquefiable layer depends on factors such as the thickness, density (SPT or CPT tip value), and permeability (soil type) of the layer and the duration of earthquake shaking (magnitude). It should be noted that the criteria are only guidelines to allow the Designer to be aware of the potential settlement contributions from certain non-liquefiable soil layers present in a layered system.

D.3 Other Collateral Hazards

The potential risk to bridges located in SDR 3 and higher from collateral hazards not associated with liquefaction must also be considered. These other collateral hazards include fault rupture, landsliding, differential compaction, and flooding or inundation.

If the risk of the ground displacement hazard from one or more of these sources is determined to be unacceptable by the owner for the desired performance level, then the hazard should be mitigated through use of ground improvement methods or by selecting an alternative bridge location.

CD.3 Other Collateral Hazards

With the exception of flooding and inundation, these other collateral hazards involve ground displacements. These ground displacement hazards can sometimes be very large, on the order of meters, and quantification of the amount of displacement can be difficult. Detailed geotechnical explorations and analyses are usually required to identify the potential for these displacement hazards and their consequences.

D.3.1 Fault Rupture

Ground displacements generally are expected to reoccur along preexisting fault traces. The development of a new fault or reactivation of a very old (pre-Quaternary) fault is uncommon and gen-

CD.3.1 Fault Rupture

To evaluate the potential hazards of surface fault rupture, a number of evaluations are necessary, including determination of the location of fault traces, the nature and amount of near-surface

erally does not need to be considered for typical bridges. Faults are generally considered active and present a potential risk to a bridge if they have displaced in the past 11,000 years. Bridges should not be constructed across active faults, unless specialized studies are performed to quantify the amount of potential fault movement and to determine the consequences of this movement to the bridge.

deformations, and the history of deformations. Maps showing the location of active faults have been developed by many state geological agencies and by the United States Geological Survey. The potential amount of movement can be estimated from empirical relationships between magnitude of the seismic event on the fault and displacement (e.g., Wells and Coppersmith, 1994).

The evaluation of fault displacement involves skills and techniques not commonly used in geotechnical or geologic investigations, and therefore should be done by an individual or organization with specific expertise in making these estimates. The owner must consider the uncertainty in these estimates and the consequences of incorrect estimates when deciding whether to locate a bridge across a fault.

D.3.2 Landsliding

Earthquake-induced landsliding represents a significant hazard to roadways in seismically active areas, and can be a hazard to bridges. Damage can be in the form of ground movement either at the abutment or extending to the central piers of a bridge. Sites that are most susceptible to earthquake-induced landslides include locations with slopes of 18 degrees or greater, or a history of rock falls, avalanches, or debris torrents.

CD.3.2 Landsliding

Pseudo-static stability methods are often used to evaluate the potential for landsliding at soil sites (in the absence of liquefaction). These methods involve conducting slope stability analyses using a seismic coefficient equal to two-thirds to one-half the predicted peak ground acceleration. Conditions are normally considered acceptable if the computed factor of safety under the imposed loads is 1.0 or higher. If the factor of safety is less than 1.0, a sliding block analysis using the Newmark (1965) method, as discussed in Article D.2.5.2, is conducted to estimate the magnitude of displacement during the landslide. A detailed discussion of seismic-induced landslides is presented in MCEER (2000).

Where cliffs or steep slopes occur, earthquake-induced rock fall hazards may exist. The Colorado Rock Fall Simulation Program (Pfeiffer and Higgins, 1991) can be used to evaluate the potential danger from this mechanism.

Numerous more rigorous two- and three-dimensional computer methods, which model the nonlinear response of the soil or rock, can be used to investigate the potential for landsliding, pending the owner's approval. In some cases these more rigorous methods may be the only reasonable method for making the evaluation.

D.3.3 Differential Compaction

Loose cohesionless soil above the water table will tend to densify during the period of earthquake ground shaking. This potential should be considered when evaluating the potential for dif-

CD.3.3 Differential Compaction

Procedures describe by Tokimatsu and Seed (1987) can be used to estimate the amount of settlement. The Tokimatsu and Seed procedure for estimating seismically-induced settlements in dry

ferential displacement between the bridge abutment and the closest central pier or between central piers in a multi-pier bridge.

D.3.4 Flooding or Inundation

Tsunamis and seisches can be triggered by earthquakes, causing wave impact and inundation. Failure of reservoirs or aqueducts, and canals located upslope of the bridge can also result in flooding. With the exception of coastal areas in the western United States, the risk associated with these mechanisms is low for most bridge sites.

D.4 DESIGNING FOR COLLATERAL HAZARDS

Collateral hazards discussion described in previous paragraphs identify methods for quantifying the occurrence of collateral hazards. In most cases it is also possible to quantify the amount of displacement associated with the hazards. These estimates are normally made assuming free-field conditions, and therefore don't consider the effects on or from a bridge structure located on the hazards. In some cases the foundations of the structure will either limit or prevent the amount of predicted displacement. Procedures for evaluating the effects of soil movement are summarized in the following paragraphs. Additional requirements for foundations and abutments are presented in Sections 7 and 8 of these *Guidelines*.

D.4.1 Spread Footing Foundations

Spread footing foundations located above liquefiable layers must consider the potential for loss in bearing support and for liquefaction-induced settlement if liquefaction is predicted below the foundation. Either of these occurrences can result in displacements of the bridge support system that lead to damage of the structure.

(and unsaturated) sand requires that the settlement estimates be multiplied by a factor of 2.0 to account for the effect of multidirectional shaking.

CD.3.4 Flooding or Inundation

For some performance levels in SDR 3, 4, 5, and 6, it may be desirable to confirm that flooding and inundation will not jeopardize the bridge. Maps have been developed for some areas, such as the west coast of the United States, showing areas where tsunami danger exists. Most states also have identified possible areas of inundation from failure of reservoirs.

CD.4 DESIGNING FOR COLLATERAL HAZARDS

The occurrence of a collateral hazard is normally determined by an engineering geologist and a geotechnical engineer. Often results are presented in terms of a factor of safety or an estimated amount of deformation. The bridge designer is then left with the decision on how this information should be used in the selection and design of the bridge foundation system. Too often, little communication occurs between the geotechnical engineer/geologist and the bridge designer regarding the uncertainties and implications associated with the prediction and quantification of the hazard. This approach to seismic design is undesired and not recommended. The best and most efficient design for handling the collateral seismic hazards described above will be achieved only if the geotechnical and bridge engineers work as a team.

CD.4.1 Spread Footing Foundations

The state-of-the-practice for predicting the consequences of liquefaction, whether it is loss in bearing support or settlement, is one of the least precise of the predictions made by geotechnical engineers. This imprecision reflects the complexity of the overall liquefaction mechanisms and the uncertainties on how these will affect a spread footing foundation. For this reason spread footing foundations are normally discouraged if liquefaction is predicted below the footing.

If liquefaction is predicted to occur below a planned spread footing foundation, this potential should be brought to the attention of the owner, and a decision made as to the appropriateness of the spread footing foundation in this particular situation.

D.4.1.1 Loss of Bearing Support for Spread Footings

Liquefaction can cause the loss of bearing capacity beneath spread footing foundations supported on "stable" strata above the liquefiable soils. In view of the possible loss in support, spread footing foundations for bridge structures are not recommended above liquefiable soil layers, except in SDR 1 and SDR 2. For SDR 3 and above the liquefiable layer should be at least two foundation widths below the bottom of the footing. At this depth the induced vertical stress in the soil from the footing is less than 10% of the bearing pressure imposed at the base of the foundation. Even with the low overburden stress increase, the potential for settlement should be determined.

Spread footing foundations typically should not be used when lateral spreading or flow failures that would load the foundations are predicted. In most cases the spread footing will move with the soil, resulting in excessive bending and possible collapse of the column supported by the footing.

CD.4.1.1 Loss of Bearing Support for Spread Footings

Spread footings supporting bridge structures should not normally be used above layers that will liquefy in SDR 3, 4, 5, and 6 because of the potential for loss in bearing capacity and post-earthquake settlement as porewater pressures dissipate. As bearing pressure is lost the foundation will displace downward, likely resulting in differential settlement between column supports. While numerical methods can be used to predict the amount of settlement, the accuracy of the numerical prediction is not usually sufficient to make accurate estimates of distortion between columns. At least part of the difficulty in making these predictions, either numerically or by simple methods, is the inherent variability of soils.

For non-critical spread footing foundations, it is possible to design the footing for the occurrence of liquefaction. For these situations, Ishihara's method of analysis (Ishihara, 1993) for surface manifestation can be used for shallow footings, using the elevation of the bottom of the footing as the top of the surface layer. If Ishihara's criteria cannot be met, consideration should be given to alternative mitigation methods. In the event that an explicit bearing capacity analysis is performed, the undrained residual strength of liquefied layers can be used in assessing the bearing capacity.

If spread footing foundations must be used above liquefiable layers, whether it is for an SDR 3 or an SDR 6 site, another alternative to consider is to improve the ground below the footing using stone columns, compaction grouting, or a similar improvement procedure. The area improved should extend a distance from the footprint of the footing such that liquefaction of surrounding soils will not cause loss in bearing capacity for the footing. Mitchell et al. (1998) provide guidance in designing liquefaction mitigation methods.

D.4.1.2 Settlement of Spread Footing

Settlement of spread footings located above loose granular soils should be quantified using the procedures identified in D.3.3. These evaluations should be made whenever liquefaction is predicted to o2ccur below the footing or, in the case of dry or unsaturated soils that are not expected to liquefy, if the $(N_1)_{60}$ value is less than 30.

Where there are relatively uniform conditions at a site with deep sediments (if demonstrated by the field program), minimum differential settle-

CD.4.1.2 Settlement of Spread Footing

The differential settlement between adjacent columns, or distortion, is normally needed by the structural designer to evaluate effects of settlement on the structure. While differential settlement estimates based on one-half to two-thirds of the total settlement provide an indication of the differential settlement, this approach does not account for location specific soil conditions.

For a location specific estimate, total settlement must be determined at each support location. This

ment of less than one-half of the total settlement may be used in the design. When the subsurface condition varies significantly in lateral directions and/or the thickness of soil deposit (Holocene deposits and artificial fills) varies within the site, a minimum value of one-half to two-thirds of the total settlement is suggested. Once again, it should be noted that the settlement and differential settlement estimates are valid only for level-ground sites that have no potential for lateral spread. If lateral spreading is likely at a site and is not mitigated, the differential settlements could be much greater than the above-suggested values.

D.4.2 Deep Foundations

Deep foundations extending through liquefiable soils will require special consideration. The lateral capacities of piles or drilled shafts may be reduced if the surrounding soils liquefy. Lateral spreading or flow slides can also result in the imposition of significant additional lateral demands on the deep foundations. Liquefaction also can result in settlement of the liquefied strata and the strata above the liquefied strata. This settlement will cause downdrag or negative friction to be imposed on the deep foundations. The potential for these must be addressed for bridges located in SDR 3, 4, 5, and 6.

D.4.2.1 Loss in Lateral Support for Deep Foundations

A well-designed deep foundation should extend beyond the deepest depth of liquefaction. Liquefaction of a layer above the toe of the pile or drilled shaft may have limited effects on the axial capacity of the foundation but can result in loss of lateral support of the pile or drilled shaft. This can reduce the lateral stiffness of the soil-pile system if the loss in lateral support occurs within 10 pile diameters of the bottom of the pile cap or the ground surface. The effects of this loss should be quantified in accordance with procedures given in Article 7.4 or 8.4 of these *Guidelines*.

determination would require a soil boring to establish thickness of layers that could settle, thereby adding to the exploration costs. In the absence of this approach it is suggested that the differential settlement estimates from the one-half to two-thirds factor be used as representative of the minimum differential settlement between adjacent supports. If these settlements are approaching unacceptable levels, a more detailed site investigation should be performed to obtain location specific estimates.

CD.4.2 Deep Foundations

If the effects of liquefaction cannot be adequately accommodated in deep foundation design, consideration should be given to alternative mitigation methods. Liquefaction effects on deep foundations can be mitigated by the implementation of ground improvement techniques prior to, or after deep foundation installation.

CD.4.2.1 Loss in Lateral Support for Deep Foundations

The change in stiffness of a pile or drilled shaft extending through liquefied soil can be determined by conducting a lateral pile analysis using a beam-column-type computer software. Common examples of these software are LPILE+ and COM624. These programs allow modeling of individual layers within the soil profile. Liquefied layers are assigned a residual strength and treated as a cohesive soil. The strain necessary to mobilize 50% of ultimate resistance (ε_{50}) is assumed to be 0.02.

If a cohesionless layer does not liquefy but the factor of safety against liquefaction is less than 1.5, a reduced soil friction angle and a reduced subgrade modulus should be used. It is suggested that the reduced friction angle be taken as 10 degrees for FS of 1.0 and should be interpolated for FS between 1.0 and 1.5. Modulus of subgrade reaction values are reduced in a similar manner with the modulus at FS of 1.0 equal to the modulus of a soft clay.

D.4.2.2 Loads from Lateral Spreading/Flow

If lateral flow or spreading of the ground is predicted during a seismic event, deep foundations that would be loaded by the deforming ground need to designed to withstand the loads from the moving soil. The recommended design approach for evaluating this condition involves the following four steps:

1. Slope stability analyses are conducted to determine the yield acceleration. This step may include the pinning effects of the deep foundation or the increased resistance of soil that has been improved by some type of ground improvement method.
2. Newmark sliding block analyses are performed to estimate displacements of the soil-deep foundation system.
3. The passive force that can ultimately develop ahead of a pile or foundation as soil movement occurs is estimated, and
4. The likely plastic mechanisms that may develop in the foundations and substructure are evaluated.

The rationale behind the proposed method is to determine the likely magnitude of lateral soil movement and assess the ability of the structure to both accommodate this movement and/or potentially limit the movement.

The concept of considering a plastic mechanism in the foundation under the action of spreading forces is tantamount to accepting substantial damage in the foundation. This is a departure from seismic design for vibration alone, and the departure is believed to be reasonable because it is unlikely that the formation of a mechanism in the foundation will lead to structure collapse. The reasoning behind this is that lateral spreading is essentially a displacement-controlled process. Thus the estimated soil displacements represent a limit on the structure displacement, excluding the phenomena of buckling of the piles or shafts below grade and the continued displacement that could be produced by large P-Δ effects. Buckling should be checked, and methods that include the soil residual resistance should be used. Meyersohn, et al. (1992) provide a method for checking buckling as an example. The effects of P-Δ amplification are discussed in this section.

CD.4.2.2 Loads from Lateral Spreading/Flow

A flowchart of the proposed methodology for evaluating spreading is given in Figure D.4.2-1. Key components of this methodology are numbered in the flowchart, and this chart along with the following commentary provide a 'roadmap' to the recommended procedure for lateral spreading resistance design. The primary feature of the proposed methodology is the use of passive piles to restrict the movement of soil and foundations to levels that are tolerable by the structure.

- *Step 1:* The soil layers that are likely to liquefy are identified.
- *Step 2:* A stability analysis is conducted to determine the likelihood of soil movements, and to determine the extent of such movements. This would include the depths of soil likely to move and the plan extent of the likely soil failure block. Assessment of the impacts to a bridge structure can then be made by considering the proximity of the failure block to the foundation system.
- *Step 3:* The maximum displacement of the soil is estimated. This can be accomplished using the simplified Newmark charts or the Newmark Time History Analysis described in Article D.2.5.2. The Designer is permitted to apply more advanced techniques if the benefits justify the additional engineering costs and with the concurrence of the owner. In some cases, substantial improvements and reduction in overall estimated displacements can be achieved.
- *Step 4:* An assessment is made whether soil moves past the foundation, (i.e., foundation is relatively fixed) or movement of the foundation occurs. The assessment requires a comparison between the estimated passive soil forces that can be exerted on the foundation system and the ultimate structural resistance that can be developed by the structure, itself. This assessment requires estimating the forces that can develop if soil is to actually flow around the foundation system and comparing them with the likely resistance the structure will provide. In cases where a crust of non-liquefied material exists at or near the ground surface, the full structural resistance is likely to be less than the movement-induced passive

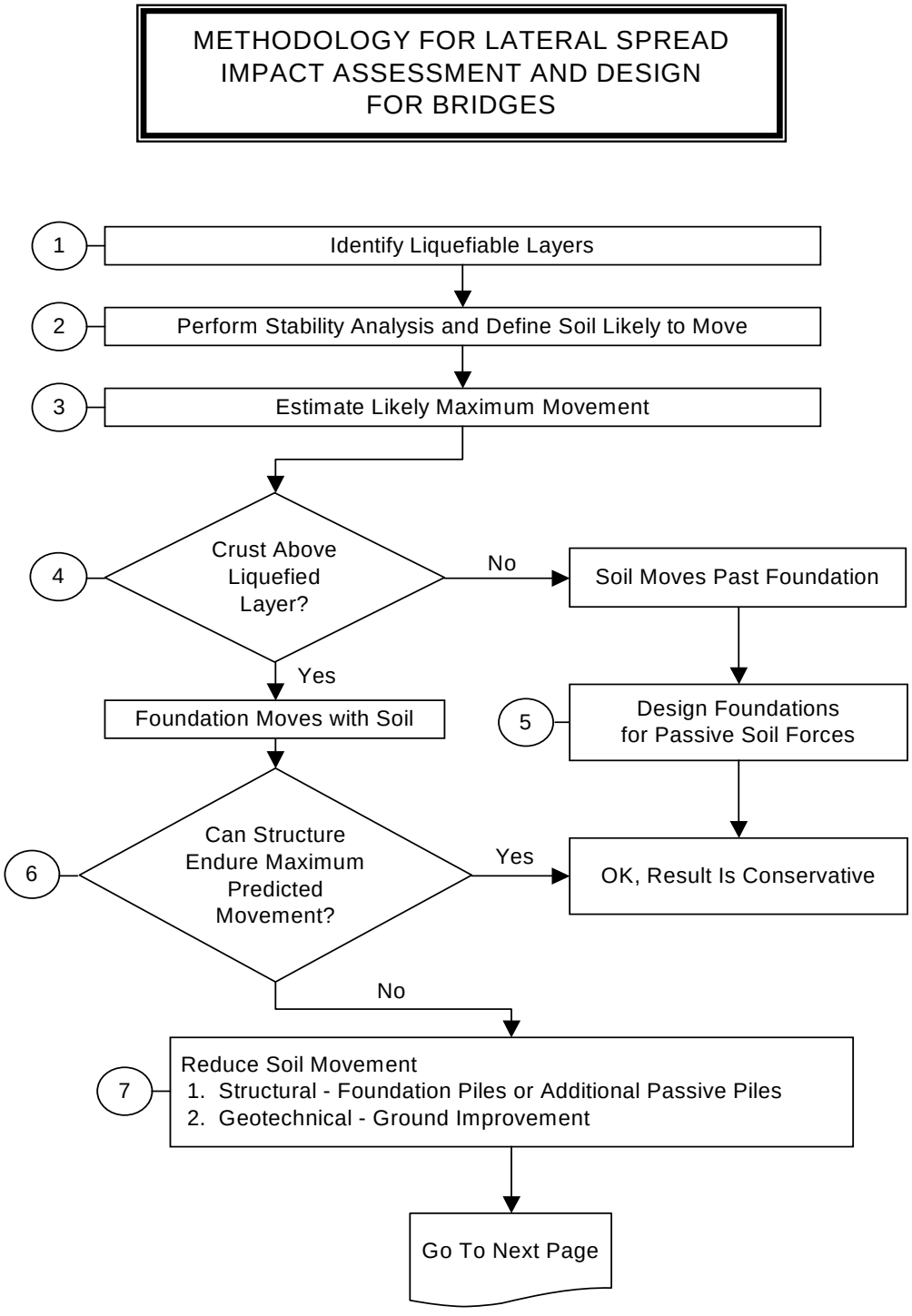

Figure D.4.2-1 Flowchart Showing Process for Evaluating the Effects of Lateral Spread and Flows on a Bridge Foundation

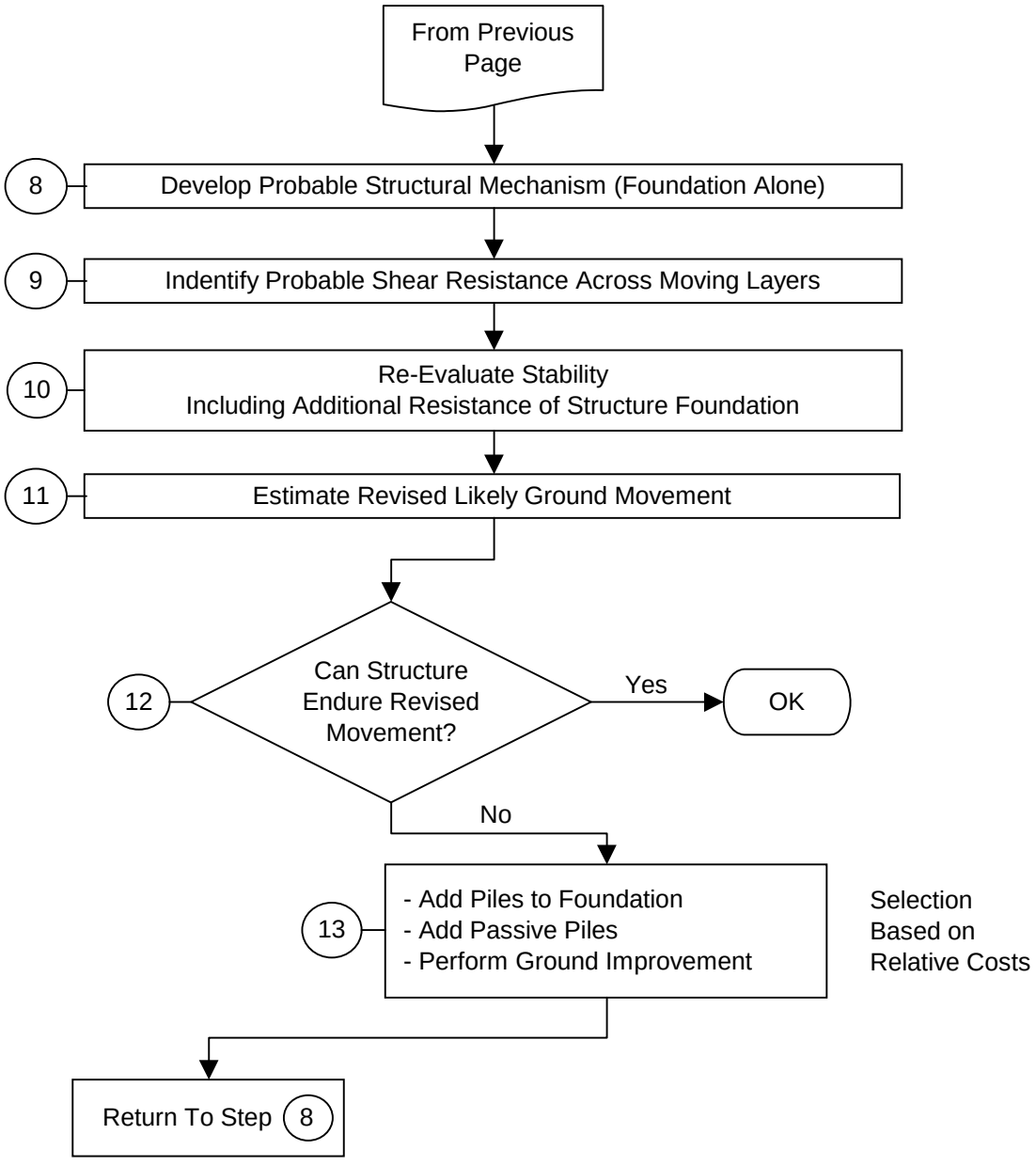

Figure D.4.2-1 Flowchart Showing Process for Evaluating the Effects of Lateral Spread and Flows on a Bridge Foundation (cont.)

forces, and in such cases the foundation is likely to move with the soil. In many cases, it may be immediately obvious which condition, soil or foundation movement, is more likely. Qualitative illustrations of the two scenarios are given in Figure D.4.2-2 and Figure D.4.2-3.

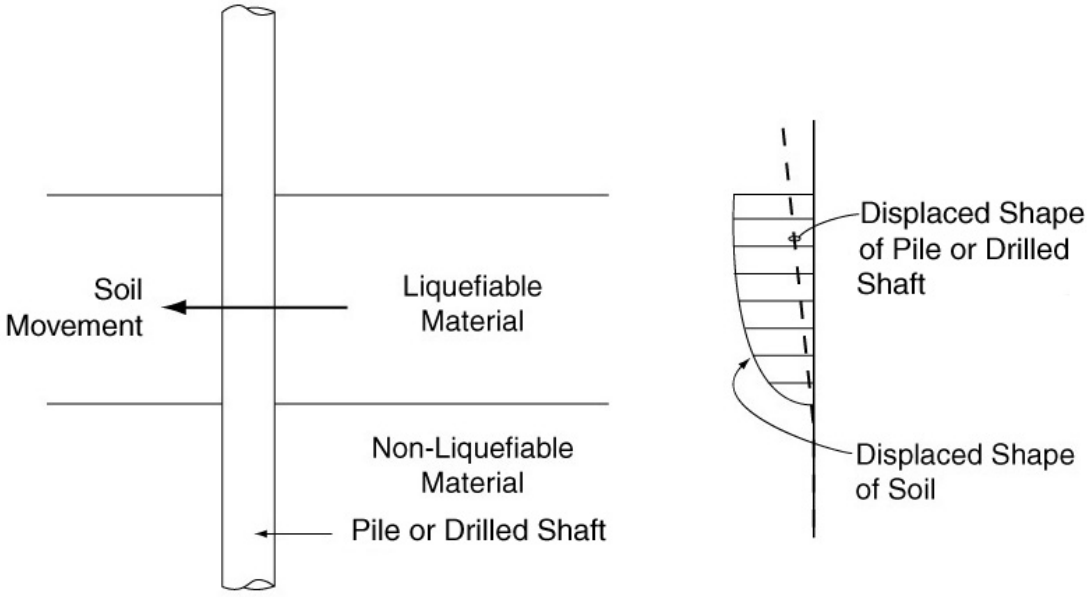

Figure D.4.2-2 Movement of Liquefied Soil Past Pile or Drilled Shaft

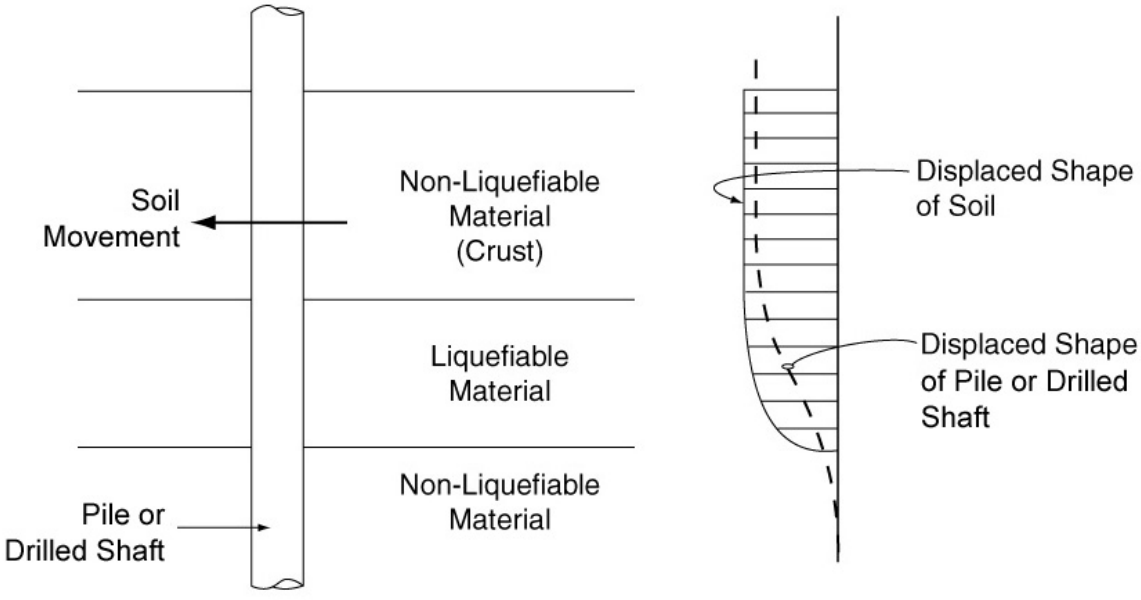

Figure D.4.2-3 Movement of Liquefied Soil with Crust with Pile or Drilled Shaft

- *Step 5:* If movement of soil around the structure is indicated, then the foundation is designed to withstand the passive pressures created by the soil moving around the structure. The induced forces are effectively the largest forces that the structure will experience, and for this reason it is conservative to design a structure for such forces.

- *Step 6:* If on the other hand, the assessment indicates that movement of the foundation is likely, then the structure must be evaluated at the maximum expected displacement. This check is shown in Step 6. The implication of this assessment is that for relatively large ground movements, soil displacements are likely to induce similar magnitude movements of the foundation. In this context, "large" is taken relative to the structural yield resistance. The resulting induced movements of the foundations may produce substantial plasticity in the foundations, and may induce relatively large reactions in the superstructure. Guidelines for the acceptablerotation are provided in Articles 7.7.9, 7.8.6, 8.7.9, and 8.8.6 of these *Guidelines*. For an upper level event, the recommended acceptance criterion is a plastic rotation of 0.05 radians. The allowance of plasticity in the foundation is believed to be reasonable, even though plasticity may occur below grade, because damage in the foundation is not likely to pose a collapse hazard.

  Step 7: If deformations are not acceptable, there are realistically only two ways to restrict the foundation and substructure forces to acceptable values. The first method is to design the foundations to resist the full passive pressure forces that would accompany passive movement of the soil around the foundations. The other method would be to limit the ground movement by providing either ground or structural remediation. It is the structural option that provides the simplest first option, and this makes use of the "pinning" or dowel action that pile or shaft foundations contribute asthey cross the potential failure plane of the moving soil mass.

- *Step 8:* The determination of the plastic mechanism that is likely to occur in the presence of spreading should be done in a reasonable manner. Due to the range of inherent uncertainties, great precision in the determina-

tion may not produce more accuracy. Thus a simple estimate of the mechanism and its corresponding lateral resistance capability is often adequate. For instance, one method is to use the upper bound method of plasticity and postulate potential mechanisms, then using judgment assess the mechanism that is likely to control. The acceptance criteria are basically the structural deformation criteria for SDAP E, which uses the push-over method. In fact, the piles are the elements that limit the acceptable displacements of the system.

The lateral shear that produces the plastic mechanism can be adjusted downward to account for the driving effect of the *P*-Δ effect. The lateral soil force that produces a plastic mechanism in the foundation/substructure system is required; therefore, the reduction in shear required to produce a mechanism due to *P*-Δ should be considered. Figure D.4.2-4 and Figure D.4.2-5 illustrate first-order corrections for *P*-Δ effects for a stub abutment and for an

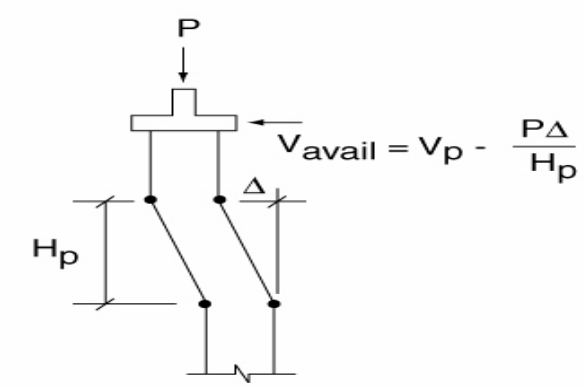

Figure D.4.2-4 *P*-Δ Effects to Stub Abutment

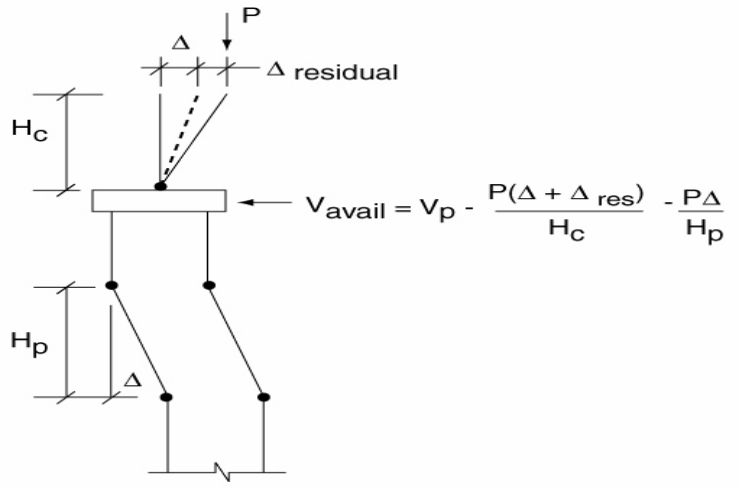

Figure D.4.2-5 *P*-Δ Effects for an Intermediate Pier with Piles and Pile Cap

intermediate pier with piles and pile cap, respectively.

A more precise method of determining the plastic mechanism would be to use an approach that ensures compatibility of deformations between the soil and piles (e.g., similar to that incorporated in LPILE) and which accounts for plastic deformations in the piles themselves. This second requirement could be satisfied by using software that is capable of performing push-over-analysis, then using p-y curves from a program such as LPILE to produce boundary support elements that ensure compatibility.

- *Step 9:* The system then must be assessed for a prescribed displacement field to represent the likely soil spreading deformation. From this analysis, an estimate of the likely shear resistance the foundation will provide is estimated and this shear can then be incorporated back into the stability analysis.
- *Step 10:* If substantial resistance is provided, then its effect on limiting the instability driven movement of the soil block should be introduced into the stability analysis. This step is typically not included in current assessments of potential foundation movements, although inclusion of this resistance could improve the expected performance of the structure.
- *Step 11 and 12:* The overall displacement is re-calculated with the revised resistance levels considered. Once a realistic displacement is calculated, then the foundation and structural system can be assessed for this movement. It is at this point that more permissive displacements than for substructure design can be relied upon. This implies that plastic rotations, and potentially large ones, may be allowed to occur in the foundation under such conditions.
- *Step 13:* If the behavior of the structure is acceptable then the design is complete; if not, then the Designer must assess whether to try to produce adequacy either through additional piles or shafts, and these may not need to connect to the foundation (passive piles). Alternately ground improvement approaches may be considered, for instance stone columns. The selection of structural or geotechnical remediation methods is based on the relative economy of the system being used.

The process is repeated by returning to *Step 8* and modifying the available resistance until the slope is stabilized. The fact that inelastic deformations may occur below grade during the upper level seismic event and that these may be difficult to detect and inspect should be considered. However, typically the presence of large ground movements induced by earthquake motions is discernible. Thus it should be possible to postulate whether inelastic deformations have occurred from the post-earthquake inspection information. Additionally, inclinometer tubes could be installed in selected elements of deep foundations to allow quantitative assessment of pile or shaft movement following an earthquake.

D.4.2.3 Settlement and Downdrag

Deep foundations should also be designed for settlement that occurs during the seismic event. The settlement can be estimated based on settlement below the neutral plane of the pile or drilled shaft. Procedures given in Section 10 of the AASHTO LRFD Bridge Design Specifications can be used to estimate the location of the neutral plane. The Tokimatsu and Seed (1987) method described in Article D.2.5.3 can be used to estimate the settlement.

Vertical drag loads will be imposed on a deep foundation as liquefied layers settle. These loads should be used to estimate the total settlement of the deep foundation (i.e., added to the settlement estimated by the Tokimatsu and Seed (1987) method) and the structural capacity of the pile under the drag loads.

CD.4.2.3 Settlement and Downdrag

The drag load will develop along the side of the deep foundation from settlement of all layers above the bottom of the liquefied layer. The drag load in non-liquefied layers will be the same as the ultimate side resistance developed under compressive loading. The drag load along the portion of the deep foundation that is in liquefied soil will initially be the residual strength of the liquefied soil, but will then increase gradually as porewater pressures dissipate. For design purposes it is conservative to assume that maximum drag occurs at the end of porewater pressure dissipation, when the soil strength has returned to its initial condition.

D.4.3 Ground Improvement

Ground improvement methods can be implemented to mitigate the effects of liquefaction. A number of these methods are available, including grouting (compaction, permeation, and jet), vibro systems (vibratory probe, vibro-compaction, vibro-replacement), surcharge and buttress fills, reinforcement and containment (root piles, mixed-in-place walls and columns) and drains. Cooke and Mitchell (1999) provide detailed guidelines for mitigating the effects of liquefaction at bridge sites. The suitability of these methods will depend on the soil conditions at the site, the location of the ground water, and project logistics.

A critical phase in any ground improvement method is confirmation that the ground improve-

CD.4.3 Ground Improvement

Two of the more common procedures for accomplishing this remediation are described below:

- *Vibro-Replacement:* The most widely used densification method is the vibro-replace-ment technique. This method involves the repeated insertion and withdrawal of a large vibrating probe in the soil, to the desired depth of densification. As vibration-induced liquefaction occurs, crushed stone backfill is placed around the vibrator leading to the development of a stone column approximately 1 m in diameter. The stone column provides for an increased effectiveness of vibration transmission, and facilitates drainage of excess pore water pressures as densification occurs. The procedure is

ment goals have been achieved. Pre- and post-field explorations are required using SPT or CPT methods to confirm that required ground improvements have been achieved. In many cases it will be desirable to conduct a test program before the actual ground improvement program to confirm that the proposed improvement methods will work in the particularly conditions occurring at the project site.

repeated at grid spacing of 2 to 3 feet. Relative densities of the order of 80%, can be accomplished by the method. The method has been shown to be effective if sands to be densified contain less than 15 to 20% fines, although the use of wick drains placed at the midpoints of stone column grid points to aid drainage, can potentially lead to densification of sandy silts (Luehring et al., 1998). Details on design information and equipment applications can be found in many publications such as Baez (1995, 1997), Hayden and Baez (1994), and Martin (1998).

- *Compaction Grouting:* This method involves pumping a stiff mix of soil, cement, and water into the ground under high pressure to compress or densify the soil. For sites where vibratory techniques may be impractical, compaction grouting can be used. Typically, a very stiff (25 to 50 mm slump) soil-cement-water mixture is injected into the soil, forming grout bulbs which displace and potentially densify the surrounding ground, without penetrating the soil pores. A grid or network of grout columns formed by bottom up grouting, results in improved liquefaction resistance over a required areal extent, similar to the use of a network of stone columns described above for vibro-replacement. An overview of this approach is documented by Boulanger and Hayden (1995).

D.4.3.1 Bearing Capacity and Settlement

Ground improvement methods can be used to limit settlements of approach fills and improve bearing capacity or lateral capacity of soil that is predicted to liquefy. The amount of improvement is determined by the type and extent of improvement. Cooke and Mitchell (1999) provide guidance on evaluating these improvement methods.

CD.4.3.1 Bearing Capacity and Settlement

When used to improve the bearing capacity for spread footings or the lateral capacity of deep foundations, the ground is usually improved to a level where it will not liquefy during the seismic event. However, material beyond the improved zone will likely liquefy. Porewater pressures in these liquefied zones can migrate into the improved area, reducing the capacity of the improved zone. Similarly, loss in strength in the liquefied zone can lead to loss in either vertical or lateral support within the improved ground, due to loss of soil reaction in the liquefied zone. This loss in capacity can lead to increased vertical or lateral displacements. The placement of a zone with a radius of 1.5 to 2 times the thickness of the liquefiable layer can be used to eliminate post liquefaction downdrag on a pile, and the potential effects of cyclic ground lurch (progressive unidirectional movement of soil due to high ground accelerations).

The improved ground will also propagate ground motions more effectively than will the liquefied zone. Site conditions following ground improvement will likely be stiffer than what existed before ground improvement. This increased stiffness should be considered when defining the site category for determining peak ground and spectral accelerations.

These factors must be considered during the design process.

D.4.3.2 Lateral Spreading and Flow

Ground improvement methods can be used to control or limit the amount of lateral flow or spreading. The approach used in design is to increase the strength of the ground enough that it either causes the liquefied soil to flow around the improved ground or provides sufficient resistance to stop the lateral spread or flow. In most bridge designs one goal will be to prevent movement of the approach fill, either transverse or in line with the bridge alignment. Conventional slope stability methods are used to make these assessments. Initially, the potential for flow failure should be evaluated, with the improved ground characterized by a higher strength. If the resulting factor of safety is less than 1.0, then either the Newmark Charts or the Newmark Time History Analyses can be conducted to determine the amount of ground deformation. Procedures described in Article D.4.2.2 can then be used to evaluate whether the resulting deformations meet design criteria for the bridge structure and foundation.

CD.4.3.2 Lateral Spreading and Flow

A Newmark approach can be used to determine the buttress width that leads to acceptable displacement performance of abutment or bridge pier piles in the failure zone. This involves determining the yield acceleration for slope movement through the improved ground, and then using the simplified charts, equations, or integrated earthquake records to revise the displacement procedure. As the width of the improved zone increases, the amount of deformation will decrease. This relationship allows a cost-benefit study to be conducted to determine the minimum area of improved ground (minimum costs) that will result in deformations that can be tolerated by the bridge structure-foundation system.

Appendix E
LIQUEFACTION EFFECTS AND ASSOCIATED HAZARDS

E.1 PURPOSE AND SCOPE

In support of the NCHRP 12-49 effort to develop the next generation of seismic design provisions for new bridges, a study of the effects of liquefaction and the associated hazards of lateral spreading and flow, was undertaken. This appendix presents a summary of the results of that study (NCHRP 12-49 Liquefaction Study), which is presented in its entirety in the companion MCEER/ATC-49-1 Report, *Liquefaction Study Report, Recommended LRFD Guidelines for the Seismic Design of Highway Bridges* (ATC/MCEER, 2003a)

The motivation for the study was the recommended change in the design return period for ground motions for a rare or "Maximum Considered Earthquake" (MCE) used in the recommended provisions. The recommended provisions are based on using ground motions for the MCE that correspond to a probability of exceedence of 3% in 75 years (2,475-year return period) for most of the United States. In areas near highly active faults, ground motions are bounded deterministically to values that are lower than ground motions for a 2475 year return period. In contrast, the design ground motion hazard in the current AASHTO Division 1-A seismic provisions has a probability of exceedence (PE) of 10% in 50 years (approx. 15% PE in 75 years or 475-year return period). With the increase in return period comes an increase in the potential for liquefaction and liquefaction-induced ground movements. These ground movements could damage bridge structures. Concerns that liquefaction hazards under the recommended provisions may prove to be too costly to accommodate in construction led to this study.

The project team believed that, along with increases in the likelihood or extent of liquefaction at a particular site, there also exists some conservatism in current design practices. If such conservatism exists, then the use of state-of-the-art design procedures could lead to designs that perform satisfactorily in larger earthquakes, and may not be much more expensive than those being currently built.

The scope of the study was limited to two sites in relatively high seismicity locations, one in the western United States in Washington State and one in the central United States in Missouri. The Washington Site is located near the Cascadia subduction zone, and the Missouri site is located near the New Madrid seismic zone. Actual site geologies and bridge configurations from the two states were used as an initial basis for the study. The site geologies were subsequently idealized by providing limited simplification, although the overall geologic character of each site was preserved.

The investigation of the two sites and their respective bridges focused on the resulting response and design differences between the recommended ground shaking level (3% PE in 75 years) and that corresponding to the current AASHTO Division I-A provisions (15% PE in 75 years). The scope of the study for each of the two sites and bridges includes:

1. Development of both 15% PE in 75 year and 3% PE in 75 year acceleration time-histories;
2. Simplified, conventional liquefaction analyses;
3. Nonlinear assessment of the site response to these accelerations including the time history of pore pressure increases;
4. Assessment of stability of abutment end slopes;
5. Estimations of lateral spreading and/or flow conditions at the sites;
6. Design of structural systems to withstand the predicted response and flow conditions;
7. Evaluation of geotechnical mitigation of liquefaction related ground displacement; and
8. Evaluation of cost impacts of the structural and geotechnical mitigation strategies.

The results for the 15% PE in 75 year and 3% PE in 75 year ground motions were compared against one another to assess the implications of using ground motions for the longer return period (lower probability of exceedance level) for design. Additionally, the conduct of the study helped syn-

thesize an overall approach for handling liquefaction-induced movements in the recommended design provisions. The study for the Washington site is described in Articles E.3 through E.8 and for the Missouri site in Article E.9, with lesser detail.

E.2 DESIGN APPROACH

The design approach used in the study and recommended for the new AASHTO LRFD provisions involves four basic elements:

1. Stability analysis;
2. Newmark sliding block analysis;
3. Assessments of the passive force that can ultimately develop ahead of a pile or foundation as liquefaction induces lateral spread; and
4. Assessment of the likely plastic mechanisms that may develop in the foundations and substructure.

The rationale behind this approach is to determine the likely magnitude of lateral soil movement and assess the structure's ability to both accommodate this movement and/or potentially limit the movement. The approach is based on use of a deep foundation system, such as piles or drilled shafts. Spread footing types of foundations typically will not be used when soil conditions lead to the possibility of liquefaction and associated lateral spreading or settlement.

The concept of considering a plastic mechanism, or hinge, in the piles under the action of spreading forces is tantamount to accepting damage in the foundation. This is a departure from seismic design for structural inertia loading alone, and the departure is felt reasonable for the rare MCE event because it is unlikely that the formation of plastic hinges in the foundation will lead to structure collapse. The reasoning behind this is that lateral spreading is essentially a displacement-controlled process. Thus the estimated soil displacements represent a limit on the structure displacement, excluding the phenomena of buckling of the piles or shafts below grade and the continued displacement that could be produced by large P-Δ effects. Buckling should be checked, and methods that include the soil residual resistance should be used. Meyersohn, et al. (1992) provides a method for checking buckling as an example. The effects of P-Δ amplification are discussed later in this Appendix.

The fact that inelastic deformations may occur below grade, and that these may be difficult to detect and inspect, should be considered. However, the presence of large ground movements induced by earthquake motions is discernible. Thus, it should be possible to evaluate whether inelastic deformations could have occurred from the post-earthquake inspection information. Additionally, inclinometer tubes could be installed in selected elements of deep foundations to allow quantitative assessment of pile/shaft movement following an earthquake. Also post earthquake investigation using down hole video cameras can be used to assess damage.

A flowchart of the methodology for consideration of liquefaction induced lateral spreading is given in Figure D.4.2-1 and key components of the methodology are numbered in the flowchart and discussed in detail in the commentary to Article D.4.2.2. The figure, together with the commentary, provides a 'roadmap' to the procedure used in this study for the lateral spreading resistance design. The primary feature of the recommended methodology is the use of inelastic action in the piles to accommodate the movement of soil and foundations. If the resulting movements are unacceptable, then mitigation measures must be implemented. Mitigation measures are discussed in Article D.4.3 and are discussed in more detail in the full liquefaction study report (ATC/MCEER, 2003a).

E.3 SITE SELECTION AND CHARACTERIZATION

Because the purpose of the study was to investigate sites that are realistic, an actual site was chosen as the prototype for a Western U.S. Site and another actual site for a mid-America site. The western site is the primary focus of this Appendix although a brief summary of the results of the Mid-America site are given in Article E.9. The Western site is located just north of Olympia, Washington in the Nisqually River valley[1]. The location is within a large river basin in the Puget Sound area of Washington State, and it is situated

[1] This site was selected and the liquefaction evaluation was completed before the February 2001 Nisqually earthquake. Ground motions associated with the Nisqually earthquake were considerably less than those used in this study. While liquefaction occurred at some locations near the selected site no bridge damage apparently occurred likely because of the limited extent of liquefaction.

near the mouth of the river in the estuary zone. The basin is an area that was over ridden by glaciers during the last ice age and therefore has overconsolidated material at depth. Additionally, the basin contains significant amounts of recently deposited, loose material over the glacially consolidated materials.

Soil conditions for the site were developed from information provided by Washington State Department of Transportation (WSDOT) for another well characterized site located in a geologically similar setting near Seattle. The actual site was moved to the Olympia area to avoid the effects of the Seattle fault. At the prototype site, the material at depths less than 150 feet is characterized by alluvial deposits. At greater depths some estuarine materials exist and below about 200 feet dense glacial materials are found. This then produces a site with the potential for deep liquefiable soils.

For the purposes of this study, the site profile was simplified such that fewer layers exist, and the profile is the same across the entire site. The simplified profile retains features and layering that produce the significant responses of the actual site. The simplified soil profile is given in Figure H-1. This figure also includes relevant properties of the soil layers that have been used for the seismic response assessments and bridge design. Shear wave velocity (V_s), undrained shearing strength (c_u), soil friction angle (φ), and residual soil strength (S_{ur}) were interpreted from the field and laboratory data provided by WSDOT. The cyclic resistance ratio (CRR) was obtained by conducting simplified liquefaction analyses using both the SPT and CPT methods to obtain CRR values. These CRR values are plotted in Figure H-2. Average CRR values were determined for liquefiable materials, and represent clean sand values for a M7.5 event.

The prototype site profile and the structure elevation are shown in Figure H-3. The modified site is a smaller river crossing than the original since the total length of the bridge was substantially shortened for the study. Only enough length was used to illustrate the issues of soil movement and design. In this case the total length of the bridge is 500 feet. The ground surface is shown in Figure H-3 as the 0-foot elevation. As can be seen in the figure, approach fills are present at both ends of the bridge, and in this case, they are relatively tall at 30-feet each.

An approach fill comprised of a relatively clean sandy gravel was assumed at each abutment. The sandy gravel was assigned a friction angle of 37 degrees.

E.4 BRIDGE TYPE

The prototype bridge from which the study data were drawn is a river crossing with several superstructure and foundation types along the structure. Again for the study, the actual structure was simplified. The 500-foot long structure comprises of a 6-foot deep concrete box girder that is continuous between the two abutments. The intermediate piers are two-column bents supported on pile caps and 24-inch steel piles filled with reinforced concrete. The roadway is 40-feet wide. The two 4-foot diameter columns for each pier are approximately 23 feet apart, and due to the relatively large size of the pile caps, a single combined pile cap was used for both columns at each pier. Figure H-4 shows the general arrangement of an intermediate pier.

The centermost pier in this example is located at the deepest point of the river channel, as shown in Figure H-3. While this is somewhat unusual, in that a longer span might often be used to avoid such an arrangement, the river pier was used here for simplicity. The columns of this pier are also relatively slender, and they were deliberately left so to allow any negative seismic effects of the slenderness, for instance P-Δ, to be assessed. In a final design, the size of these columns might likely be increased. In fact, non-seismic load combinations/conditions may require the columns to be enlarged.

The abutments are of the overhanging stub abutment type. Figure H-5 shows the transverse and longitudinal elevations of the abutments used for the bridge. For this type of abutment, the backfill is placed directly against the end diaphragm of the superstructure. This has the seismic advantage of providing significant longitudinal resistance for all displacement levels, since the passive resistance of the backfill is mobilized as the superstructure moves. This type of abutment also eliminates the need for expansion joints at the ends of the structure, and for this reason, is limited to the shorter total length structures.

E.5 DESIGN RESPONSE SPECTRA AND TIME HISTORIES

The design response spectra for the current AASHTO *Standard Specifications for Highway*

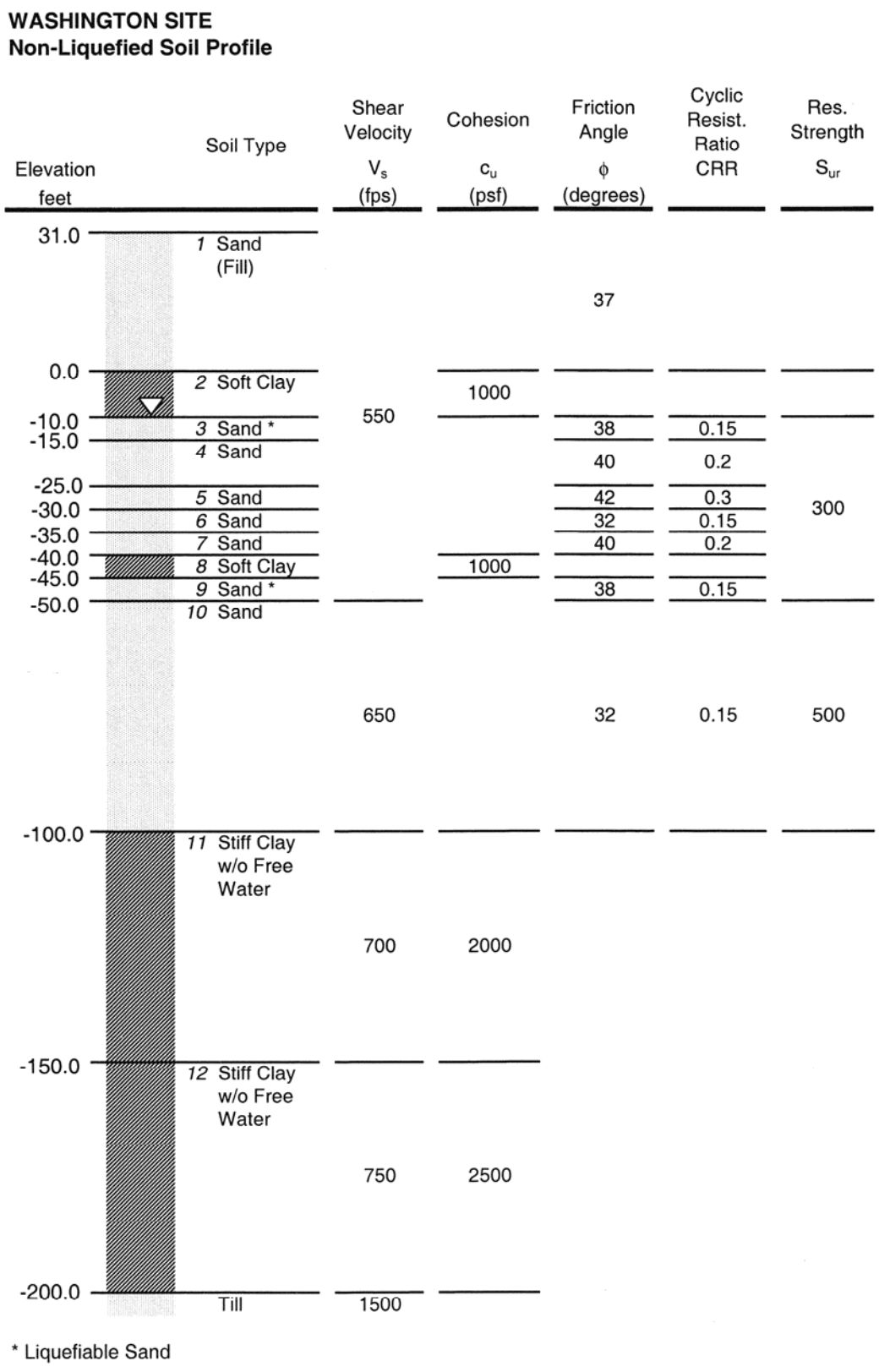

Figure E-1 Simplified Soil Profile for the Western U.S. (Washington State) Site

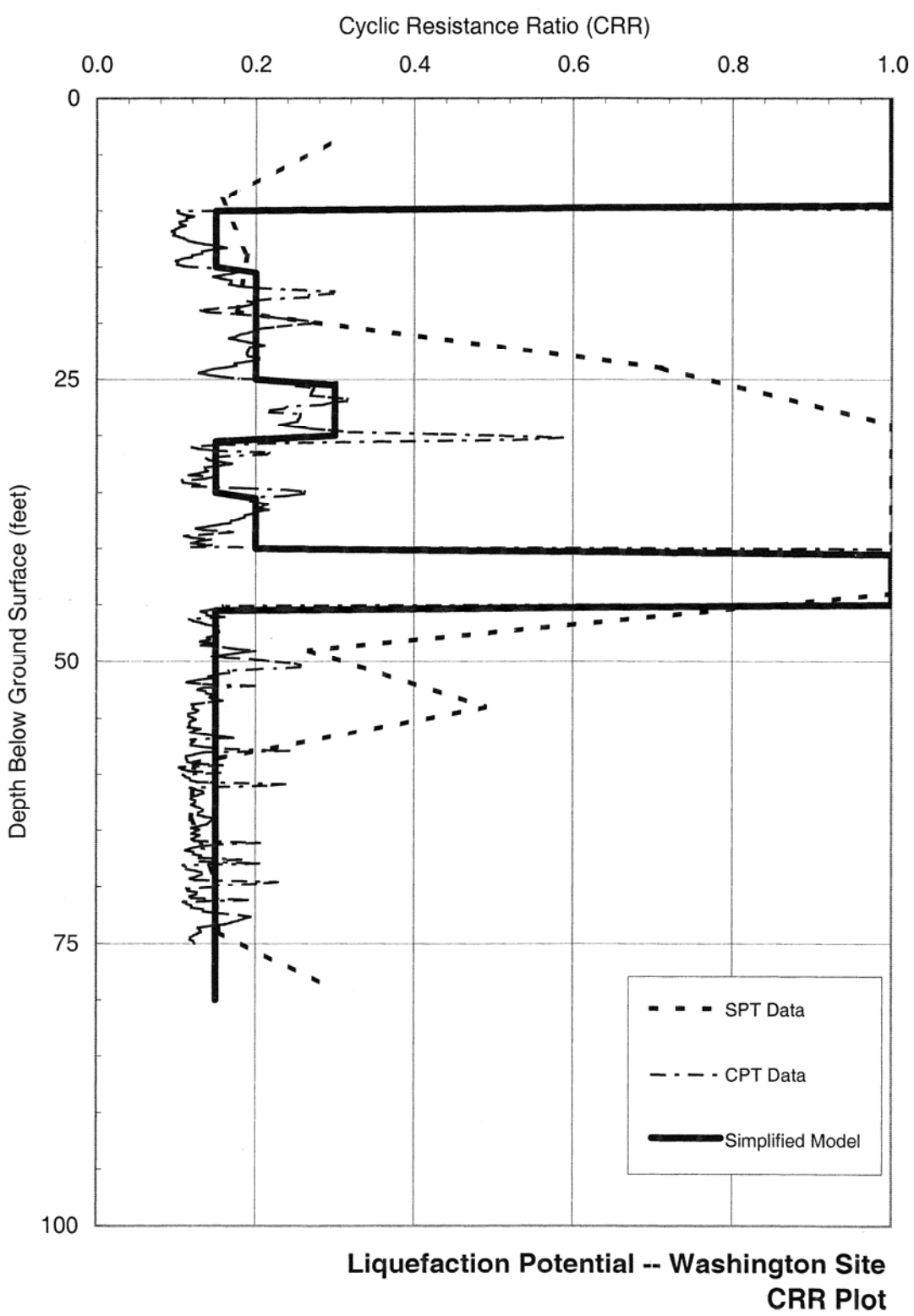

Figure E-2 Washington State Department of Transportation Location H-13 CRR Plot

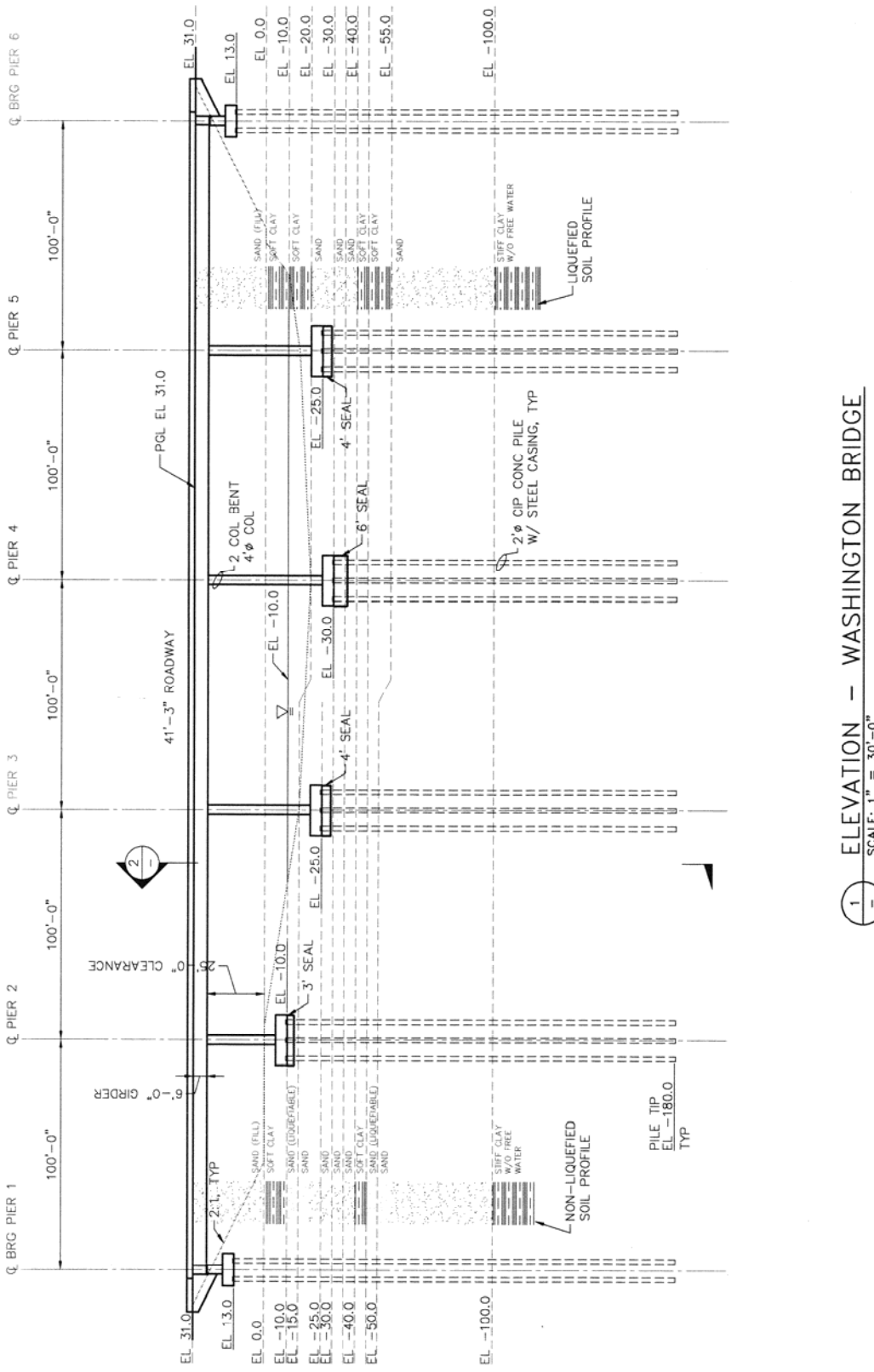

Figure E-3 Site Profile and Structure Elevation, Washington State Bridge

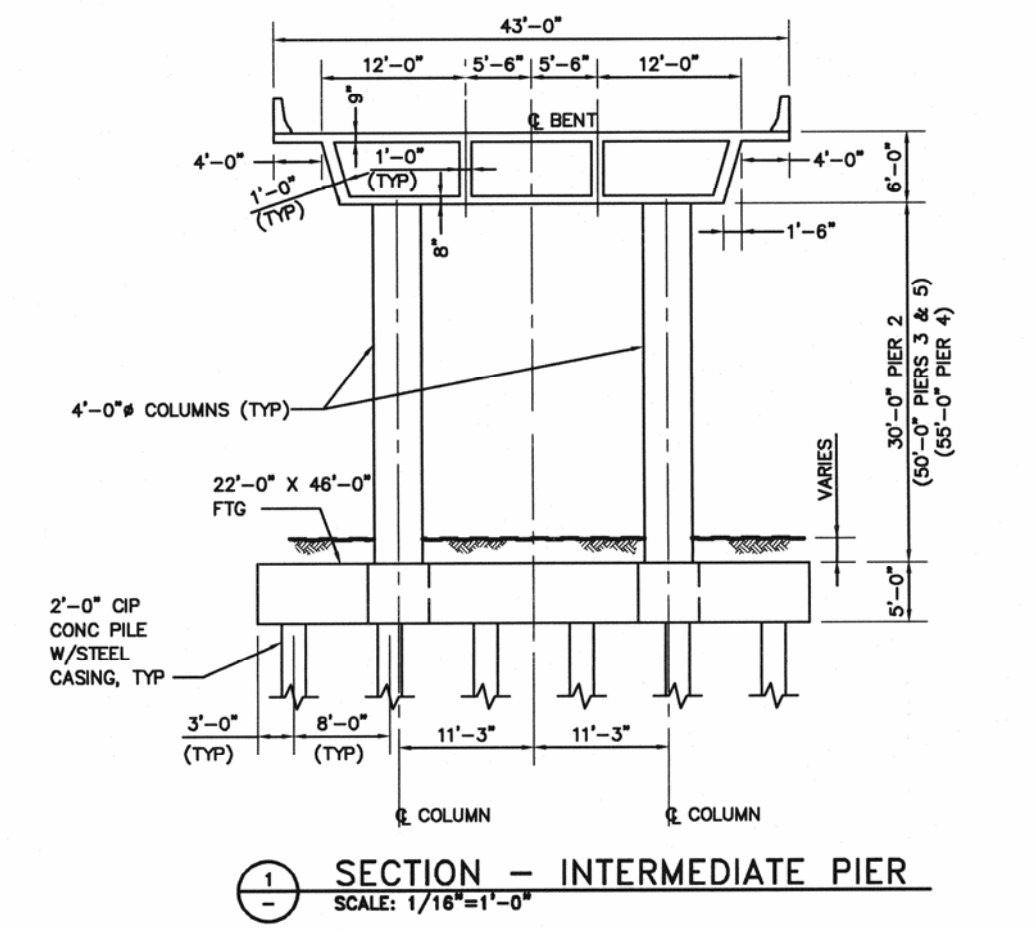

Figure E-4 Elevation of an Intermediate Pier, Washington State Bridge

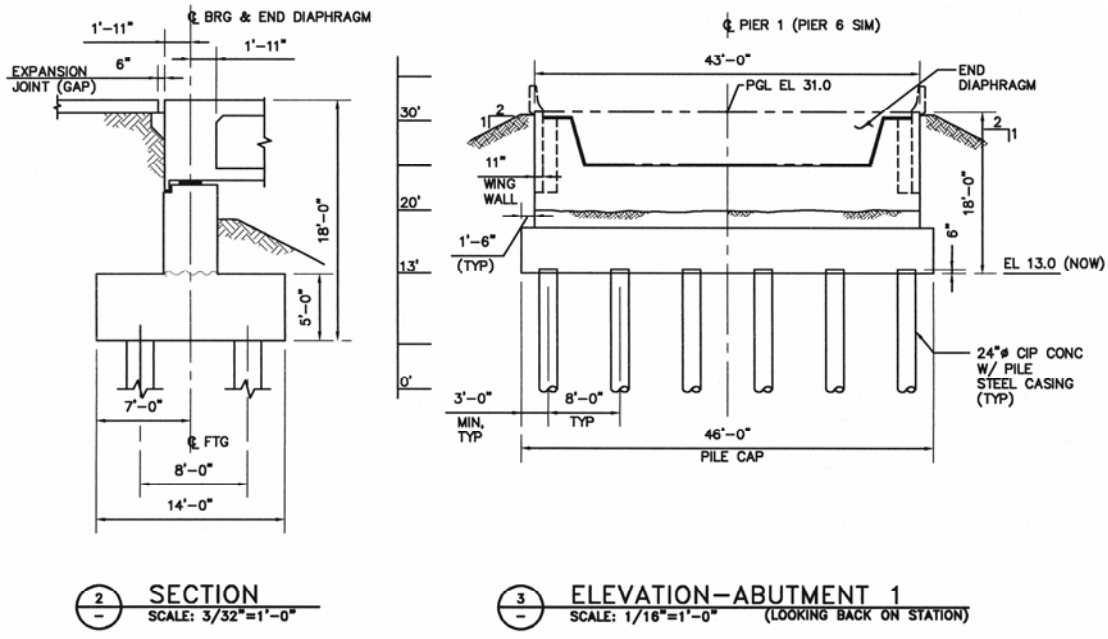

Figure E-5 Elevations of the Abutment, Washington State Bridge

Bridges (hereinafter referred to as the current AASHTO *Specifications*) and the NCHRP 12-49 recommended LRFD seismic design provisions were constructed using the procedures and site factors described in the respective specifications. For the current AASHTO *Specifications*, the hazard level of 10% probability of exceedance in 50 years was used. For the recommended LRFD provisions, both the rare earthquake (Maximum Considered Earthquake or MCE) having a probability of exceedance of 3% in 75 years with deterministic bounds near highly active faults, and the frequent earthquake (also termed the Expected Earthquake) having a probability of exceedance of 50% in 75 years, were used as design earthquakes.

Design response spectra based on the current AASHTO *Specifications* were constructed using a (rock) peak ground acceleration (PGA) of 0.24g for the Olympia site. This peak ground acceleration value was determined from the AASHTO map contained in the current AASHTO *Specifications*. Design spectra for the MCE of the recommended LRFD provisions were constructed using rock (Site Class B) spectral accelerations at 0.2-second period and 1.0-second period. These two spectral values were obtained from maps published by the U.S. Geological Survey (USGS). The PGA for the MCE was defined as 0.4 times the spectral acceleration at 0.2 seconds as required by the recommended LRFD provisions. Design spectral accelerations for the Expected Earthquake were obtained from the hazard curves of probabilistic ground motions on the CD-ROM published by the USGS.

Rock spectra based on AASHTO and the recommended LRFD provisions were adjusted for local site soil conditions. According to the AASHTO *Specifications* the site is a Soil Profile III; the recommended LRFD provisions define the site as Class E. Figure H-6 presents the design response spectra for the current AASHTO *Specifications*, on Soil profile Type III, and for the MCE and the frequent earthquake of the recommended LRFD provisions, on Site Class E. These site classifications represent the assessed soil profile below the ground surface where response spectra are defined for structural vibration design and peak ground accelerations are used for simplified liquefaction potential analyses. Note in Figure H-6 that the short-period branch of the AASHTO spectra are assumed to drop from the acceleration plateau at a period of 0.096 second to the peak ground acceleration at 0.02-second period, the same as for the MCE spectra. Also note that, because the long-period branch of the AASHTO spectra declines more slowly with period than those of the MCE (as $1/T^{2/3}$ in the current AASHTO *Specifications* compared to 1/T in the recommended LRFD provisions), the AASHTO and MCE spectra come closer together as the period increases.

Acceleration time histories consistent with current AASHTO *Specifications* and with MCE ground motions of the recommended LRFD provisions were developed as firm soil outcropping motions for input to the one dimensional, non-linear site response analyses to assess the liquefaction hazard of the site. These time histories were developed in accordance with the requirements and guidelines of the recommended LRFD provisions. Deaggregation of the probabilistic results for the Olympia site indicates that significant contributions to the ground motion hazard come from three magnitude-distance ranges: (1) magnitude 8 to 9 earthquakes occurring at a distance of 70 to 80 km distance; (2) magnitude 5 to 7 events occurring at a distance of 40 to 70 km distance; and (3) magnitude 5 to 6.5 earthquakes occurring at distances less than 20 km. These three magnitude-distance ranges are associated, respectively, with (1) large-magnitude subduction zone interface earthquakes, (2) moderate magnitude earthquakes occurring within the subducting slab of the Juan de Fuca plate at depth beneath western Washington and in the shallow crust of the North American plate at relatively large distances from the site, and (3)moderate magnitude earthquakes occurring in the shallow crust of the North American plate in the near vicinity of the site. Time histories were developed for each of these earthquake sources. The selected source for (1) was the 1985 Chile earthquake, for (2) it was representative of the events occurring within the subducting slab, of the type that occurred near Olympia in 1949 and the 2001 Nisqually earthquake, and for (3) it was the 1986 North Palm Springs earthquake, a moderate magnitude local shallow crustal earthquake.

E.6 LIQUEFACTION STUDIES

The liquefaction study for the Washington bridge site involved two phases. In the first, a series of liquefaction analyses were conducted using the SPT and CPT simplified methods. Results of these analyses were used to determine the depths at which liquefaction could occur during the 15% probability of exceedance (PE) in 75 year and 3%

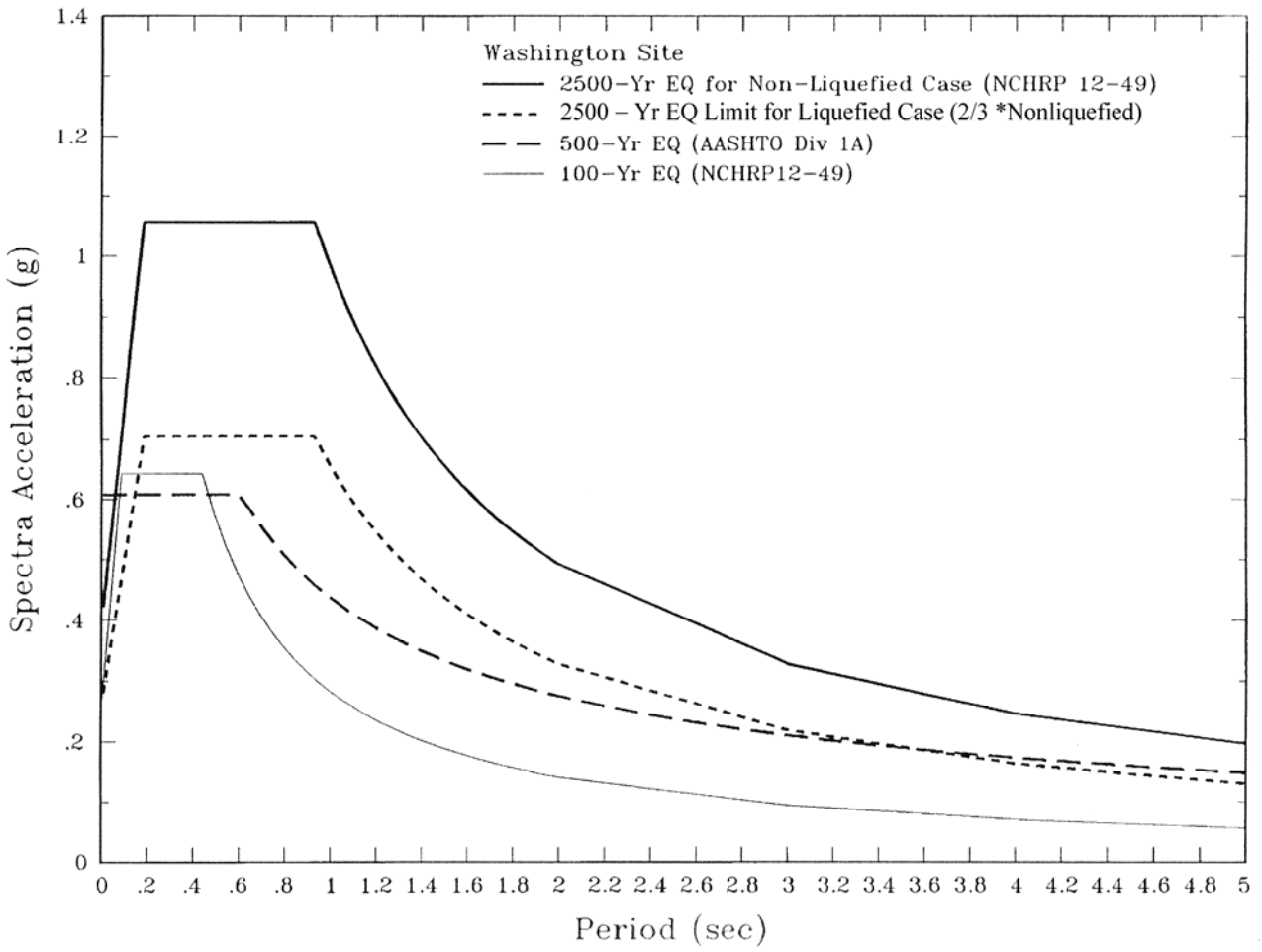

Figure E-6 Design Response Spectra Based on Current AASHTO *Specifications*, Site Class III, and for the MCE and the Expected Earthquake Events in the Recommended NCHRP 12-49 Design Provisions, Site Class E, Washington Site

PE in 75 year earthquake ground motions. These results were also used as a basis for determining H the residual strength of the soil. Concurrent with these analyses, a series of one-dimensional nonlinear, effective stress analyses was conducted to define more explicitly the mechanisms for pore water pressure increase within the soil profile and the changes in ground accelerations and deformations resulting from the development of liquefaction.

E.6.1 Simplified Liquefaction Analyses

The first step of the procedure outlined in the commentary to Article D.4.2.2 is to determine whether liquefaction is predicted to occur.

Simplified liquefaction analyses were conducted using the procedures given in Youd and Idriss (1997). Two levels of peak ground acceleration (PGA) were used, one representing the acceleration from the current AASHTO *Specifications* with its 10% PE in 50 year ground motion and the other representing the recommended 3% PE in 75 year ground motion. The PGA for the 10% in 50 year ground motion was not adjusted for site effects: this is consistent with the approach recommended in the current AASHTO *Specifications*[2]. Ground motions with a 3% PE in 75 years were adjusted to Site Class E, as recommended in

[2] Common practice is to adjust the PGA for the site soil factors given in Table 2 of Division 1-A of the current AASHTO *Specifications*. While this adjustment may be intuitively correct, these site factors are not explicitly applied to the PGA. If the site coefficient were applied at the Washington site, the PGA would be increased by a factor of 1.5, making it only slightly less than the PGA for the 2,475-year event.

Article 3.4. The resulting PGA values for each case are summarized below.

Input Parameter	10% PE in 50 Years	3% in 75 Years
Peak ground acceleration	0.24g	0.42g
Mean Magnitude	6.5	6.5

The magnitude of the design earthquake was required for the SPT and CPT simplified analyses. Results of deaggregation studies from the USGS database suggest that the mean magnitude for PGA for the 10% PE in 50 year and 3% in 75 year ground motions is 6.5. This mean magnitude reflects contributions from the different seismic sources discussed above. However, common practice within the State of Washington has been to use a magnitude 7.5 event, as being representative of the likely size of a subduction zone event occurring directly below the Puget Sound area. In view of this common practice, a range of magnitudes (6.5, 7.0 and 7.5) was used during the liquefaction analyses.

For these analyses, ground water was assumed to occur 10 feet below the ground surface for the non-fill case. Evaluations were also performed using a simplified model to evaluate the effects of the fill. For the fill model, the soil profile with the associated soil properties was the same as the free-field case. However, an additional 30 feet of embankment was added to the soil profile. This change results in a lower imposed shearing stress (i.e., demand) because of the lower soil flexibility factor (R_d). No adjustments were made to the normalized CRR values for the greater overburden. As discussed in Youd and Idriss (1997), the recommended approach for a site where fill is added is to use the pre-fill CRR value, under the assumption that the overburden effects from the fill will not have an appreciable effect on the density of the material.

Factors of safety (FOS) results from the liquefaction evaluations at the three magnitudes (6.5, 7.0 and 7.5) are shown in Figures H-7a and H-7b for the 10% PE in 50 year and 3% PE in 75 year ground motions, respectively, for the case of no approach fill. These results indicate that liquefaction could occur at two depths within the soil profile for the 10% PE in 50 year ground motion, depending somewhat on the assumed earthquake magnitude. For the 3% PE in 75 year ground motions liquefaction is predicted to depths of 75 feet, regardless of the assumption on the earthquake magnitude[3].

Results of the liquefaction analyses with the approach fill are compared in the companion *Liquefaction Study Report* (ATC/MCEER, 2003a). The fill case results in somewhat lower liquefaction potential (i.e., higher FOS) due to the lower imposed shearing stress.

E.6.2 DESRA-MUSC Ground Response Studies

A more detailed and refined approach to assess if liquefaction occurs and the resulting ground motion is to use a nonlinear dynamic effective stress approach. For this assessment, one-dimensional nonlinear effective stress site response analyses were conducted using the program DESRA-MUSC (Martin and Ping, 2000).

The idealized site profile and related soil properties adopted for the response analyses are shown in Figure H-1. Response analyses were performed for the three ground motions, assuming a transmitting boundary input at a depth of 200 feet, corresponding to the till interface. Analyses were conducted for both the 10% PE in 50 year and 3% PE in 75 year ground motions and for site profiles with and without embankment fill. The DESRA-MUSC parameters utilized for analyses for the various soil strata (G/G_{max} curves, backbone curves and liquefaction strength curves) are documented in the case study report together with the results of response analyses for all cases defined above. A representative set of results for the time history matching the site spectra, but based on the 1985 Chile Earthquake, which has the highest energy levels of the three events used for analyses (representative of a M 8 event), are described below.

[3] The maximum depth of liquefaction was cut-off at 75 feet, consistent with WSDOT's normal practice. There is some controversy whether a maximum depth of liquefaction exists. Some have suggested that liquefaction does not occur beyond 55 feet. Unfortunately, quantitative evidence supporting liquefaction beyond 55 feet on level ground is difficult to find; however, cases of deep liquefaction were recorded in the 1964 Alaskan earthquake. For expediency liquefaction in the simplified analysis was limited to 75 feet.

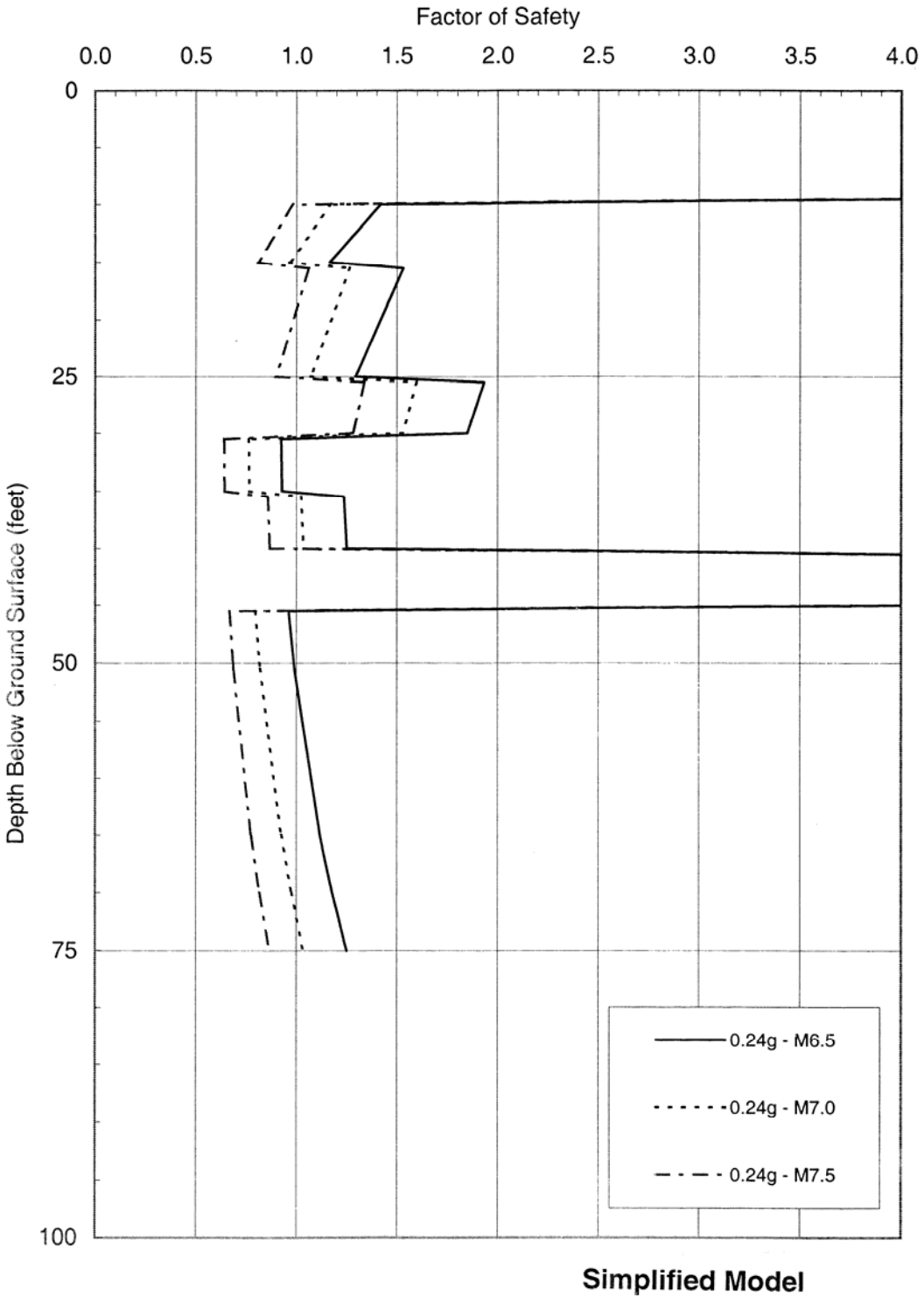

Figure E-7a **Liquefaction Potential – 475-Year Return Period (10% PE in 50-Year Ground Motion), Washington State Case Study**

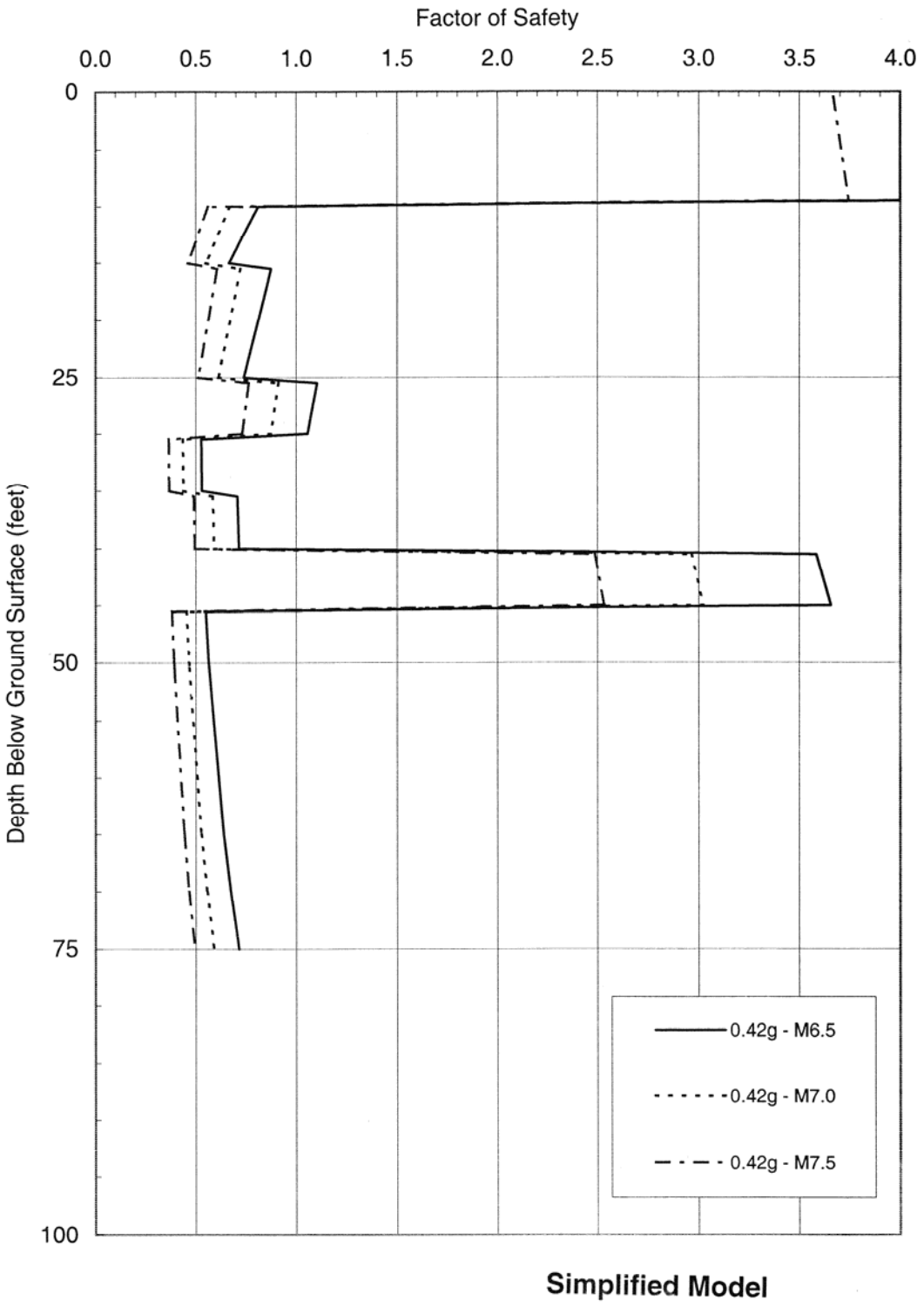

Figure E-7b **Liquefaction Potential – 2,475-Year Return Period (3% PE in 75-Year Ground Motion), Washington State Case Study**

E.6.2.1 Without Embankment Fill

The site response for the 10% PE in 50-year ground motion is summarized in four figures:

- Figure H-8 – input and output acceleration time histories and response spectra
- Figure H-9 – maximum shear strains induced as a function of depth
- Figure H-10 – time histories of pore water pressure generation at various depths
- Figure H-11 – shear stress-shear strain hysteretic loops at various depths

A similar set of figures summarize data for the 3% PE in 75 year ground motion (see ATC/MCEER, 2003a). The following are key observations from the data plots:

- The pore water pressure time history response and output accelerations are very similar for the 10% PE in 50 year and 3% PE in 75 year cases. The underlying reason for this is the fact that the higher input accelerations for the 3% PE in 75 year case are more strongly attenuated when transmitted through the clayey silts between 100 to 200 feet, such that input accelerations at the 100-foot level for both cases are of the order of 0.25g.
- All liquefiable soils between 10 and 100 feet eventually liquefied for both cases. However liquefaction was first triggered in the 45- to 50-foot layer, which became the focal point for shear distortion and associated ground lurch (see Figures H-9 and H-11). Maximum shear strains of about 6 and 10% for the 10% PE in 50 year and 3% PE in 75 year ground motions, respectively, over the 5-foot depth of this layer, would suggest maximum ground lurches of about 0.3 and 0.5 feet respectively. Liquefaction also occurred at about the same time for the layer between 10 and 20 feet. Maximum shear strains in this and other layers were relatively small, but still sufficient to eventually generate liquefaction. The strong focal point for shear strains for the 45- to 50-foot layer suggests that this layer would also be the primary seat of lateral spread distortion.
- Liquefaction at the 45- to 50-foot depth, which was triggered at about a time of 17 seconds, effectively generated a base isolation layer, subsequently suppressing the transmission of accelerations above that depth, and generating a much "softer" soil profile. This is graphically illustrated in Figure H-8 which shows suppression of input accelerations and longer period response after about 17 seconds. Such behavior is representative of observations at sites that liquefied during the Niigata and Kobe earthquakes.

Similar trends to those described above were seen for the other two time histories based on the Olympia and Desert Hot Springs earthquakes. However, for the Desert Hot Spring event, more representative of a M6.5 event, liquefaction did not occur at depths greater than 55 feet and only barely occurred at depth between 20 and 30 feet, for the 475-year event, which corresponds to 10% PE in 50 year ground motion.

The above results are generally consistent with the factor of safety calculations using the simplified method. However, one notable difference is the observation that the sand layer between 25 and 30 feet (CRR = 0.3) tends to build up pore water pressure and liquefy in a similar manner to the layers above (CRR = 0.2) and below (CRR = 0.15) due to pore water pressure redistribution effects in DESRA-MUSC, whereas the simplified method which assumes no drainage during earthquake shaking, indicates factors of safety greater than one for 475-year events. The effects of redistribution, also tend to suppress the rate of pore water pressure build up in the layer between 30 and 35 feet.

E.6.2.2 With Embankment Fill

The site response for the 475- and 2,475-year earthquakes is summarized in a similar manner to the no fill case above. As in the simplified method, the effect of the fill is to suppress the rate of pore water pressure build up in the DESRA-MUSC analyses (or increased factor of safety in the case of the simplified method). However, the overall response is similar for both the 10% PE in 50 year and 3% PE in 75 year cases, as for the no fill case.

Liquefaction was first triggered in the 45 to 50-foot layer, which became the focal point for shear distortion as in the no fill case. Liquefaction also occurred at about the same time for layers between 10 and 20 feet. However, liquefaction was suppressed in layers between 20 and 40 feet. The strong focal point for shear strains for the 45- to 50-foot layers, again suggests that this layer would be the primary seat of lateral spread distortion. Similar trends to those described above were

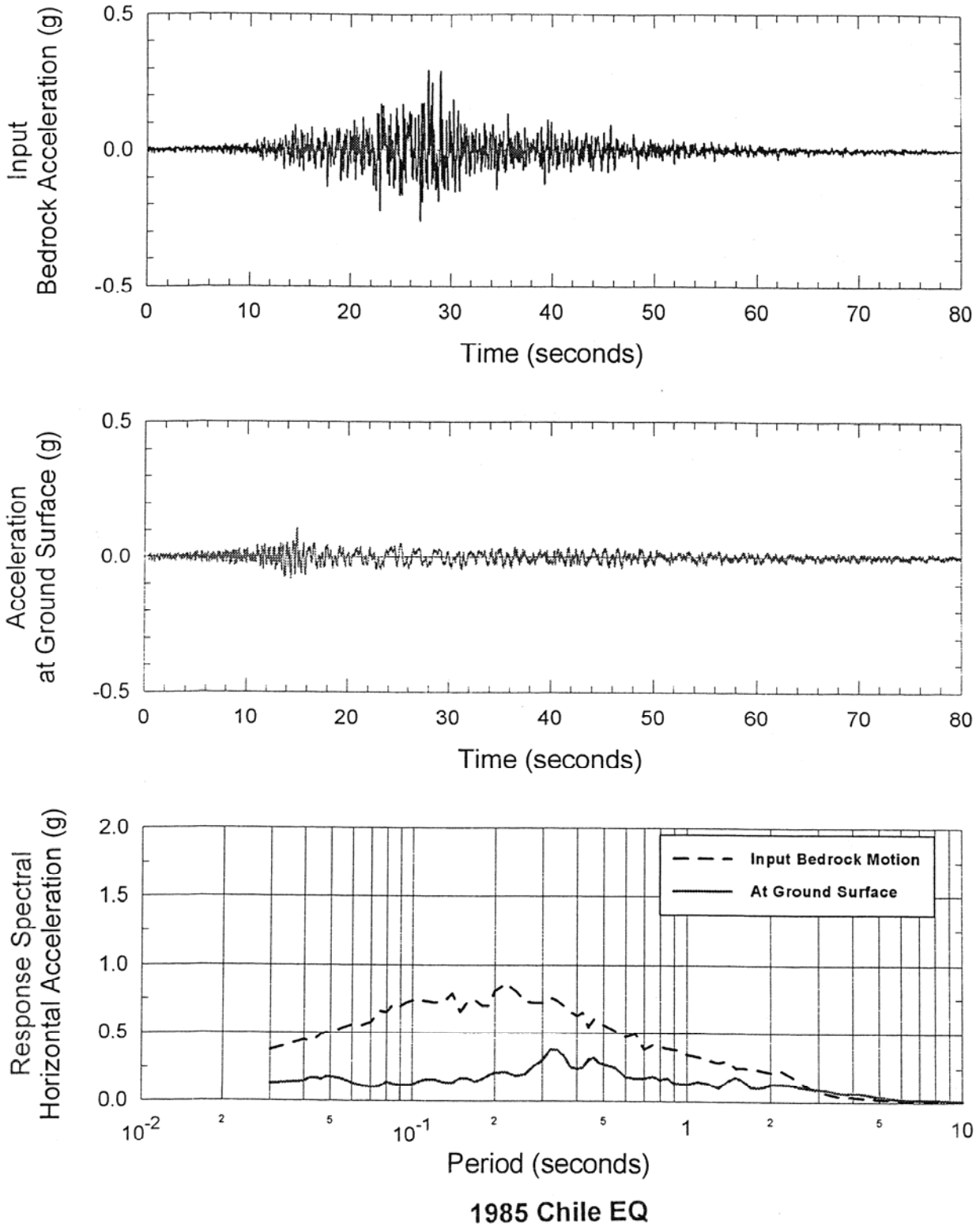

Figure E-8 **Input and Output Acceleration Histories and Response Spectra, 475-Year Earthquake (10% in 50-Year PE Ground Motion) Without Fill, Washington State Case Study**

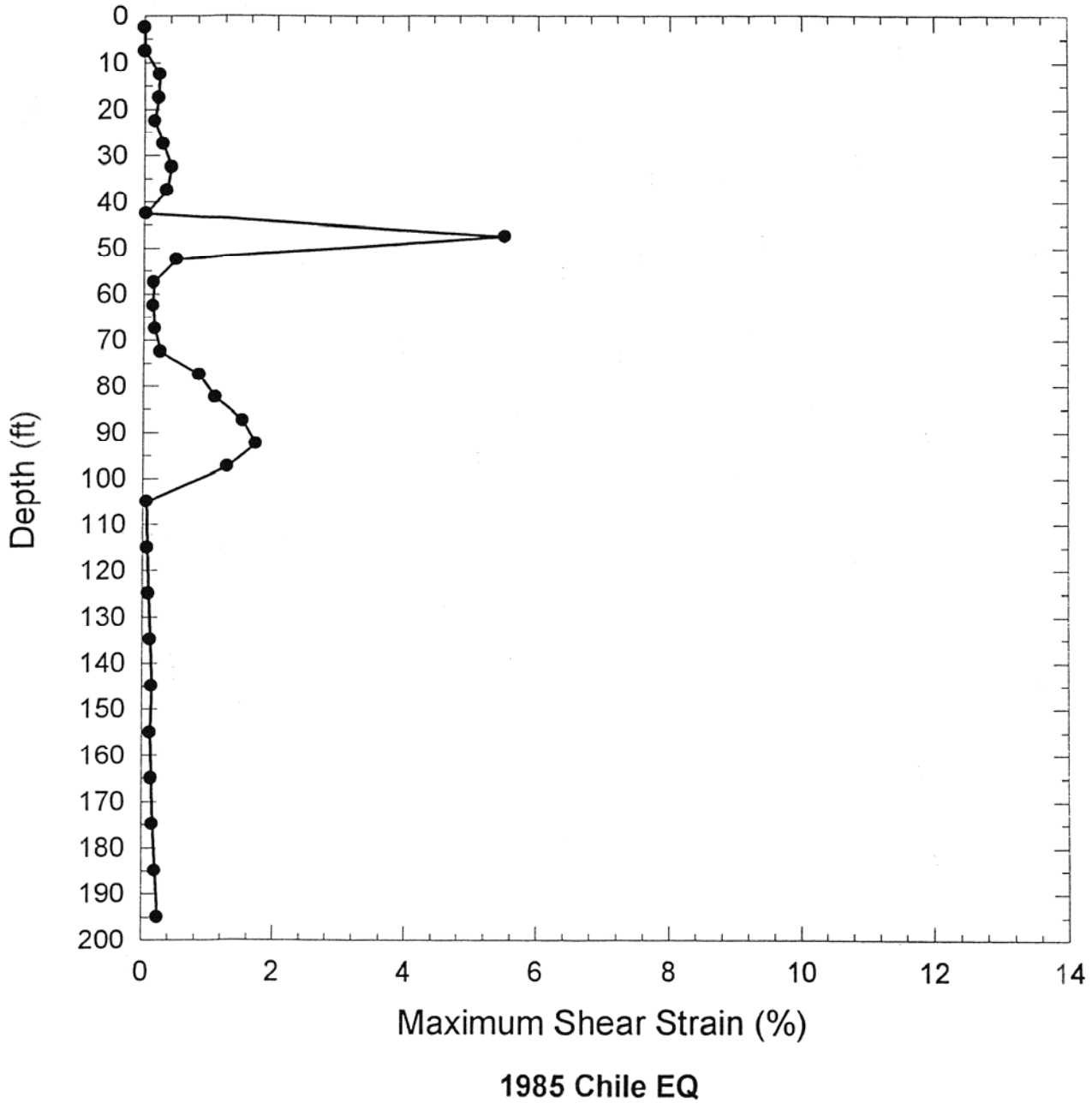

Figure E-9 **Maximum Shear Strains Induced as a Function of Depth, 475-Year Earthquake (10% PE in 50-Year Ground Motion) Without Fill, Washington State Case Study.**

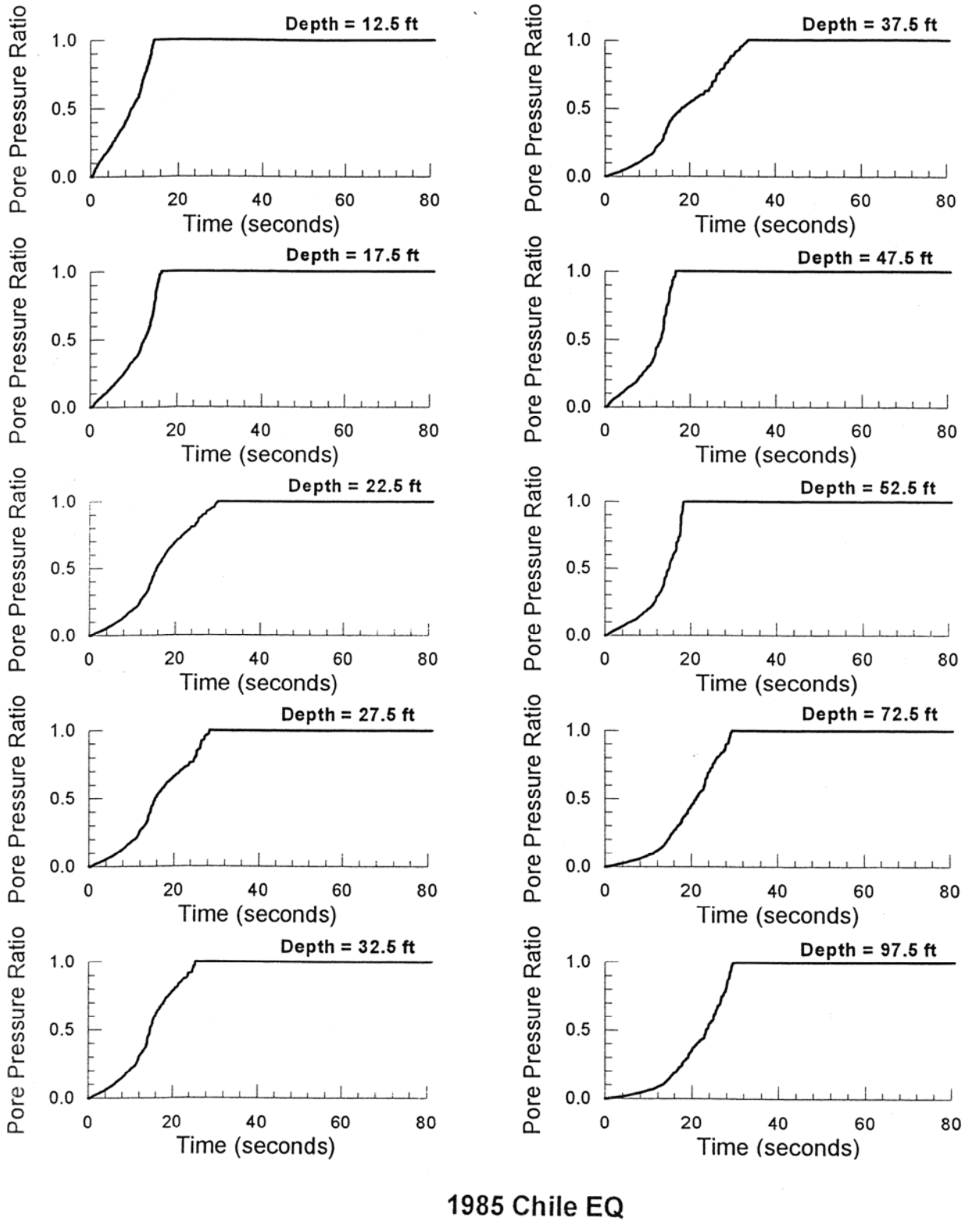

Figure E-10 **Time Histories of Pore Pressure Generation at Various Depths, 475-Year Earthquake (10% PE in 50-Year Ground Motion) Without Fill, Washington State Case Study.**

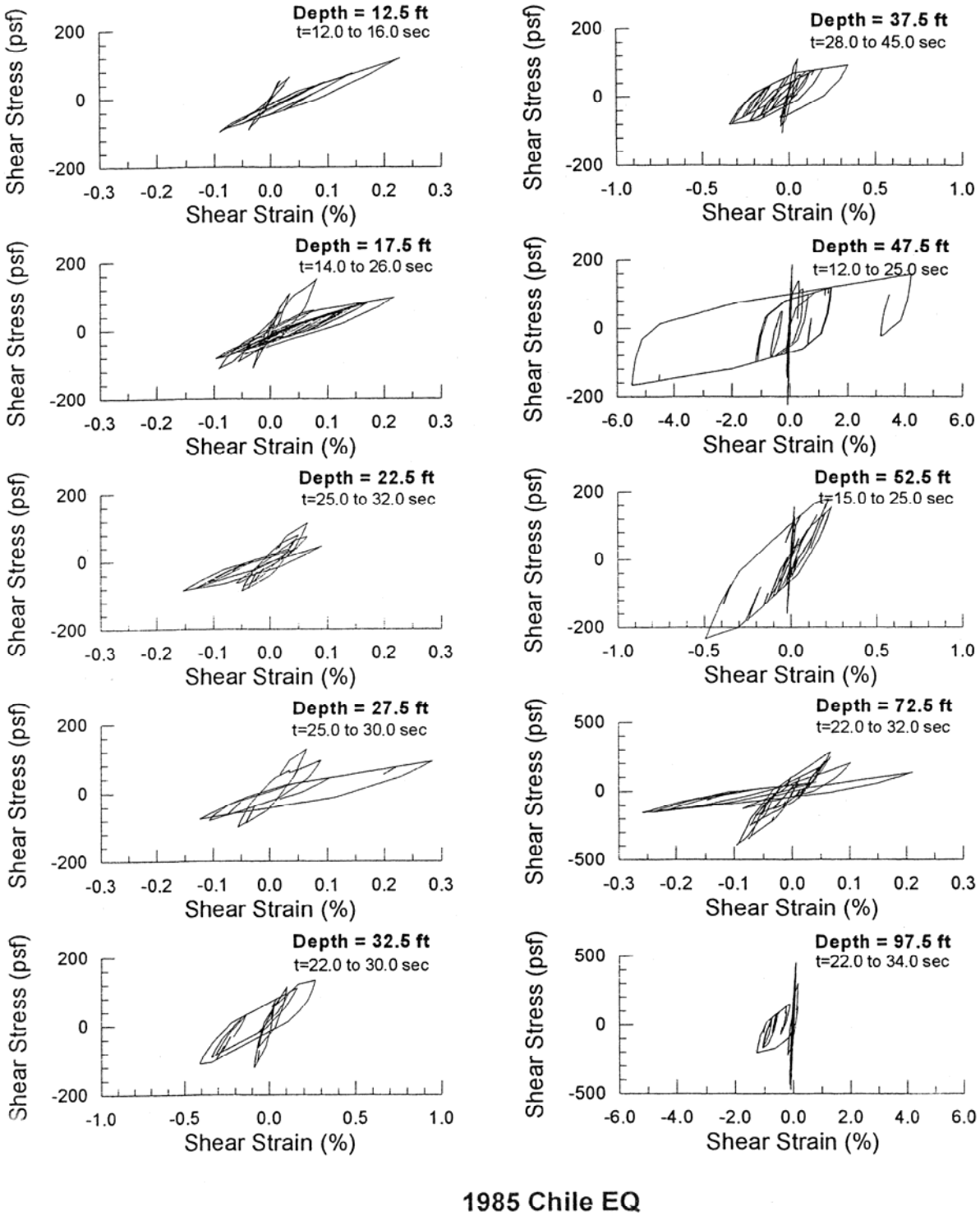

Figure E-11 **Shear Stress – Shear Strain Hysteretic Loops at Various Depths, 475-Year Earthquake (10% PE in 50-Year Ground Motion) Without Fill, Washington State Case Study**

also seen for the time histories based on the Olympia and Desert Hot Spring earthquakes, although as for the no fill case, liquefaction did not occur at depths greater than 55 feet for the 475-year Desert Hot Springs event.

The above results are again generally consistent with the factor of safety calculations using the simplified method, but with the notable differences that for the 475-year Olympia and Chile events, liquefaction occurred at depths between 70 and 100 feet, whereas factors of safety would have been greater than one based on the simplified method. This reflects the "bottom up" wave propagation used in DESRA-MUSC, versus the "top down" inertial loading from the simplified method.

E.6.3 Lateral Ground Displacement Assessment

From the results of the simplified liquefaction studies, two liquefiable zones were identified for stability and displacement evaluations. One extends from a depth of 10 feet to 20 feet below the ground surface. The other extends from 45 to 55 feet below the ground surface. The residual strength of these two liquefied zones was selected as 300 psf based on the SPT blow counts in each layer. Soils between 20 and 40 feet below the ground surface and between 55 and 100 feet below the ground surface were assumed to have partial build-up in pore water pressure, resulting in some reduction in the friction angle of the non-liquefied sand layers, as shown in the DESRA-MUSC analyses. For these conditions, the response of the end slope for the approach fill on each side of the channel was estimated by conducting pseudo-static stability evaluations followed by simplified deformation analyses using chart-based Newmark analyses. These correspond to Steps 2 and 3 of the design procedure of Article D. 4.2.2.

E.6.3.1 Initial Stability Analyses

Once liquefaction has been determined to occur, a stability analysis is performed to assess the potential for soil movement as indicated in Step 2 of the design procedure.

The computer program PCSTABL was used during these analyses. Most analyses were conducted using a simplified Janbu failure method of analysis with a wedge failure surface. This geometry was believed to be most representative of what would likely develop during a seismic event. Checks were also performed for a circular failure surface and using the modified Bishop and Spencer methods of analysis. Both pre-liquefaction and post-liquefaction strengths were used during these analyses.

Results of the pre-liquefaction studies indicate that the static FOS for the end slopes on each side of the channel was 1.5 or more, confirming acceptable static conditions. Yield accelerations (accelerations that produce FOS's of 1 on postulated failure surfaces in the pre-liquefaction state) were typically greater than 0.15, suggesting that some deformation would occur within the end slopes, even without liquefaction.

The FOS values dropped significantly when residual strengths were assigned to the two liquefied layers, as summarized in the following table. For these analyses the geometry of the failure surfaces was constrained to force failure through the upper or lower liquefied zone. Results given in the following table are for post-liquefaction conditions; i.e., no seismic coefficient for the right-hand approach fill.

Case	Abutment	Factor of Safety	Comment
Upper Wedge	Right	0.71	Modified Janbu
Lower Wedge	Right	0.79	Modified Janbu
Upper Circle	Right	0.81	Modified Bishop
Lower Circle	Right	0.86	Modified Bishop

Results of the stability analyses for the right-hand abutment indicate that for liquefied conditions and no inertial force in the fill (i.e., after the earthquake), factors of safety range from 0.7 to 0.9 for different assumptions of failure surface location and method of analysis. FOS values less than 1.0 indicate that lateral flow failure of the material is expected during any event that causes liquefaction in the two layers, whether it is associated with the 10% PE in 50 year or 3% PE in 75 year ground motion. The potential for instability is similar for failure surfaces through the upper and lower layers of liquefied soil, suggesting that any mitigation procedure would have to consider displacements through each layer. In other words, it would not be sufficient to improve only the upper 20 feet of soil where the FOS was lower, as a liquefaction-related failure could also occur at deeper depths.

Given the predicted occurrence of a liquefaction-induced flow failure, it would be desirable to quantify the amount of displacement expected dur-

ing this flow, which corresponds to Step 3 of the design procedure. Unfortunately, this is quite difficult when flow failures are predicted to occur. The simplified chart methods or the Newmark time history analysis, cannot be used to compute displacements for flow failures. However, flow displacements could be expected to be large, and such large displacements would indicate mitigation might be needed. More detailed analyses considering both structural pinning effects and ground modifications for mitigation of displacements are discussed in the following section of this Appendix.

E.6.3.2 Lateral Spread Implications from DESRA-MUSC Analyses

A key conclusion from the DESRA-MUSC analyses was the strong likelihood that lateral spread deformations would be controlled by a failure zone in the 45- to 50-foot layer. Displacement time histories for a rigid block sliding on this layer (assuming a Newmark sliding block analogy) were generated for a range of yield accelerations, using input acceleration time histories generated at the base of the 50- to 55-foot layer. The analyses were performed using the DISPMNT computer program (Houston et. al., 1987). "Upslope" deformations were suppressed assuming a strong one directional driving force from the embankment. At time zero, drained strengths for the liquefied layer were assumed. Strengths were degraded as a function of pore water pressure increase and reduced to the assumed residual strength of 300 psf when liquefaction was triggered. As would be expected, most of the computed displacements occurred subsequent to triggering.

Results showing displacement time history plots for the 3% PE in 75 year ground motion, based on the Chile earthquake as a function of yield acceleration, are shown in Figure H-12. Total accumulated displacements as a function of yield acceleration are shown in Figure H-13 for the three earthquake records. These plots became a basis for discussion on remediation analyses, as described in Article E.6.3.4. Similar analyses for potential failure surfaces in the depth zone of 10 to 20 feet, gave a maximum displacement of only 0.06 feet.

E.6.3.3 Stability Analyses with Mitigation Measures

Since it has been determined that significant soil movements will occur, Step 7 of the design procedure requires an evaluation of measures that will reduce the amount of movement.

Two procedures were evaluated for mitigating the potential for lateral flow or spreading: structural pinning and ground improvement. For these analyses the additional resistance provided by the improved ground or by the structural pinning of the soil was incorporated into the stability analyses described above. If the FOS for the revised analysis was greater than 1.0, the yield acceleration for the mitigated condition was determined, which then allowed displacements to be estimated. If the FOS was still less than 1, then flow would still occur and additional mitigation measures would be required.

For the structural pinning evaluation, shear forces were calculated to be 90 kips per pile for sliding on either the upper or lower failure surfaces. Procedures for determining the amount of pinning force are given in Section E.7.2. The abutment has 12 piles which extend through the sliding zone, resulting in 1,080 kips of additional shear reaction to sliding. Pier 5 of the bridge has 16 piles that produce 1,440 kips of pinning force. The abutment and the columns for Pier 5 are expected to develop reaction forces from passive pressure and column plastic shear. These forces were calculated to be 400 kips and 420 kips, respectively. This reaction occurs over the 48-feet abutment and pile cap widths, resulting in a total resistance of 31 and 70 kips per foot of width (or 1480 kips and 3340 kips, total) for displacement along the upper and lower liquefied zones, respectively.

This reaction force was introduced into the slope stability analysis using two methods:

1. A thin vertical slice the width of the pile group was placed at the location of the pile. This slice was assigned a strength that gives the same total pile resistance per unit width.

2. The resistance per unit width was converted into an equivalent shear strength along the shear plane in the liquefied zone, and this equivalent strength was added to the residual strength of 300 psf. For these analyses the upper failure plane was determined to be 104 feet in length giving an added component to

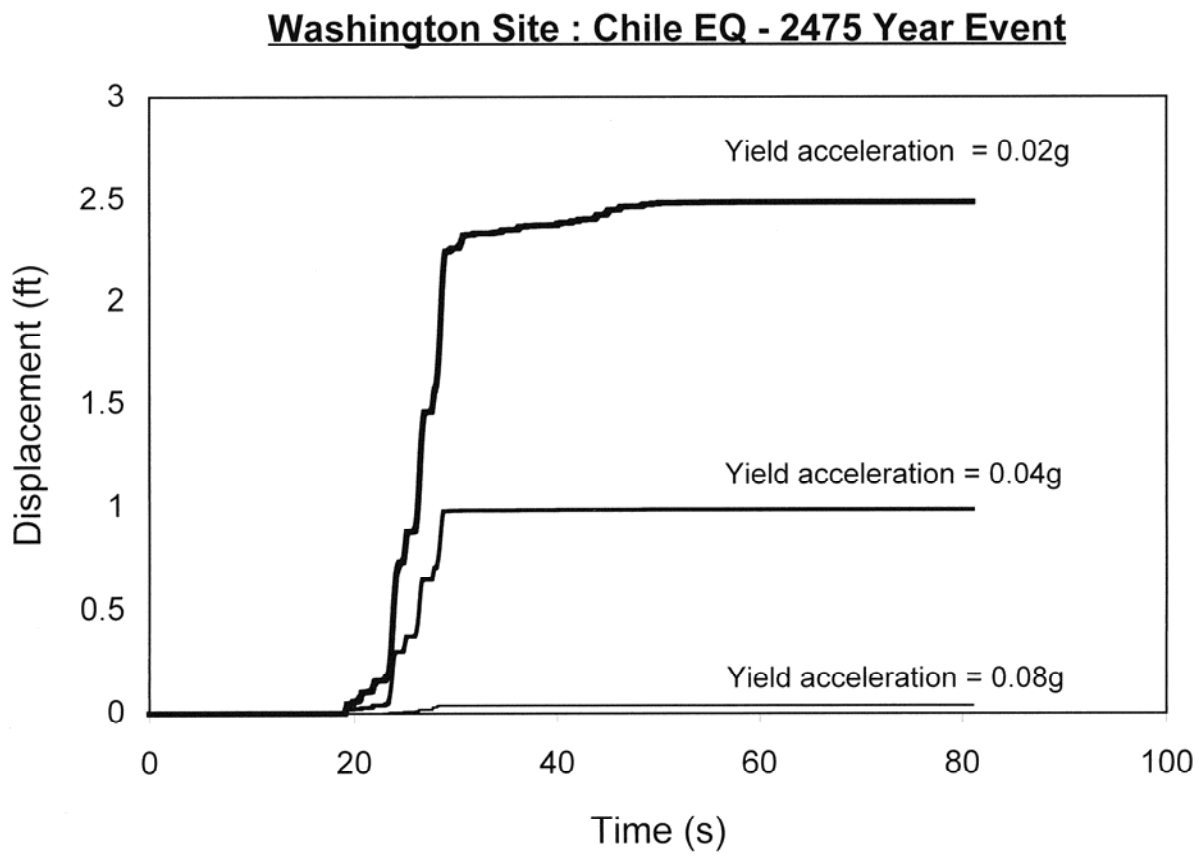

Figure E-12 Displacement vs. Time for 2475-Year Earthquake (3% PE in 75-Year Ground Motion), Washington State Case Study.

the liquefied strength of 300 psf. The resulting strength assigned to the liquefied layer was 600 psf (i.e., 300 psf + 300 psf = 600). For the lower zone, the surface is 132 feet in length, resulting in an average pinning resistance of 530 psf and a total resistance of 830 psf.

Both procedures gave generally similar results.

The FOS for the lower surface is greater than 1.0 for the post-liquefaction case, indicating that a post-earthquake flow failure would not occur. However, under the slope inertial loading, displacement of the slope could develop, and this can be assessed using the Newmark sliding block analysis once the yield acceleration is determined. The upper surface has a FOS of 1.0, indicating that a flow failure is on the verge of occurring.

The yield acceleration for the lower surface was determined by varying the seismic coefficient within the slope stability analysis until the factor of safety was 1.0. This analysis resulted in the lower surface yield acceleration given below. For the upper surface, it was assumed that the yield acceleration was zero, since the FOS was 1.0 without any additional inertial force.

Case	Yield Acceleration (g)
Upper Surface	0
Lower Surface	0.02

For the ground improvement case, different widths of improved ground were used below the abutment. The improved ground extended through each of the liquefied zones. Soil in the improved ground was assigned a friction angle of 45 degrees. This increase in strength was assumed to be characteristic of stone columns or a similar improvement procedure. As with the structural pinning case, two procedures were used to represent the improved zone. One was to model it explicitly; the second involved "smearing" the reaction from the improved strength zone across the failure surface by increasing the strength of the soil in the liquefied zone to give the same reaction. The re-

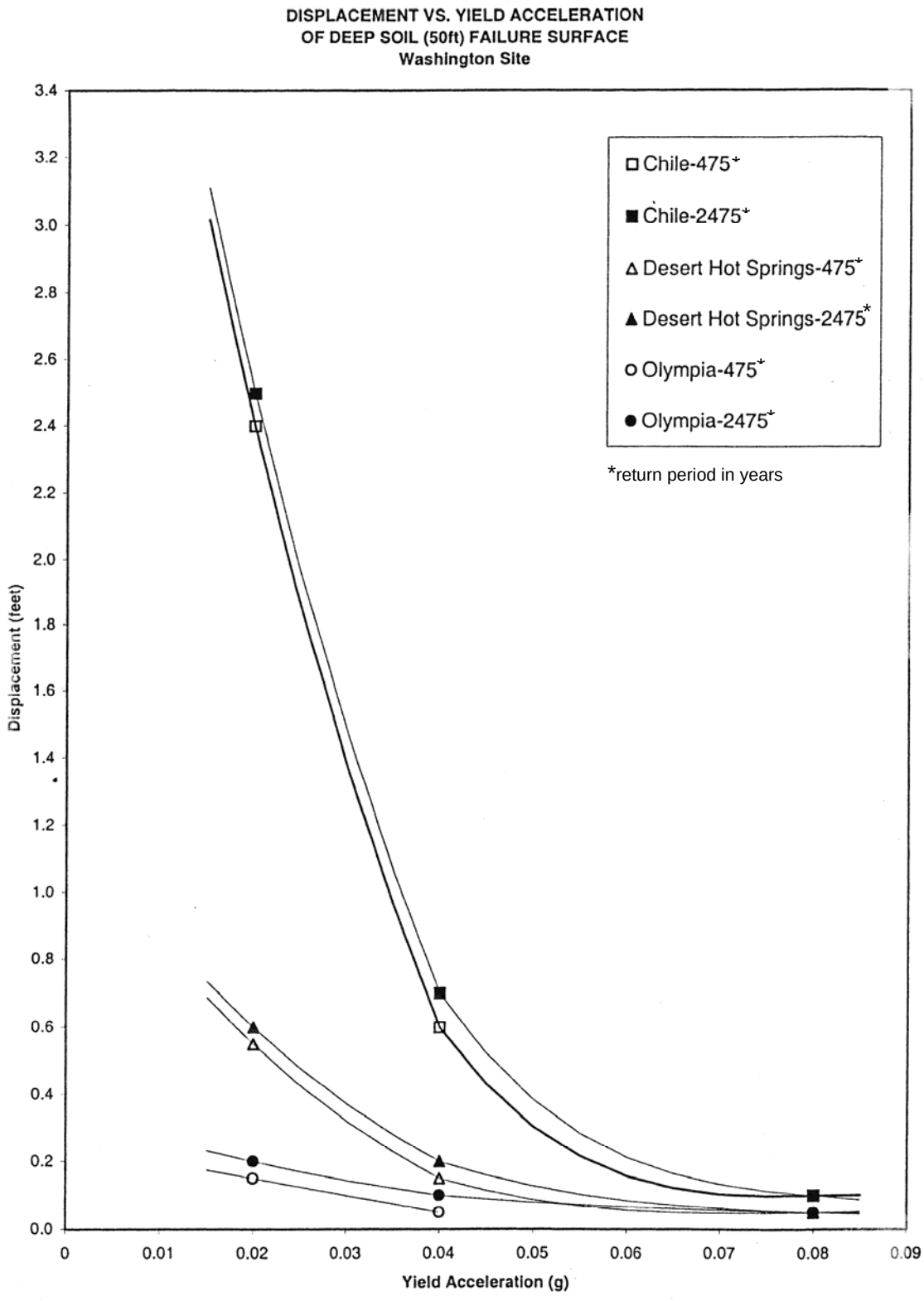

Figure E-13 **Displacement vs. Yield Acceleration for the Deep Sliding Surface of the Washington State Site**

sulting FOS was greater than 1.0 for all cases, indicating that flow would not occur. This allowed yield accelerations to be computed as a function of the width of the improved zone, in order to estimate the displacements that may occur. These values are summarized below.

Width (feet)	Yield Acceleration (g)
30	0.12
50	0.33
70	0.65

E.6.3.4 Displacement Estimates from Simplified Methods

Once lateral flow has been prevented, the amount of displacement that occurs from inertial loading on the failure wedge is estimated. This corresponds to Steps 3 and 11 of the design procedure.

Displacements were estimated for the yield accelerations given above using simplified methods. For these estimates, methods recommended by Franklin and Chang (1977), Hynes and Franklin (1984), Wong and Whitman (1982), and Martin and Qiu (1994) were used. All three methods approach the problem similarly. However, the Hynes and Franklin, as well as the Wong and Whitman and Martin and Qiu methods, eliminate some of the conservatism that is implicit to the Franklin and Chang method. For the Franklin and Chang method, it is necessary to define both the peak acceleration and velocity. The ratio of velocity to acceleration was assumed to be 30 for this study based on typical observations from recording of more distant events. For near-source events (epicentral distances less than about 15 km) this ratio can be as high as 60. In the case of the Hynes and Franklin method, displacements can be obtained for the mean, mean plus one standard deviation, and upper bound displacements. The mean displacements are used for this study. The Martin and Qui study was based on the Hynes and Franklin database, but included the peak ground acceleration as an additional variable in the data regression analyses. Mean values were also used in their regressions. Each of these simplified methods relates displacement to the ratio of yield acceleration to the peak ground acceleration (k_{max}). For these evaluations k_{max} was 0.24g and 0.42g for the 10% PE in 50 and 3% PE in 75-year ground motions, respectively. The resulting displacements for the cases cited above are summarized as follows.

Displacements (inches)				
	475-Year Event (10% PE in 50-Year Ground Motion)			
Case	Franklin & Chang	Hynes & Franklin	Wong & Whitman	Martin & Qiu
1	>36	16	10	28
2	<1	<4	<1	5
3	<1	<4	<1	<1
4	<1	<4	<1	<1
	2,475-Year Event (3% PE in 75-Year Ground Motion)			
Case	Franklin & Chang	Hynes & Franklin	Wong & Whitman	Martin & Qiu
1	>36	31	23	42
2	13	<4	3	8
3	<1	<4	<1	<1
4	<1	<4	<1	<1

Table notes: Case 1: Pile Pinning/Lower
Case 2: Stone Columns – 30 ft
Case 3: Stone Columns – 50 ft
Case 4: Stone Columns – 70 ft

It is the recommendation of the new provisions that a designer use the Martin and Qiu results. The Franklin and Chang, and Wong and Whitman, results provide possible upper and lower bound ranges on the displacements, but they are not believed to be as credible as the Hynes and Franklin, and Martin and Qiu, results.

The approximate displacement from the Martin and Qiu method for the 10% PE in 50 year ground motion is 28 inches. For the 3% PE in 75 year ground motion the displacement is 42 inches. (See table above.)

E.6.3.5 Displacement Estimates Using Site Response Analysis Results

This section corresponds to Steps 3 and 11 of the design procedure, as they apply to site-specific analysis of potential displacements using the nonlinear, effective stress method.

Similar estimates to the simplified methods described above may be made using the displacement versus yield acceleration curves shown in Figure H-13. As the curves are essentially identical for the 10% PE in 50 year and 3% PE in 75 year ground motions, the displacement estimates

shown in the table below are for both probability levels and for the lower yield surface (45-55-foot depth).

Case	Displacements (inches)		
	Chile	Olympia	Desert Hot Springs
Pile Pinning	29	7	3
Stone Columns (> 30 foot width)	< 1	< 1	< 1

These estimates are generally consistent with the estimates from the simplified methods, although the site-specific results indicate that the event representative of the large mega-thrust subduction zone earthquake (Chile) will produce the largest displacements. The displacements from a moderate magnitude subduction zone intraslab earthquake (Olympia) and a moderate magnitude local shallow crustal earthquake (Desert Hot Springs) produce much more modest displacements that could be accommodated by the foundations.

E.7 STRUCTURAL ANALYSIS AND DESIGN

The design of bridge structures for liquefaction effects generally has two components. The first is that the bridge must perform adequately with just the liquefaction-induced soil changes. This means that the mechanical properties of the soil that may liquefy are changed to reflect their liquefied values (i.e., properties such as stiffness are reduced). Design for these cases is in reality a design for structural vibration effects, and these are the effects that the code-based procedures typically cover for design. The second component of the design is the consideration of liquefaction-induced ground movements. The potential interaction or combination of these effects must be addressed in the design, and at the present, there is not sufficient understanding of the phenomena to normally warrant performing a combined analysis. Therefore, the recommended methodology is to simply consider the two effects independently; i.e., de-coupled. The reasoning behind this is that it is not likely that the peak vibration response and the peak spreading or flow effect will occur simultaneously. In fact, for most earthquakes the peak vibration response is likely to occur somewhat in advance of the maximum ground movement loading. Furthermore, the de-coupling of response allows the flexibility to use separate and different performance criteria for design to accommodate the two phenomena. In some areas where extended shaking could result in the two phenomena occurring concurrently, it may be desirable to use more rigorous coupled effective stress computer models to evaluate this.

E.7.1 Vibration Design

Vibration design was done for both the current AASHTO *Specifications* and for the recommended NCHRP 12-49 LRFD provisions. For the recommended LRFD provisions, both the 3% PE in 75 year and 50% PE in 75 year ground motions were considered. Since the primary objective of the study was to compare the existing and recommended provisions, the designs were more of a preliminary nature, which was felt to be sufficient to highlight the major differences. In this study, the same bridge was evaluated for each of the two specification requirements. Comparisons were then based on the amounts of reinforcing, for example, and in the case where sizes should be altered, recommendations are given. To this end, the designs represent preliminary designs that highlight the differences between the two specifications. A very brief summary follows.

The bridge is comprised of multi-column bents so the existing provisions use an *R*-factor of 5, and the recommended provisions allow an *R*-factor of 6 provided a nonlinear static displacement check is done. For the 100 year design the proposed provisions allow an *R* of 1.3.

For the tallest columns and the recommended LRFD provisions, ground motion for the 2,475-year event required a steel content in the columns of 1.4%, and this was controlled by the 100-year event ground motion. The 100-year event ground motion produced a design moment that was approximately 20% larger than the 2,475-year event. This is due to the relative magnitudes of *R* and of the input spectra. For the 475-year event ground motion a design using 1% steel resulted. For Pier 2 the results were similar.

The foundation (piling), used as starting point for both the existing and recommended provisions, was the same. This is because one objective of the study was to evaluate a system that worked for the existing provisions when subject to the effects of the larger design earthquake ground motion.

The pier designs were checked for displacement capacity, using an approximate push over analysis. The assessment considered the super-

structure and the pile caps as rigid restraints against rotation for simplicity. While the check is only required for the recommended provisions, the checks were performed on the designs to the existing provisions, as well. All the columns met the checks (i.e., the displacement capacity exceeded the demands).

The recommended LRFD provisions also require that the displacements be checked for P-Δ effects. In other words, the lateral shear capacity of the bents defines a maximum displacement that can occur without suffering problems from displacement amplification due to P-Δ. Both piers are adequate as-designed with respect to P-Δ.

E.7.2 Lateral Spreading Structural Design/Assessment

The material in this section generally represents Steps 4, 5, 6, 8, 9 and 12 of the recommended Design Procedure, and the material addresses the structural aspects of the procedure.

In Section E.6.3 the tendency for the soil near Piers 5 and 6 to move during or after a major earthquake was assessed. Once it had been determined that lateral spreading would occur, the next step (Step 7) was to evaluate the beneficial pinning action of the foundation system in the analysis. This section describes the method of determining the pinning force to add to the stability analyses of Section E.6.3, and it describes the process of determining whether flow around the foundation would occur or whether the foundation will move with the soil. This involves Steps 4 and 5 of the design procedure.

E.7.2.1 Modes of Deformation

As outlined above there are two potential sliding surfaces during liquefaction for the Pier 5/6 end of the bridge. One is at the base of the upper liquefiable layer, and the other is at the base of the lower liquefiable layer. These potential deformation modes must be determined to evaluate the forces developed by the piles and the structures resistance.

The overall foundation deformation modes may be formally assessed using models that consider both the nonlinear nature of the soil resistance and the nonlinear behavior of the piles and foundations, when subject to prescribed soil displacement profiles. In this study, the deformations and structural behavior have been approximated using assumed displaced structural configurations that are approximately compatible with the constraints provided by the soil. Examples of these configurations are given in Figures D.4.2-4, D.4.2-5, and H-14. In this example, the abutment foundation will move in a manner similar to that shown in Figure D.4.2-4, because there are sliding bearings at the substructure/superstructure interface. In the figure, the frictional forces transferred through these bearings have been conservatively ignored.

Pier 5 will move similar to the mode shown in Figure D.4.2-5. Under such a displaced shape both the columns and the piles contribute to the lateral resistance of the foundation. The columns contribute because there is an integral connection between them and the superstructure. In the current assessment, the residual displacements have been ignored. There exists some question as to whether this should be included or not. The reductions in resistance due to P-Δ effects are likewise given in the figure, but for many of the deformations and column height combinations considered in this study, this reduction is small, and therefore it has not been included in the calculations.

E.7.2.2 Foundation Movement Assessment

As described in Step 4 through 6 of the design procedure, an assessment should be made whether the soil will move around the foundation or whether it will move the foundation as it moves. Passive capacities of the various layered soils were extracted from the p-y curves generated by conducting LPILE analyses[4] for the piles. These forces represent the maximum force that is exerted against the piles as the soil moves around the pile. This then is the upper bound limit state of the soil force that can be developed. Additionally, the maximum passive forces that can be developed against the pile caps and abutment stem wall were developed. Two total forces were developed; one for the shallow-seated soil failure and one for the deep failure. The shallow failure will develop approximately 1100 kips/pile and the deep failure approximately 3500 kips/pile at the point where the soil is moving around the foundation. By comparison, one pile with a clear distance of 30 feet between plastic hinges can develop about 90 kips of shear at the point where a full plastic mechanism has formed in the pile. The conclusion

[4] LPILE is a computer program used to evaluate lateral response of piles subjected to loads and moments at the pile head. This program is similar to COM624.

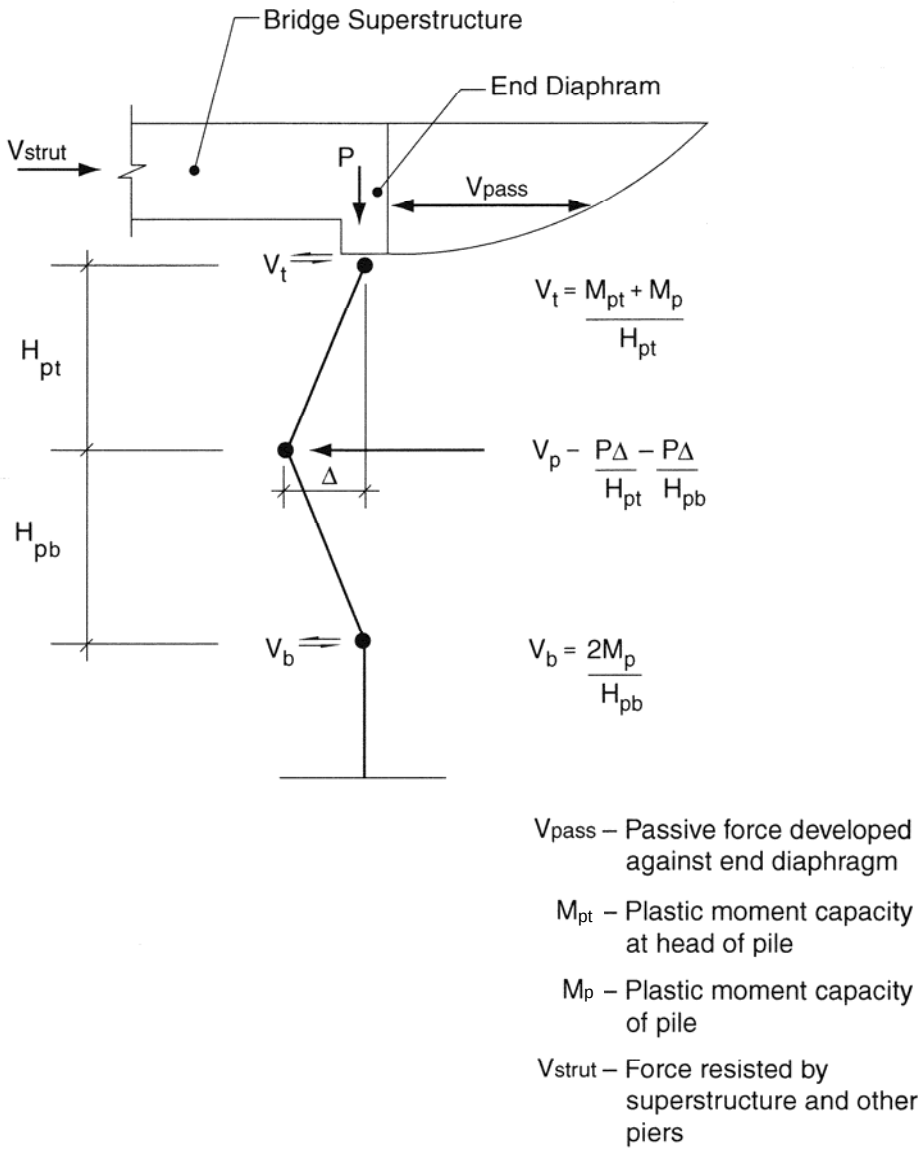

Figure E-14 Plastic Mechanism for an Integral Abutment Supported on Piles, Washington State Case Study

from this comparison is that there is no practical likelihood that the soil will move around the piles. Instead the foundations will be pushed along with the soil as it displaces toward the river channel beneath the bridge.

Intuitively, it is only reasonable to expect that soil will move around a pile if there is no crust of non-liquefied material being carried along with the displacing soil (Step 4 of the design procedure). In the case examined here, there are significant (10's of feet) non-liquefied material above the liquefiable material, and it is that material which contributes to the high passive forces. Thus if a reasonable crust exists, the foundations are likely to move with the soil.

Now the questions to be considered are: (1) can the foundation systems endure the displacement that the soil produces (Step 6), and (2) can the foundations appreciably reduce the soil movement via pinning action (Step 7).

E.7.2.3 Pinning Force Calculation

In Article E.6 various pinning forces were discussed and included with the stability analyses to investigate the effectiveness of including the exist-

ing foundation pinning. The following discussion accounts for the development of the force values used.

Figure H-15 illustrates qualitatively the forces developed against the foundations and how they are reacted using the bridge, itself, as a strut. Two soil blocks are shown, Block A on the right and B on the left. Block A represents a postulated deep-seated slide that affects both Piers 5 and 6. The shears, V_{p5} and V_{p6}, represent the pinning shear force developed by the piles of Pier 5 and 6, respectively. Shear V_{c5} is the shear contributed by the Pier 5 columns. Finally, V_{pa5} is the passive resistance provided by the backfill acting against the end diaphragm.

While Block A is the most likely of the two to move, Block B is shown in this example to illustrate where and how the forces transferred into the bridge by Block A are resisted. In this case the bridge acts as a strut. Note that if a significant skew exists, then these forces cannot be resisted without some overall restraint to resist rotation of the bridge about a vertical axis.

Figure H-16 illustrates the pinning forces acting on a soil block sliding on the lower liquefiable layer. In this case, abutment and Pier 5 piles each contribute about 90 kips, the abutment about 400 kips, and the columns at Pier 5 about 420 kips. The total abutment pile resistance is 1080 kips and corresponds to the approximate plastic mechanism shear with 30 feet clear between points of assumed fixity in the piles. This comprises 10 feet of liquefiable material and 5*D* (*D* = pile diameter) to fixity above and below that layer[5]. The upper portion of the soil block is assumed to move essentially as a rigid body, and therefore the piles are assumed to be restrained by the integrity of this upper block. The pile resistance at Pier 5 is determined in a similar manner, and the shear that the Pier 5 piles contribute is 1440 kips. The abutment passive resistance corresponds to half of the prescribed passive capacity of the backfill and is assumed to act against the end diaphragm. The abutment fill is assumed to have slumped somewhat due to the movement of the soil block, and thus half of the nominal resistance was judged to be reasonable. The column resistance at Pier 5 is 420 kips, and this assumes that plastic hinging has occurred at the top and bottoms of the columns at this pier.

These forces (3360 kips) represent maximum values that occur only after significant plasticity develops. In the case of Pier 5 the approximate displacement limit is 22 inches, which comprises 4 inches to yield and 18 inches of plastic drift. The plastic drift limit is taken as 0.05 radians. The 22-inch displacement limit of Pier 5 is controlled by the piles. Because the piles of Pier 6 are the same, their limit is also 22 inches of displacement.

Because the Pier 5 columns are longer than the distance between hinges of the piles, the column displacement limits are 34 inches total and 7 inches at yield. The fact that the piles control the displacement limit in this case implies that some margin is available in the column to accommodate any residual plastic hinge rotations that remain in the column after strong shaking stops.

Figure H-17 shows the displaced shape of the foundations for a shallow (upper layer) soil failure. In this case, the distance between plastic hinges in the piles is 30 feet, just as with the deeper failure, and thus the plastic shear per pile is 90 kips. The total contributed by the piles is 1080 kips as before.

In Section E.6.3, the estimated displacements for the lower or deeper failure wedge were 28 inches for the 10% PE in 50 year ground motion and 42 inches for the 3% PE in 75 year ground motion. Neither of these are within the plastic capacity of the piles and either additional piles could be added as'pinch' piles or ground remediation could be used[6]. It will be recalled that the yield acceleration for the upper failure was essentially zero for both the 10% PE in 50 year and 3% PE in 75 year ground motions, which indicates that some remediation would be required to stabilize the fill and its toe for both design ground motions.

E.8 COMPARISON OF REMEDIATION ALTERNATIVES

The primary intent of these analyses was to determine the potential effects of increasing the seismic design ground motion criteria from its current probability of exceedance of 10% in 50 years to 3% in 75 years. Liquefaction was predicted for both probability of exceedance levels (earthquake return periods), and as a consequence, there is little difference in what remedial work is required

[5] Fixity was assumed to develop 5*D* above the liquefied layer. In an actual design case, a lateral analysis using a computer code such as LPILE could be conducted to be more rigorous about the distance to fixity.

[6] Pinch piles refer to piles driven at close spacing to increase the shear resistance or density of a soil mass. In the Pacific Northwest, these piles are often timber.

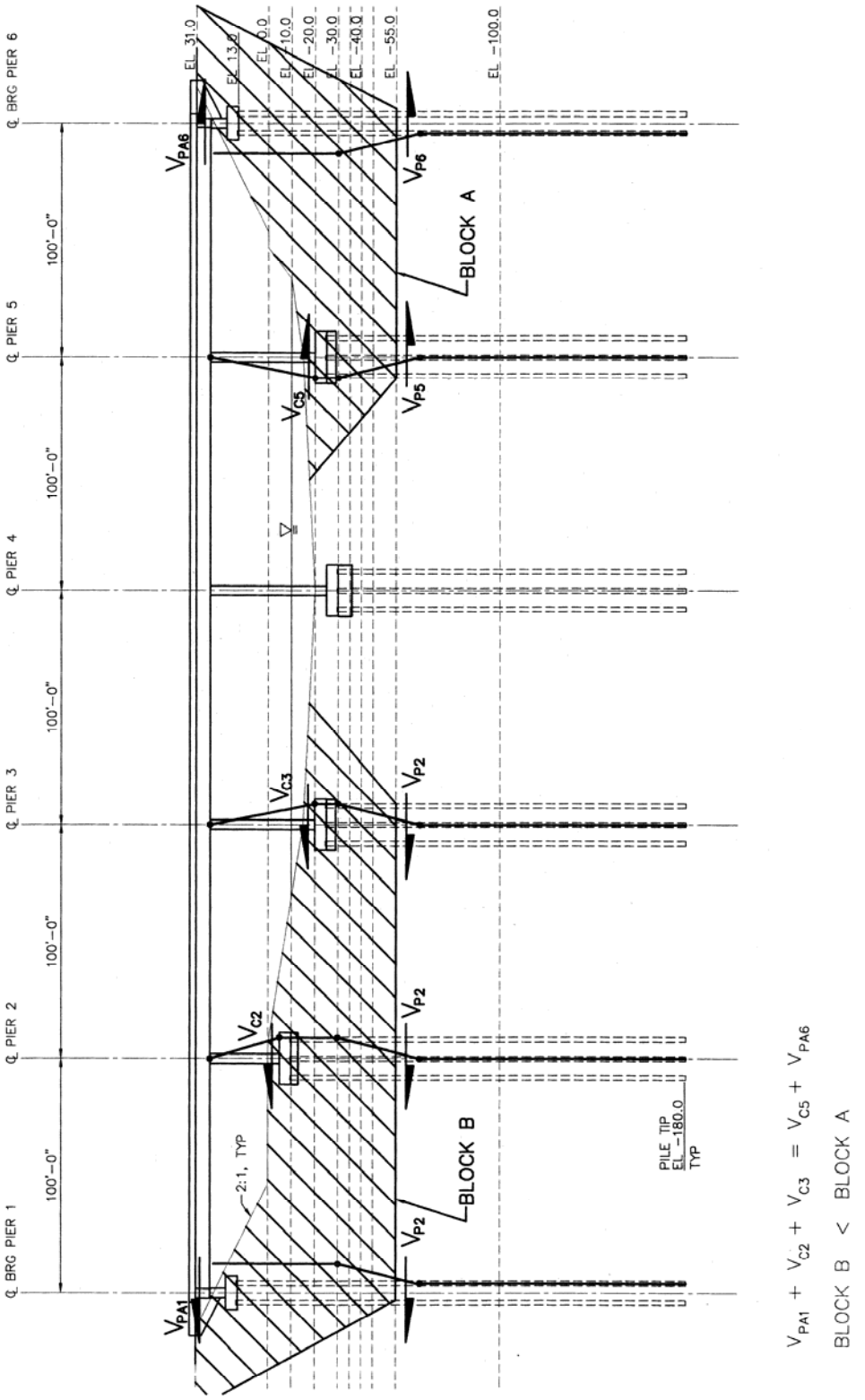

Figure E-15 **Forces Provided by Bridge and Foundation Piling for Resisting Lateral Spreading, Washington State Case Study**

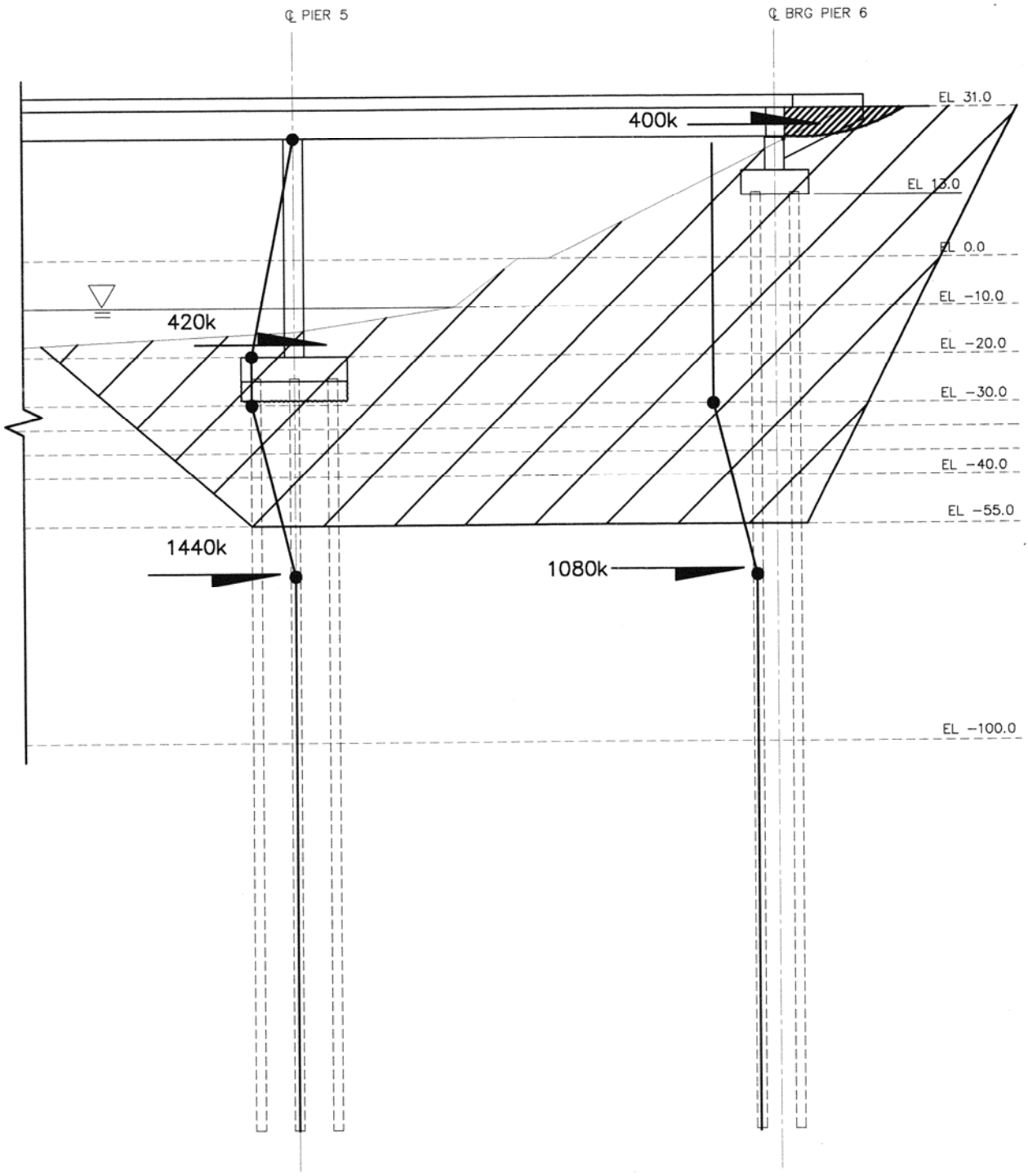

Figure E-16 **Piers 5 and 6 Resisting Lateral Spreading – Deep Wedge, Washington State Case Study**

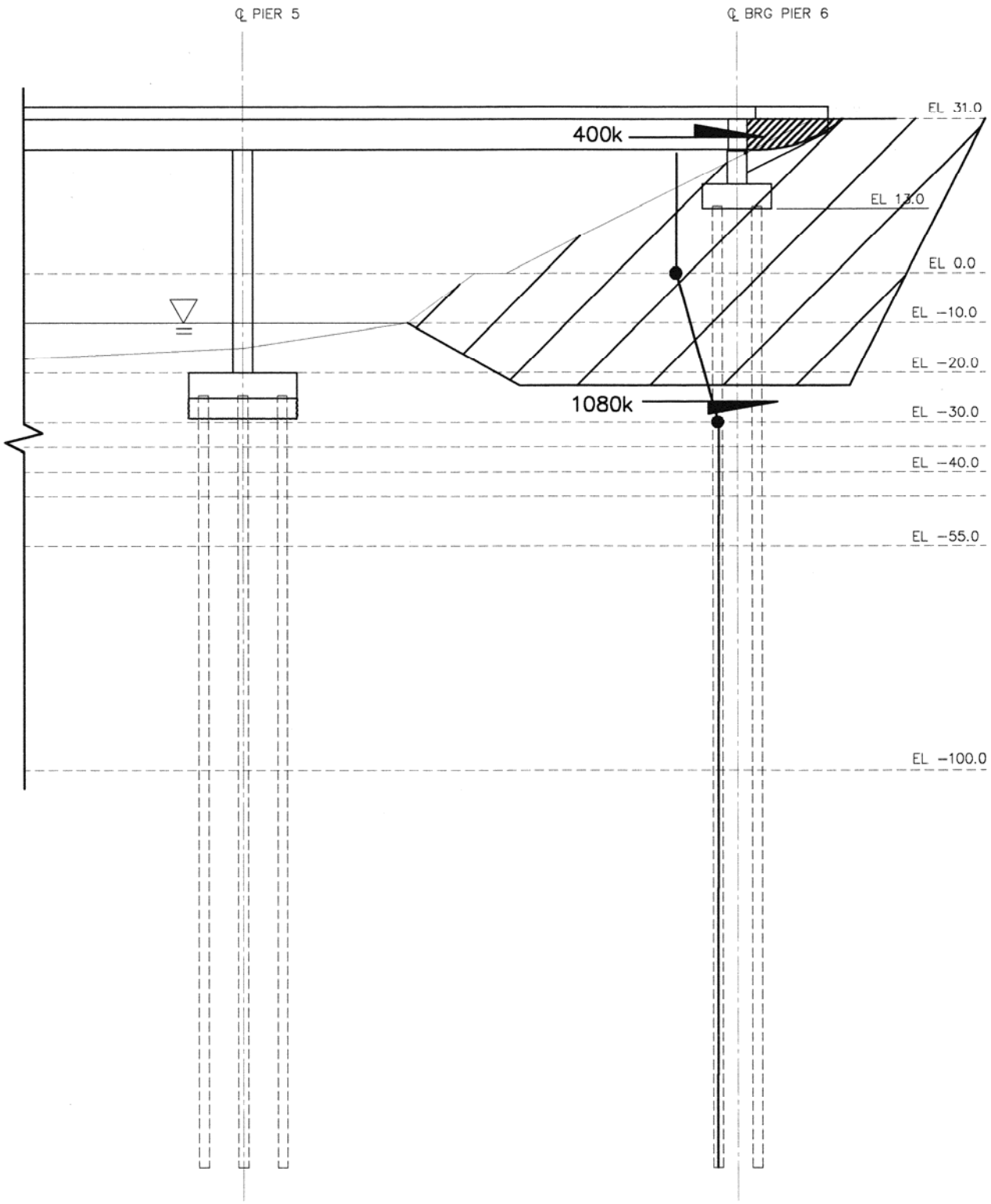

Figure E-17 Pier 6 Resisting Lateral Spreading – Shallow Wedge, Washington State Case Study

for the two probability of exceedance levels (earthquake return periods).

E.8.1 Summary of Structural and Geotechnical Options

Mitigation measures are assessed based on the desired performance requirement of the bridge. The first option is to assess the performance in its as-designed configuration. If this results in unacceptable performance, a range of mitigation measures is assessed.

For this example, some form of structural or geotechnical remediation is required at the right-hand abutment because the yield acceleration for the upper failure wedge is zero. This implies that this wedge is unstable under static conditions after the soil liquefies, which it does for both the 3% PE in 75 year ground motion and the 10% in 50 ground motion[7]. Two choices for improving the conditions were considered — use of additional piles or stone columns. Since the yield acceleration for the upper failure surface is so low, the more effective choice of the two was to use stone columns. These provide the combined advantage of increasing the residual shear strength of the sliding interface, and they can reduce pore water pressure build up, thereby postponing or possibly eliminating the onset of liquefaction.

Because the lower failure wedge also has a relatively low yield acceleration, 0.02g, it makes sense to extend the mitigation deep enough to improve the deeper soil layers, as well. This low yield acceleration results in displacements of 28 inches and 42 inches for the 10% PE in 50 year and 3% in 75 year ground motions from the simplified analyses and displacements of approximately 29 inches for both ground motion events for the time history corresponding to the mega thrust subduction zone earthquake for the site-specific Newmark analyses. The decision to improve the deeper layers requires that stone columns extend on the order of 50 feet in depth. The stone column remediation work will provide displacements that are less than 4 inches. This will keep the piles within their elastic range, and this will meet the highest level of operational performance objectives in the foundation system.

[7] The approach fill and ground profile condition for the bridge considered in this study are more severe than that used in the actual bridge that this example was modeled after. Thus, the implication of instability here does not imply instability in the prototype structure.

Although in this example the left-hand abutment was not evaluated in detail because the FOS of the initial stability analyses was greater than 1, a cost/benefit assessment would typically be made to determine if some remediation work on the left-hand abutment would be cost effective. Once a contractor is mobilized on the site, it would make some sense to provide improvement on both sides of the river. It may be that upon more in-depth investigation the stone columns could be spaced further apart or applied over a smaller width on the left-hand bank.

E.8.2 Comparisons of Costs

As noted above, the remedial work is required for both the 10% PE in 50 year and 3% PE in 75 year ground motions.

The stone column option would likely be applied over a 30-foot length (longitudinal direction of bridge), since that length produced acceptable deflections of less than 4 inches for the site specific results, which is within the elastic capacity of the piles. The width at a minimum would be 50 feet, and the depth also would be about 50 feet. If the columns were spaced roughly on 7-foot centers, then 40 stone columns would be required. At approximately $30 per lineal foot (plf), the overall cost per approach fill would be on the order of $60,000, or about $120,000 for both sides if the left-hand fill were judged to require remediation.

As a rough estimate of the cost of the overall structure, based on square-footage costs of $100 to $150 in Washington, the bridge would cost between 2 and 3 million dollars. If the higher cost were used, due to the fact that the bridge is over water and the foundation system is relatively expensive because of its depth, the cost to install stone columns on the right-hand side would run about 2% of the overall cost of the bridge. If both sides were remediated, then the costs would comprise about 4% of the bridge costs. It should be noted that this additional cost will produce a foundation performance level that meets the operational criteria for both ground motion probability of exceedance levels.

If pinch piles were used to augment the piles of the foundations, the pinch piles would not need to be connected to the foundation, and they would not need to extend as deep as the load-bearing foundation piles. The per pile costs for the foundation piles were estimated to be on the order of $10,000 to $12,000 each for 180-foot long piles. If shorter piles on the order of 80-feet long were

used, their costs would be about half as much. Thus if pinch piles were used about 10 to 12 piles per side could be installed for the same cost as the stone column remediation option. Although detailed analyses have not been performed with these pinch piles, the amount of movement anticipated would be in the range of 6 to 12 inches, rather than the 4 inches obtained with the stone columns. Therefore, the stone column option would appear the more cost effective in this situation. On a specific project, combinations of the two options would be evaluated in more depth.

It is useful to recognize that in this situation some remediation would be required for both the 10% PE in 50 year and 3% PE in 75 year ground motions because of the predicted instability of the upper failure wedge. In the case of the former, the remediation is required to a depth of 50 feet because the anticipated movement of the lower failure wedge would be on the order of 28 inches for the simplified analyses and 30 inches for the site specific analysis and thus be in excess of the 22 inch limit. For the 3% PE in 75 year ground motion, movement on the order of 42 inches is predicted by the simplified analysis, and 30 inches by the site-specific analyses. Consequently, remediation is required to a depth of 50 feet for both cases. Hence the difference in cost for this site and bridge between the two design earthquakes is minimal.

E.9 MISSOURI EXAMPLE

The second bridge considered in this study is located in the New Madrid earthquake source zone in the lower southeast corner of Missouri. This general location was selected because this zone is one where a significant seismic hazard occurs, and there are numerous stream crossings and low-lying areas where potential for liquefaction also exists. Additionally, the project team wished to include a non-western site where the effects of different source mechanisms and where the differences in shaking levels between the 475-year and 2,475-year events would be highlighted. Since the design process and procedures used for this example are the same as the Washington example, an abbreviated summary of the key results follows. The details of the work on this bridge can be found in the companion *Liquefaction Study Report* (ATC/MCEER, 2003a).

E.9.1 Site Characterization and Bridge Type

The site is located in southeastern Missouri along the western edge of the Mississippi River alluvial plane near the New Madrid seismic zone. Soils at this site consist of 20 feet of clay over a 20-foot layer of sand over dense alluvial materials at depths greater than 40 feet. The Missouri Department of Transportation (MoDOT) provided site characterization information for the prototype site, including boring logs with SPT's, CPT soundings, and shear wave velocity data. The geotechnical information was collected by MoDOT for a lifeline earthquake evaluation that they are currently conducting.

The simplified bridge used for the overcrossing is approximately 180 feet long, and comprises three, roughly equal-length spans. There are no horizontal or vertical curves on the bridge, and the bridge has no skew. A general elevation of the bridge and of the ground line is given in Figure H-18. The bridge and site plan have been simplified from that initially provided by MoDOT for illustrative purposes. The configuration of the bridge was selected, in part, due to its common nature. Many states use this type of bridge or variations to this type of bridge. Thus it was felt that the results for such a bridge type would be widely relevant to many other regions around the country.

The bridge structure comprises AASHTO-specified prestressed girders supported on three-column bents. The roadway is approximately 38 feet wide, and five 39-inch girders with a concrete deck form the superstructure. The substructure is formed of 3-foot diameter columns, which support a 40-inch dropped cap-beam. The foundations of the intermediate piers are individual pile caps for each column that are supported on 14-inch steel pipe pile foundations. An elevation of one of the intermediate piers is given in Figure H-19.

The abutments are of the integral type, where the end diaphragm is integrated with the ends of the girders and deck and is directly supported by nine 14-inch-diameter pipe piles. These piles form a single line in the transverse direction to the bridge. An elevation of the abutment is shown in Figure H-20.

The deaggregation results for the Missouri site show that, for both 475-year (10% PE in 50 year ground motion) and 2,475-year (3% PE in 75 year ground motion) return periods and for both short periods and long periods of the response spectrum,

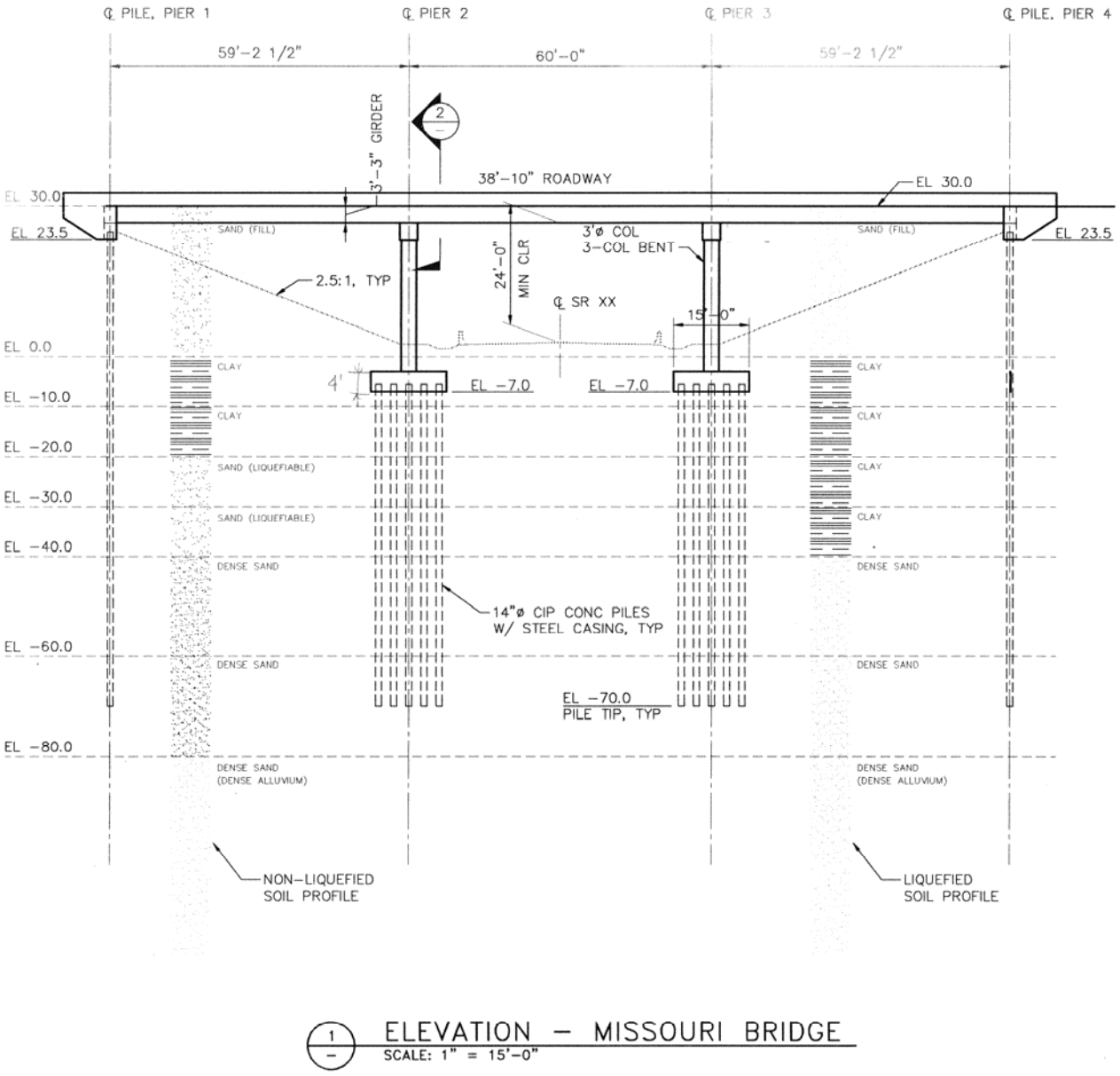

1 ELEVATION – MISSOURI BRIDGE
SCALE: 1" = 15'–0"

Figure E-18 Elevation and Ground Profile for the Mid-America (Missouri) Bridge

the ground motion hazard is dominated by magnitude 8 earthquakes occurring 30 to 80 km from the site. These earthquakes are associated with the New Madrid seismic zone. The range of distances from the New Madrid source reflects the modeling by USGS of the earthquake fault(s) within a relatively broad source zone, since the exact location of the fault(s) within the zone are not known.

The deaggregation results for the Missouri site differ from the results for the Washington site, where three different seismic source types and magnitude and distance ranges contributed significantly to the ground motion hazard. For the Missouri site a single large magnitude source mechanism dominates the seismic hazard. Three natural recordings were selected from large magnitude earthquakes in Mexico, Chile and Japan to represent the time domain characteristics of the design earthquakes. These records were frequency scaled to be consistent with the design spectra for the site.

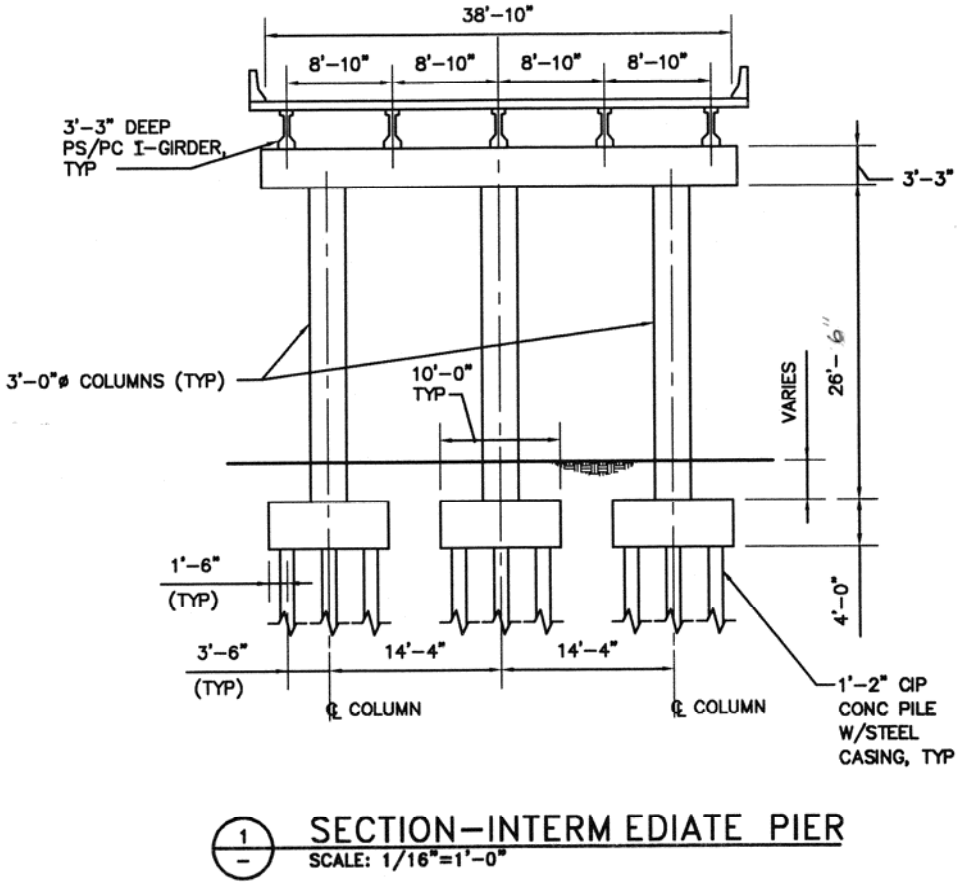

Figure E-19 Elevation of Intermediate Pier, Missouri Bridge

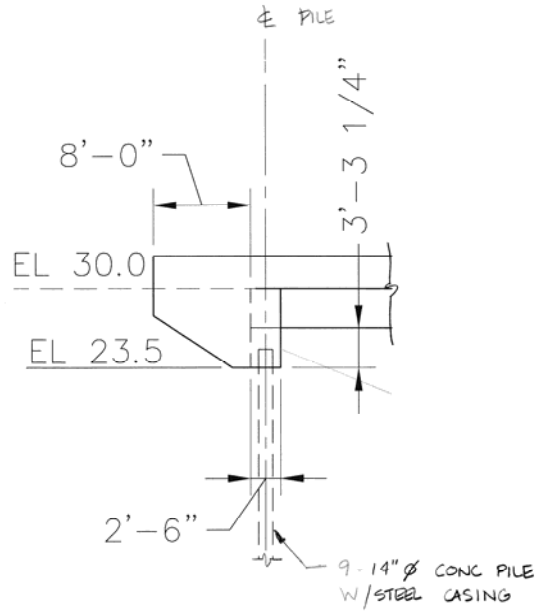

Figure E-20 Elevation of Integral Abutment, Missouri Bridge

E.9.2 Liquefaction Analyses

The first step of the procedure outlined in Section D.4.2.2 is to determine if liquefaction occurs.

Simplified liquefaction analyses were conducted using the procedures given in Youd and Idriss (1997). Two levels of peak ground acceleration (PGA) were used, one representing the 475-year event within the current AASHTO *Specifications* and the other representing the recommended 2,475-year event. The PGA for the 475-year event was not adjusted for site effects, consistent with the approach recommended in the AASHTO *Specifications*[8]. Ground motions for the 2,475-year event were adjusted to Site Class D, using the procedures given in Section 3 of the recommended LRFD provisions (see companion Part I document). The resulting PGA values for each case are summarized below.

Input Parameter	475-Year Return Period	2,475-Year Return Period
Peak ground acceleration	0.17g	0.53g
Mean Magnitude	6.6	7.5

The magnitude of the design earthquake is required for the SPT and CPT simplified analyses. As discussed previously, results of deaggregation studies from the USGS database for deaggregation suggest that the mean magnitudes for the 475- and 2,475-year events are 6.6 and 7.5, respectively. The mean magnitudes reflect contributions from small to moderate magnitude earthquakes occurring closer to the site. However, the dominant event is the characteristic Magnitude-8 earthquake in the New Madrid seismic zone. For the simplified liquefaction assessment, a range of magnitudes thought to be representative of practice was used in the evaluation. For time history analyses, acceleration time histories representative of the duration of the Magnitude-8 New Madrid earthquake and the levels of ground motion defined by the current AASHTO *Specifications* spectrum and the MCE spectrum of the recommended NCHRP 12-49 LRFD provisions were developed.

For these analyses ground water was assumed to occur 20 feet below the ground surface for the non-fill case.

Factors of safety (FOS) results from the liquefaction evaluations for the simplified soil model without fill for the three magnitudes are shown in Figure H-21 and Figure H-22 for the 475-year (10% PE in 50-year ground motion) and 2,475-year (3% PE in 75-year ground motion) return periods, respectively. These results indicate that liquefaction may or may not occur for the smaller (475 year return period) event, depending on the assumed magnitude of the earthquake. For the magnitude based on the mean of the deaggregation for the site, liquefaction is not predicted. For the 2,475-year return period event, liquefaction is predicted, regardless of the assumed magnitude.

Ground response analyses were also conducted using DESRA-MUSC, similar to those described in Section E.6.2. Results of these analyses are included in the companion *Liquefaction Study Report* (ATC/MCEER, 2003a). Based on the simplified liquefaction analyses and on the nonlinear effective stress modeling, it was concluded that lateral spread deformations would be distributed over the 20- to 40-foot depth. However, for analysis purposes, in order to compute likely displacement magnitudes of the overlying 20 feet of clay and embankment fill, it was assumed that ground accelerations, at the 40 feet interface depth, would control the displacement, assuming a Newark sliding block analogy.

E.9.3 Initial Stability Analysis

The first step in the liquefaction evaluation involved an analysis of the post-earthquake stability. In this analysis stability was evaluated for the liquefied condition but without a seismic coefficient. This check was performed to determine if a flow failure would occur in the liquefied state. Results from these analyses show that the FOS dropped significantly when a residual strength was assigned to the liquefied layer; however, the FOS was greater than 1.0, indicating that a flow failure was not expected. This allowed displacements to be estimated using the simplified Newmark method described in Section E.9.2.

Yield accelerations were initially estimated without consideration of the pinning effects of

[8] Common practice is to adjust the PGA for the site factors given in Table 2 of Division 1-A of the current AASHTO *Specifications*. While this adjustment may be intuitively correct, these site factors are not explicitly applied to the PGA. If the site coefficient were applied at the Missouri site, the PGA would be increased by a factor of 1.5, reducing the difference in the ground motions between the 475 year and the 2475 year return-period events.

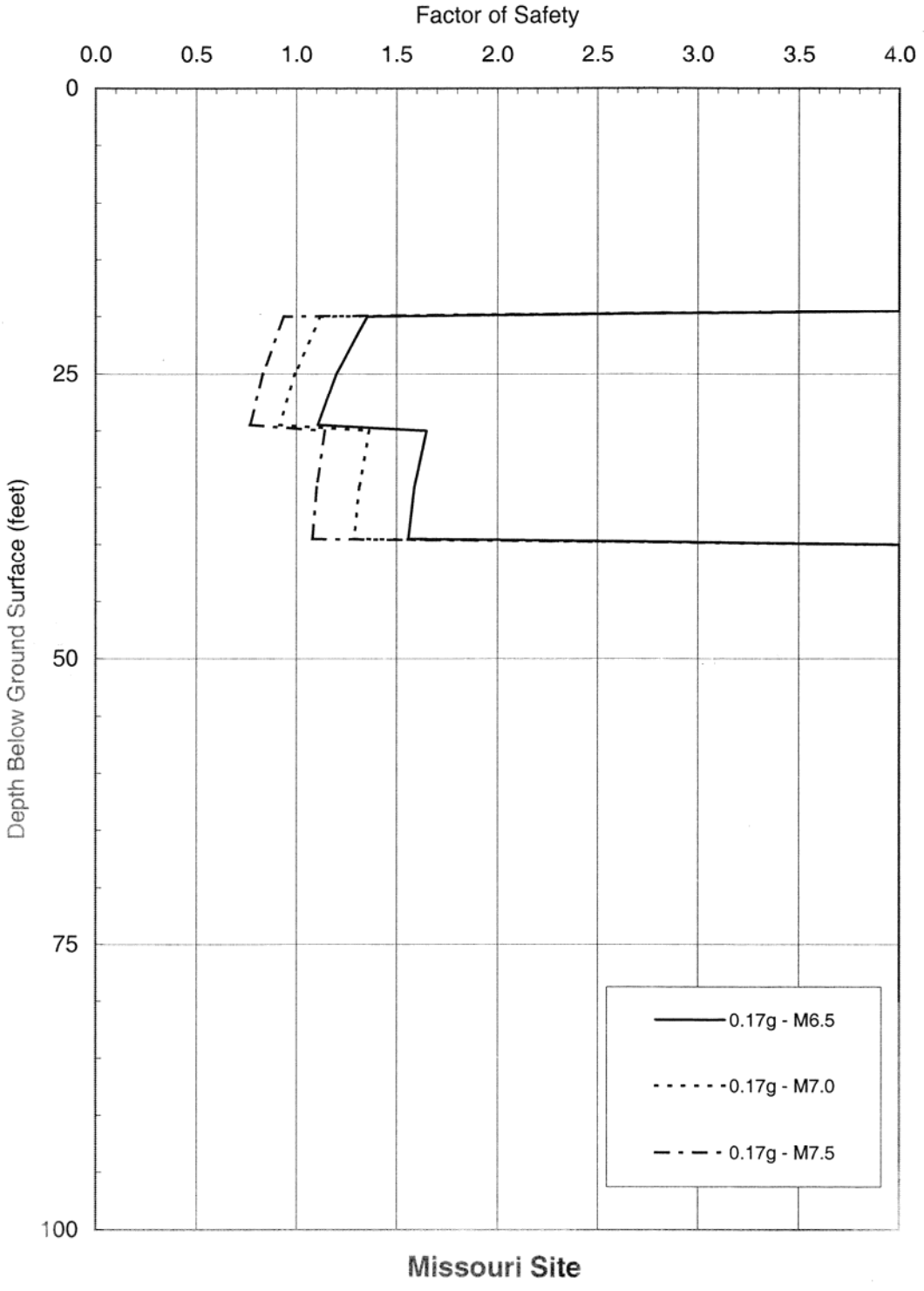

Figure E-21 **Liquefaction Potential – 475-Year Return Period (10% PE in 50-Year Ground Motion), Missouri Case Study.**

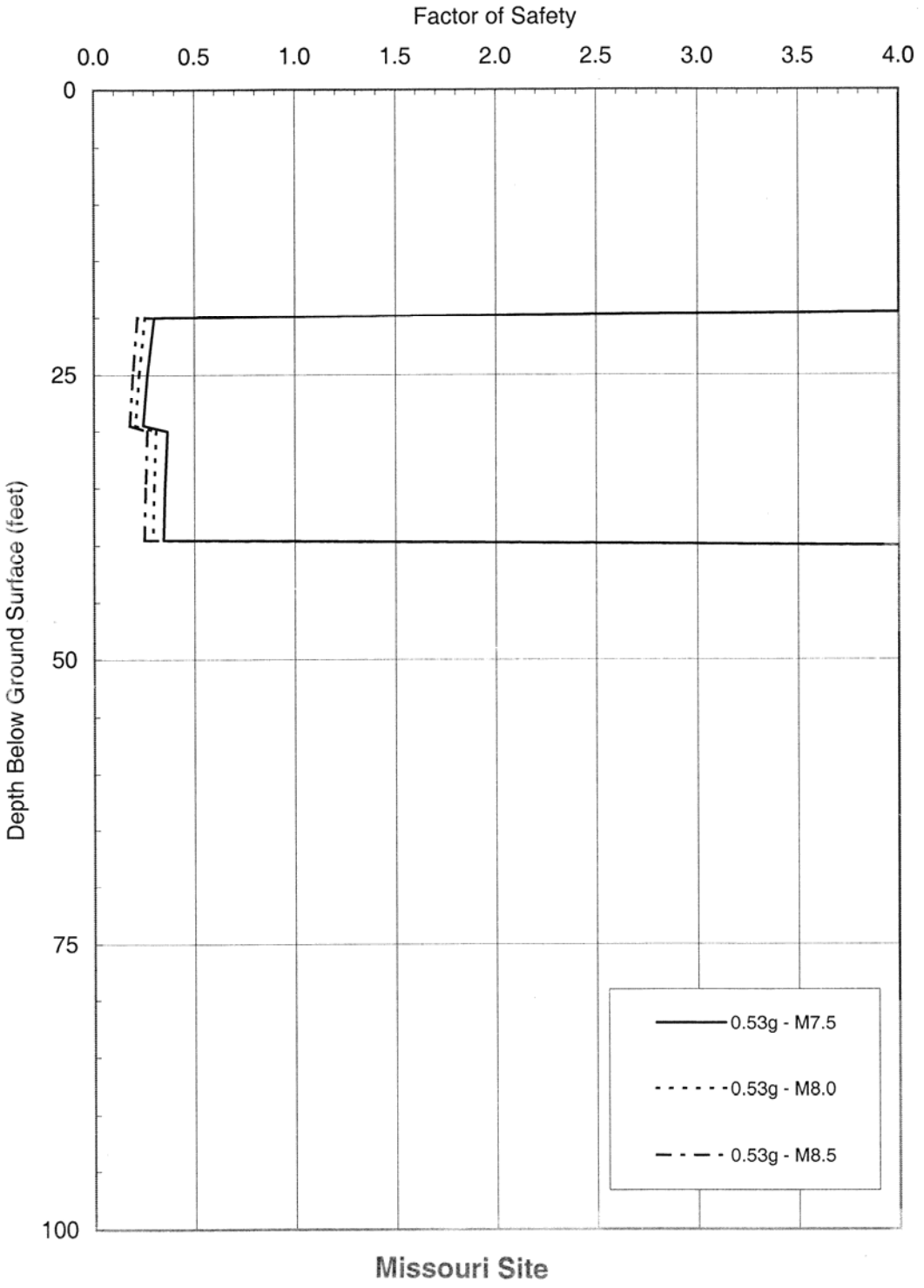

Figure E-22 **Liquefaction Potential – 2,475-Year Return Period (10% PE in 50-Year Ground Motion), Missouri Case Study.**

piles by re-running the stability analyses for the liquefied soil profile, with different applied seismic coefficients. The yield acceleration from these analyses is the inertial force required to produce a FOS of 1 and was determined to be approximately 0.02. Displacements were estimated using the same methods and assumptions as presented for the Washington State site, except that the peak ground acceleration and the yield acceleration were those for the Missouri site. The displacements determined for the two return periods are summarized at the table below.

Case: End Slope Displacements (inches)			
Franklin & Chang	**Hynes & Franklin**	**Wong & Whitman**	**Martin & Qiu**
475-Year Event (10% PE in 50-year ground motion):			
>36	>10	5	5
2,475-Year Event (3% PE in 75-year ground motion):			
>36	28	32	32

In these analyses, methods proposed by Franklin and Chang (1977), Hynes and Franklin (1984), Wong and Whitman (1982), and Martin and Qiu (1994) were evaluated. The provisions recommend that mitigation decisions be based on the results from the Martin and Qiu simplified method, which give results of 5 inches and 32 inches for the 475-year (10% PE in 50-year ground motion) and 2,475-year (3% PE in 75-year ground motion) events, respectively. These displacements are large enough, particularly for the 2,475-year return period event, that some mitigation procedures would have to be considered. These mitigation methods could involve structural pinning or ground improvement as described in the next section.

As for the WSDOT site, analyses were also performed using the DISPMNT computer program in combination with DESRA-MUSC results. "Upslope" deformations were suppressed assuming a strong one directional driving force from the embankment. Strengths on the interface were degraded as a function of pore water pressure increases for the 35-40 foot layer, and reduced to the 300 psf residual strength when liquefaction was triggered. Results showing displacement time history plots for the 2,475-year return period Michoacan earthquake, as a function of yield acceleration, are shown in Figure H-23. The input acceleration time histories used at a depth of 40 feet (70 feet with 30 feet of fill) are shown in Figure H-24. The time histories are very similar for the no fill and fill cases. Total accumulated displacements for all earthquake events are shown in Figure H-25, where it may be seen that the 2,475-year (3% PE in 75-year ground motion) events generated significantly larger displacements than the 475-year (10% PE in 50-year ground motion) events, at low values of yield acceleration. These displacements were used as a basis for discussion of remediation analyses, as described in Section E.9.4.

Similar displacement estimates to the simplified methods described above, may be made using the displacement versus yield acceleration curves shown in Figure H-25. The free field displacements without mitigation corresponding to a yield acceleration of 0.02 are summarized below.

Case: End Slope Displacement (inches)		
Michoacan earthquake	**Chile earthquake**	**Tokaji – Oki earthquake**
475-year event (10% PE in 50-year ground motion):		
21	21	16
2,475 year event (3% PE in 75-year ground motion):		
180	150	140

E.9.4 Stability Analyses with Mitigation Measures

Two procedures were evaluated for reducing the amount of displacement being predicted: structural pinning and ground improvement. For these analyses the additional resistance provided by the improved ground or by the structural pinning of the soil was incorporated into the stability analyses as described previously.

For the structural pinning evaluation, shear forces were calculated for two cases. In the first case, the shear failure occurred at the toe of the end slope in front of Pier 3 (Figure H-26). This gave an increase in resistance of 16 kips/foot for the 43-foot width of the abutment. Both pile pinning and abutment passive resistance are included in this reaction. This reaction occurs over the 35-foot abutment width, resulting in a resistance of 33 to 44 kips/foot of width. This reaction force was introduced into the slope stability analysis using

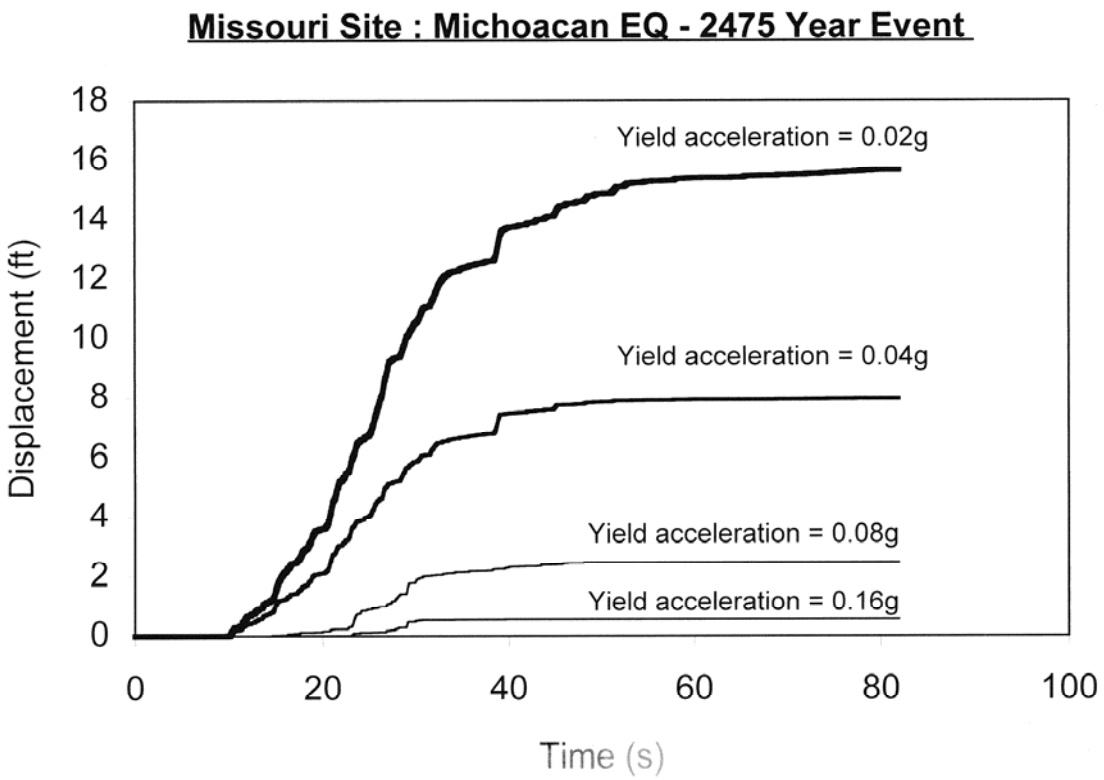

Figure H-23 Displacement vs. Time for the Missouri Site Failure Surface

the smearing method described for the Washington State study. For this method the resistance per unit width was converted into an equivalent shear strength along the shear plane in the liquefied zone, and this equivalent strength was added to the residual strength of 300 psf. For these analyses the failure plane was determined to be 90 feet in length, giving an added component to the liquefied strength of 180 psf. The resulting strength assigned to the liquefied layer was 480 psf (i.e., 180 psf + 300 psf = 480 psf).

For the second case, the shear failure was allowed to extend to the opposite embankment, as shown in Figure H-27. The pinning force for this case was 32 kips/foot, resulting in an additional 355 psf of smeared resistance. The resulting assigned strength for the layer was 655 psf (i.e., 355 psf + 300 psf = 655 psf).

Yield accelerations for both cases were determined by varying the seismic coefficient within the slope stability analysis until the factor of safety was 1.0. This analysis gave the following yield accelerations for the two cases.

Case	Yield Acceleration (g)
Toe Wedge	0.12
Deep Wedge	0.10

For the ground improvement case different widths of improved ground were used below the abutment. The improved ground extended through each of the liquefied zones. Soil in the improved ground was assigned a friction angle of 45 degrees. This increase in strength was assumed to be characteristic of stone columns or a similar improvement procedure. As with the ground improvement studies for the Washington State site, two procedures were used to represent the improved zone. One was to model it explicitly[9]; the second involved "smearing" the reaction from the improved strength zone across the failure surface by increasing the strength of the soil in the liquefied zone to give the same reaction. The resulting FOS was greater than 1.0 for all cases. This allowed yield accelerations to be computed as a

[9] The "explicit" case involved modeling the geometry of the correct width of improved ground in the computer. While fundamentally more correct, it is also time consuming to change the geometry of the problem for each width. The smearing technique involved a simple change in strength of the soil layer, which could be accomplished very quickly.

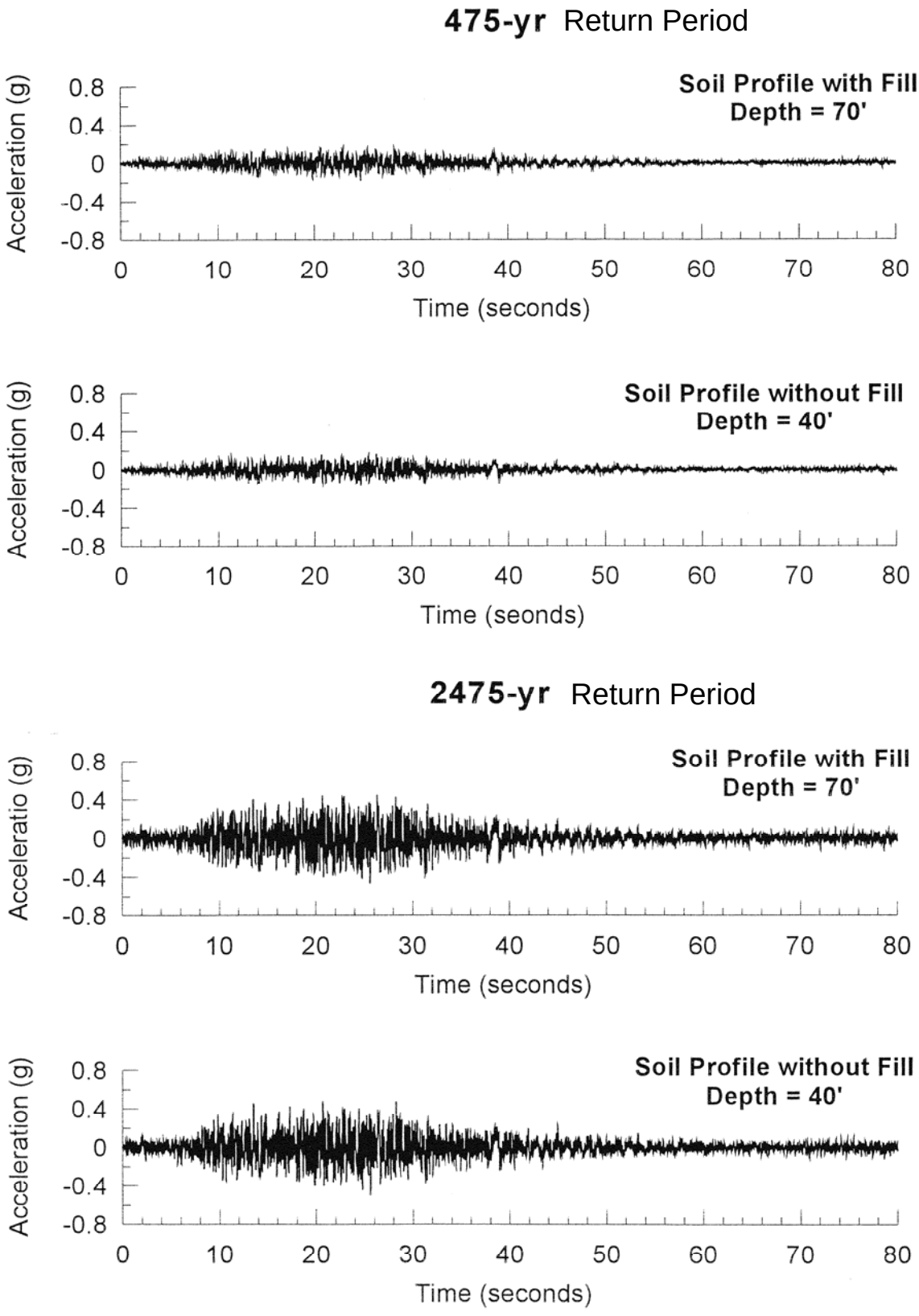

Figure H-24 **Input Acceleration History at Base of Liquefiable Layer, 1985 Michoacan Earthquake, Missouri Case Study**

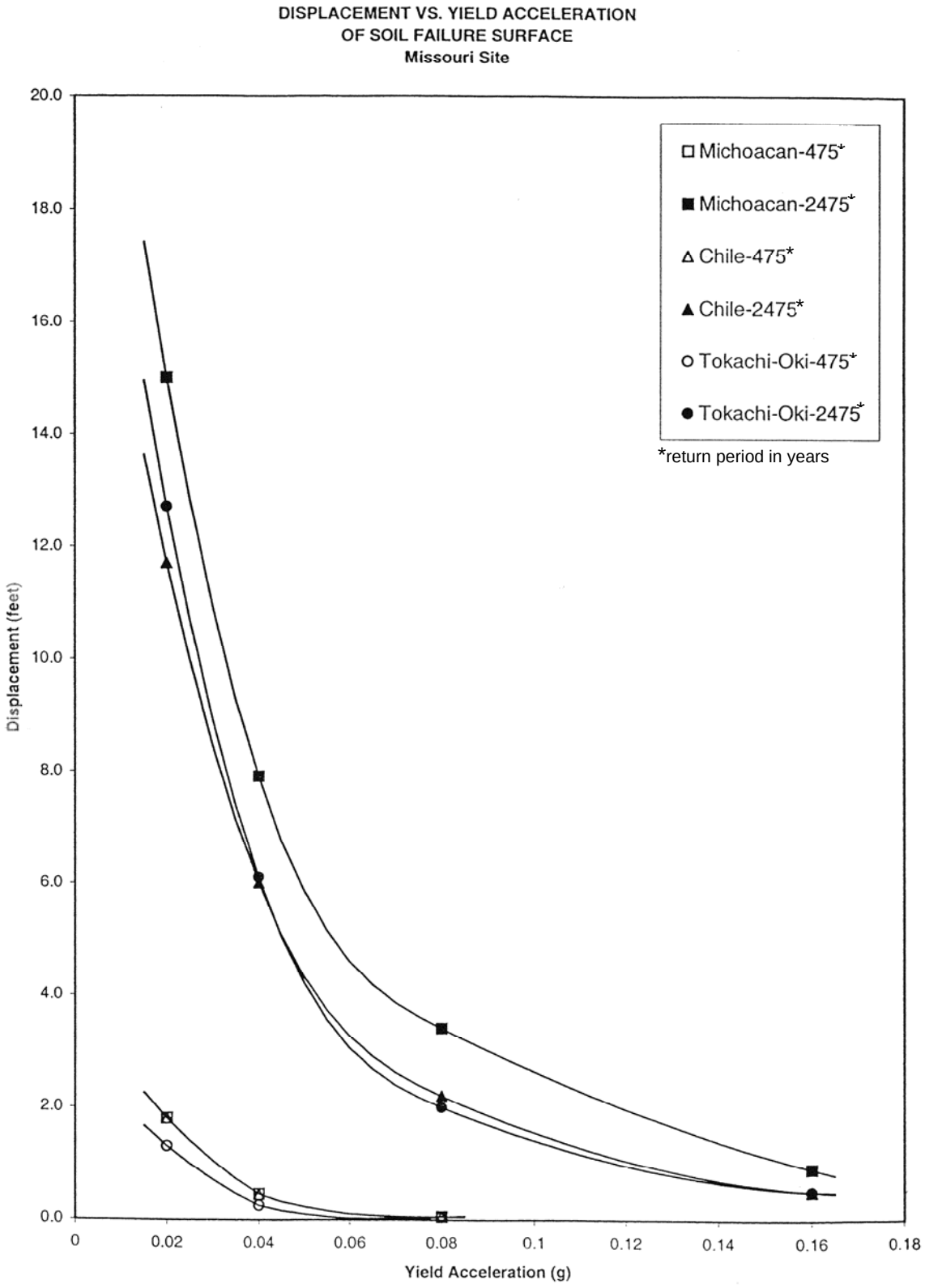

Figure H-25 Displacement vs. Yield Acceleration of the Soil Failure Surface for the Missouri Site

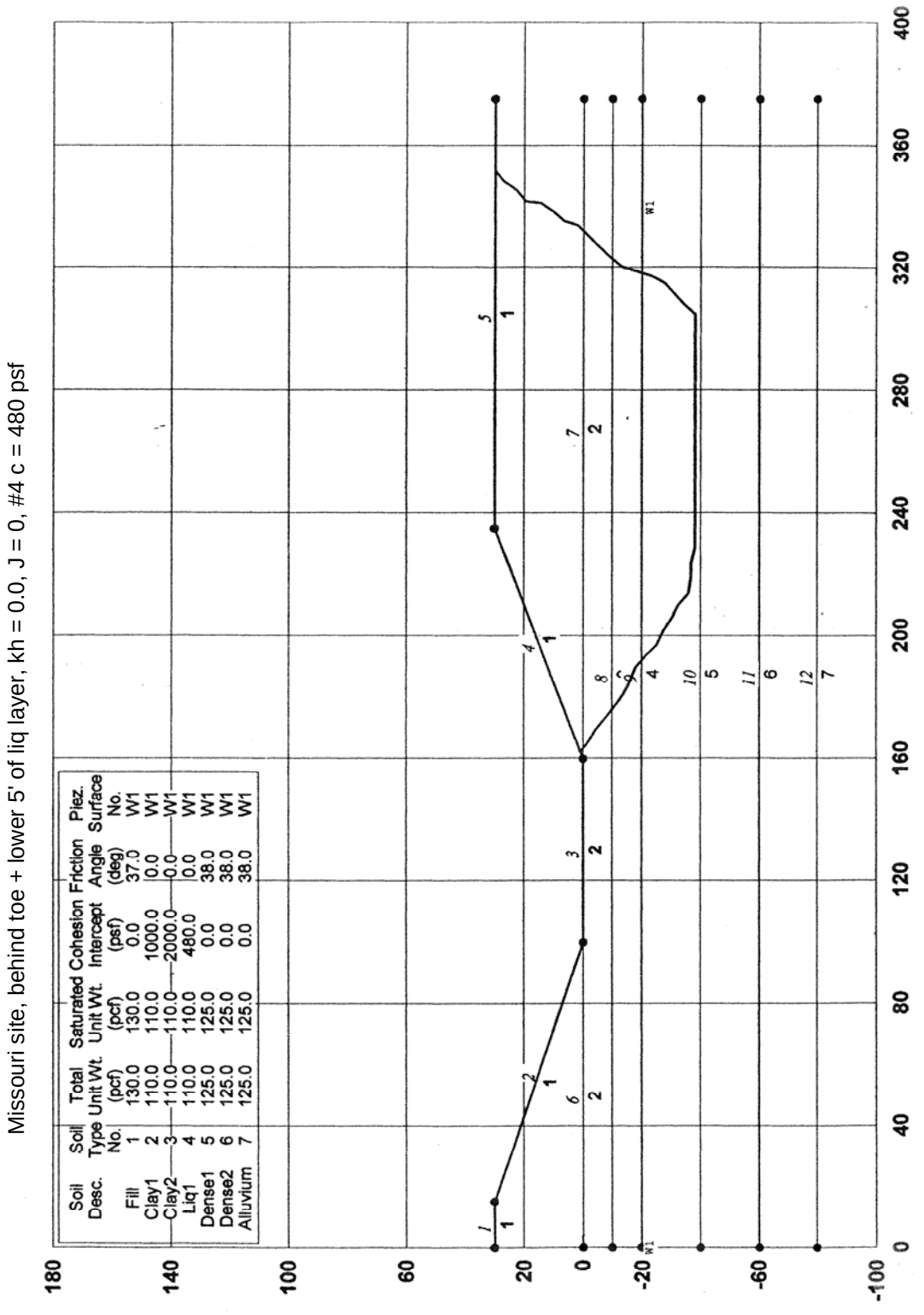

Figure H-26 Geometry of Toe Failure Wedge for Missouri Site

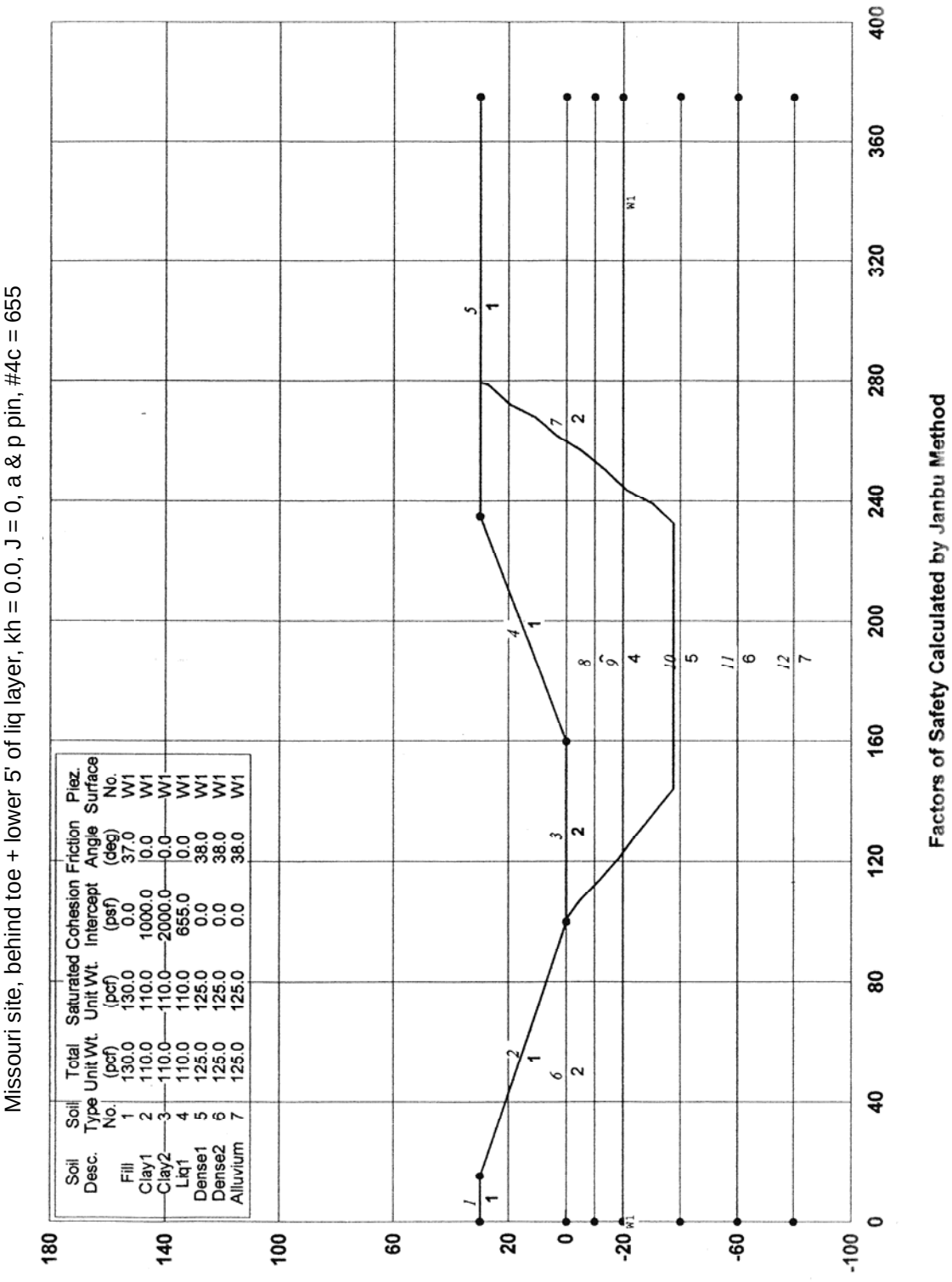

Figure H-27 Geometry of Deep Failure Wedge for Missouri Site

function of the width of the improved zone. These values are summarized as follows.

Width (feet)	Yield Acceleration (g)
10	0.18
30	0.33
50	0.53

E.9.5 Displacement Estimates from Simplified Methods

Displacements were estimated for each of the yield accelerations given above. In these analyses methods recommended by Franklin and Chang (1977), Hynes and Franklin (1984), Wong and Whitman (1982), and Martin and Qiu (1994) were used. The same assumptions as made for the Washington state site were used during these analyses. The resulting displacements for the cases cited above are summarized in the following.

Displacements (inches)				
475-Year Event (10% PE in 50-year ground motion):				
Case	Franklin & Chang	Hynes & Franklin	Wong & Whitman	Martin & Qiu
1	<1	<4	<1	<1
2	<1	<4	<1	<1
3	<1	<4	<1	<1
4	<1	<4	<1	<1
5	<1	<4	<1	<1
2,475-Year Event (3% PE in 75-year ground motion):				
Case	Franklin & Chang	Hynes & Franklin	Wong & Whitman	Martin & Qiu
1	>36	<4	5	3
2	>36	5	8	5
3	8	<4	2	1
4	<1	<4	<1	1
5	<1	<4	<1	<1

Table notes:
Case 1: Toe Wedge
Case 2: Deep Wedge
Case 3: Stone Columns – 10 ft
Case 4: Stone Columns – 30 ft
Case 5: Stone Columns – 50 ft

The estimates for the recommended Martin and Qui method indicate that for the 475-year (10% PE in 50-year ground motion) event the displacements will be <1 inch for both the toe and deep wedge cases. For the 2,475-year (3% PE in 75-year ground motion) event, the toe wedge case gives 3 inches and the deep wedge 5 inches. Virtually any pinning or ground improvement method will limit displacements to less than about 0.5 feet for the 2,475-year (3% PE in 75-year ground motion) event. (Putting aside the F-C displacements, which are based on a limited database and also reflect an upper bound.)

Similar displacement estimates to the simplified methods described above, may be made using the displacement versus yield acceleration curves shown in Figure H-25. The free field displacements without mitigation corresponding to a yield acceleration of 0.02 are summarized in Section E.9.4.

For the pile pinning and ground remediation yield accelerations described in Section E.9.4, the displacement estimates are summarized in the following.

Displacements (inches):			
	Michoacan earthquake	Chile earthquake	Tokaji – Oki earthquake
Case	475-Year Event (10% PE in 50-year ground motion):		
1	<1	<1	<1
2	<1	<1	<1
3	<1	<1	<1
4	<1	<1	<1
5	<1	<1	<1
	2,475-Year Event (3% PE in 75-year ground motion):		
Case	Michoacan earthquake	Chile earthquake	Tokaji – Oki earthquake
1	24	12	12
2	30	18	18
3	6	4	4
4	<1	<1	<1
5	<1	<1	<1

Table notes:
1: Toe Wedge
2: Deep Wedge
3: Stone Column – 10 ft
4: Stone Column – 30 ft
5: Stone Column – 50 ft

For the 2,475 earthquake (3% PE in 75-year ground motion) events, the displacements tabulated above are in general less than the Franklin and Chang estimates, but higher than the Hynes and Franklin, the Wong & Whitman, and Martin and Qiu estimates.

E.9.6 Pinning Force Calculations

As with the Washington State study, the soil movements will induce forces in the superstructure, if either the toe wedge or the deep soil wedge failure develops. The toe wedge only involves the abutment for pinning force, whereas the deep wedge involves both Pier 3 and the abutment. Additionally, the same potential failure modes exist for the left-hand end of the bridge, but since the bridge is symmetric the results for one end apply to the other.

Figure H-28 illustrates the pinning forces acting on the soil block comprising the toe wedge. In this case, the nine piles contribute 105 kips at the bottom of the slide, and they contribute 53 kips at the top. The top force is smaller than the bottom because the top is assumed to be a pinned condition. The location of the central plastic hinge is taken at mid-height of the soil column. The abutment backwall also contributes lateral force that resists the movement of the toe wedge, and that resistance is 520 kips, which is half that available typically. The reduction is taken to recognize the potential for slumping of the backfill due to movement of the toe wedge of soil.

These forces represent maximum values that only occur after significant plasticity develops. In the case of the piles, about 7 to 8 inches of lateral movement occurs at the center plastic hinge shown in the figure before full yield is attained. Subsequent to yielding the maximum deflection that can tolerated with 0.05 radians of plastic drift is 18 inches. This is the maximum total structural deflection allowed for the toe wedge movement.

Figure H-29 shows the displaced shape when the deep wedge of soil moves. This involves the abutment piles and Pier 3. For the abutment the same resistances and allowable deformations apply as with the toe wedge failure addressed above. For Pier 3 the piles can develop 531 kips of resistance, based on plastic hinges forming 5*D* above and below the liquefiable layer. This results in about 32 feet of length between plastic hinges in the piles. Additionally, the columns contribute 166 kips to the resistance. The bent was assumed to be connected to the superstructure with a pin connection. This is a reasonable bound for the common details used to connect girder superstructures, provided a full-depth diaphragm is used. The connection typically then behaves as a 'piano hinge'.

The allowable displacements for the deeper wedge failure are approximately 24 inches, which represents total displacement. Pier 3 develops yield at about 6 inches and then can tolerate roughly 18 inches of plastic deformation. However, because both the abutment piles and Pier 3 are moved by the deep wedge, the 18 inch total displacement allowed at the abutment controls. Therefore 18 inches is the allowable displacement.

In Section E.9.5 the estimated deformations for the 475-year (10% PE in 50-year ground motion) event are 7 inches for the deep wedge failure and 5 inches for the toe wedge failure. For the 2,475-year (3% PE in 75-year ground motion) event, including the pinning effect of the substructure, produces displacements of 11 and 14 inches for the toe and deep wedge failures, respectively. This is just in excess of the yield displacements for the piles, but is within their 18-inch plastic capacity, and is thus judged acceptable. This illustrates the potential beneficial effect of considering pinning.

The site-specific predictions of ground motion are given in Figure H-30, and at a yield acceleration of about 0.1g, which applies for the pinning options, the average displacement of the three time histories is about 20 inches. In this case, the site-specific data produces displacements (due mainly to the Michoacan earthquake record) that exceed the simplified methods' predictions, but are close to the plastic capacity of the piles.

The conclusion is that if one wished to be conservative and use the results of the site-specific analysis and not risk displacements close to the capacity of the piles, then some remediation would be desirable to protect the substructure. However, if one used the simplified methods for estimating displacements, then the structure, as designed could withstand the 2,475-year (3% PE in 75-year ground motion) event and the liquefaction that it induces, and the piles would be just beyond their elastic capacity. This range in predicted displacements illustrates the uncertainty associated with the prediction of ground movements.

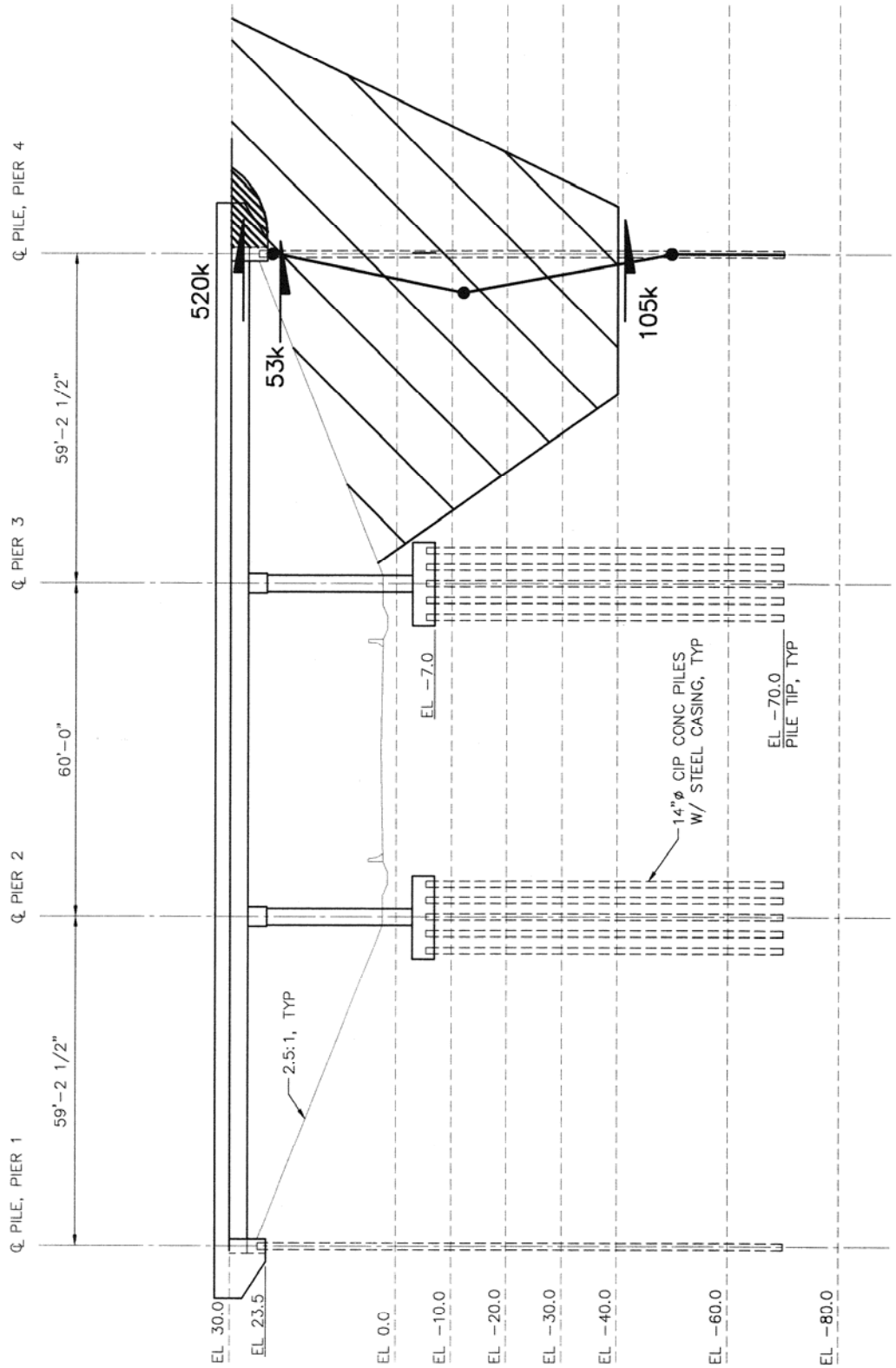

Figure H-28 Pier 4 Structural Forces Resisting Lateral Spreading, Missouri Case Study

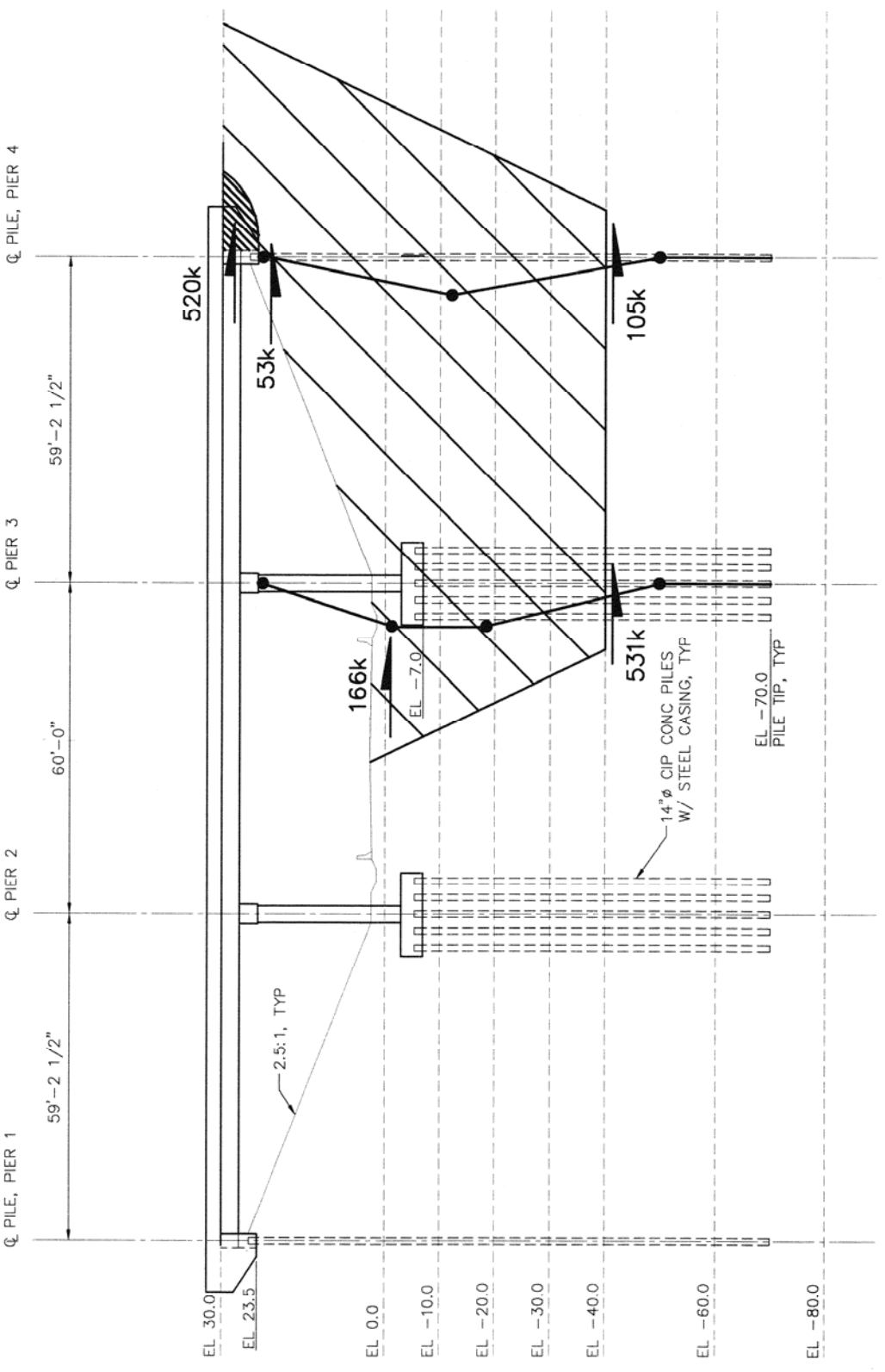

Figure H-29 Pier 3 and Pier 4 Structural Forces Resisting Lateral Spreading, Missouri Case Study

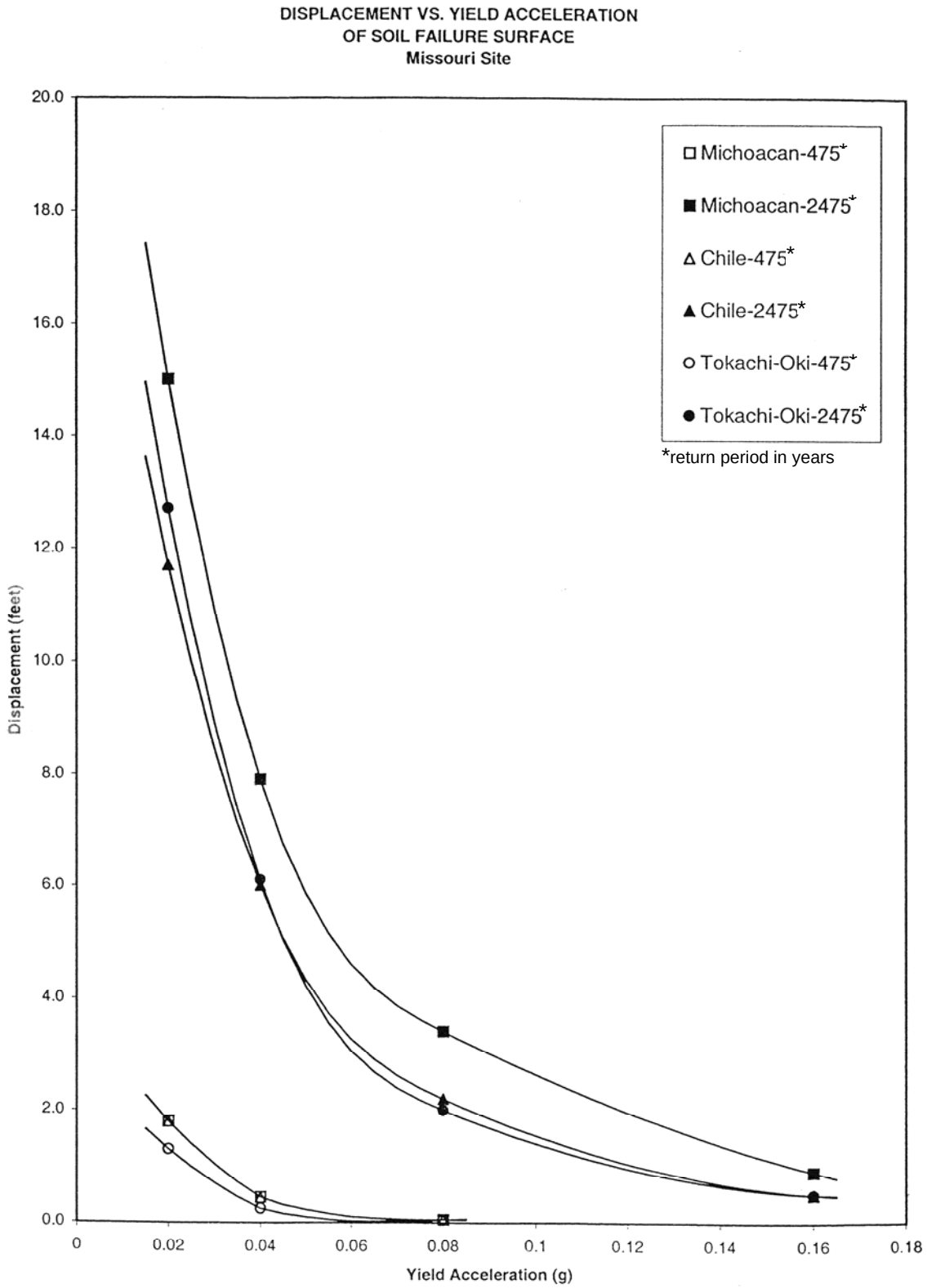

Figure H-30 **Displacement vs. Yield Acceleration of the Soil Failure Surface for the Missouri Site**

E.9.7 Comparison of Remediation Alternatives

As with the study of the Washington bridge, the intent of the Missouri study was to assess the potential consequences of changing the AASHTO seismic design provisions. This comparison met the objectives by having little if any liquefaction under the 475-year (10% PE in 50-year ground motion) event and large amounts of liquefaction and associated ground movements during the 2,475-year (3% PE in 75-year ground motion) event. It is clear that the structure, as designed, is capable of resisting the lateral spreading associated with the liquefaction without the need for any additional expenditure of funds.

Because the estimated performance under the 2,475-year (3% PE in 75-year ground motion) event produces spreading displacements that will exceed the elastic capacity of the piles, it was worthwhile to investigate mitigation measures that would produce higher levels of performance, so that the piles can remain within their elastic capacity.

Stone columns can be used to limit the displacement of the toe and deep soil wedges. In Section E.9.5, 10-foot, 30-foot, and 50-foot wide buttresses of stone columns were considered. The calculated displacements were all less than about 4 inches for the 2,475-year (3% PE in 75-year ground motion) event when the stone columns were employed, and this provides the operational performance level for the foundations. This displacement ensures the piles remain within their yield displacement.

It is evident that mitigation, if it is deemed necessary to meet higher performance levels, is only required for the longer return period (2,475-year) ground motion. All the displacements for the 475-year (10% PE in 50-year ground motion) event, when pinning is considered, are acceptable.

If additional piles are considered for limiting the overall soil displacements, then the objective would likely be to install enough to reduce the estimated displacements down to values that would be tolerable for the substructure. This would likely require a large number of piles since the existing restraint at the superstructure level currently provides over 50% of the pinning resistance. Thus the inference is that if the deformations need to be limited beyond that which the foundation pinning alone can produce, then stone columns appears to be the rational choice.

There are no additional costs necessary in order to meet the life-safety performance requirements of the 2,475-year (3% PE in 75-year ground motion) event. In this example, spreading displacements of the order of less than 14 inches would be estimated, and these can be accommodated in the piles. If a higher level of performance is desired, such that the piles remain within their elastic limits and spreading displacements are desired to be less than 4 inches, then some remediation work is necessary for the 2,475-year (3% PE in 75-year ground motion) event.

The stone column option would likely only need to be applied over a 10-foot length (longitudinal direction of bridge), since that length produced acceptable deflections of 4 inches or less in the Newmark analysis. The width at a minimum would be 50 feet, and the depth also would be about 40 feet. If the columns were spaced roughly on 7-foot centers (the width would grow to 14 feet), then about 20 stone columns would be required. At approximately $30 plf, the overall cost per abutment would be on the order of $24,000 or about $50,000 for both abutments.

As a rough estimate of the cost of the overall structure, based on square-footage costs of $80 to $100, the bridge would cost between about $600,000 and $800,000. Thus, the cost to install stone columns would run about 6 to 8% of the overall cost of the bridge. This expenditure would ensure the highest operational level of performance of the structure because foundation movements would be less than the yield level of the piles.

If pinch piles were used to augment the piles of the foundations, the piles would not need to be connected to the foundation, and they would not need to extend as deep as the load-bearing foundation piles. The per pile costs for the foundation piles were estimated to be on the order of $2500 each for 70-foot long piles. If shorter piles on the order of 40-feet long were used, their costs would be roughly $1500 each. Thus if pinch piles were used, about 15 piles per side could be installed for the same cost as the stone column remediation option. It is not likely that this number of piles would be as effective in limiting soil movement as the stone columns, although they would produce an acceptable level of performance. Therefore, the stone column option would appear the most cost effective in this situation.

E.10 SUMMARY AND CONCLUSIONS

These recommendations apply when liquefaction at a site has been determined to be likely as a result of the 2,475-year (3% PE in 75-year ground motion) earthquake. The specific criteria are given in Section 3.10.5 of the recommended LRFD provisions (see *Part I*).

There are two phenomena that must be considered in the design of a bridge on a liquefiable site. The first is the traditional vibration design based effectively on the response spectra for the site. This corresponds to the design cases dealt with in Division I-A of the current AASHTO *Specifications*. The second phenomenon is lateral forces induced by flow sliding or lateral spreading if these potential consequences of liquefaction are predicted to occur. Flow sliding describes the condition where a soil mass is statically unstable after liquefaction-induced weakening of the soil occurs. Such an unstable condition can lead to quite large deformations. Lateral spreading describes deformations that progressively occur during ground shaking due to the combined static plus transient inertial forces exceeding the resistance of the liquefied soil. Deformations due to lateral spreading typically are smaller than those due to flow sliding.

For the Maximum Considered Earthquake (MCE) event, when the recommended performance objective is life-safety, inelastic deformation is allowed in the foundation for the lateral spreading or flow spreading case. Mitigation measures are able to achieve higher levels of performance when desired, so that piles remain within their elastic capacity. The vibration cases are designed, as they always are, for inelastic response above ground and at inspectable locations. It is believed that allowing some inelastic action in the presence of large spreading movements during the MCE event is necessary. Because spreading-induced deformations are 'displacement–controlled', instability of the system is unlikely even though some damage may exist in the foundations. The implication of this decision is that a bridge and its foundations may need to be replaced after a MCE event, but it avoids a significant expenditure of funds to prevent the displacement from occurring.

The design for vibration and lateral spreading is split into two independent activities, as coupling of the vibration load case and the spreading load case is not usually warranted. The vibration design is considered separately from the spreading design, because it is unlikely that the maximum vibration effect and the maximum lateral spreading forces occur simultaneously. The de-coupled approach is considered reasonable with respect to the current state of the art.

The approach recommended is to determine the likely ground movements that may occur at the site, including the effects of altered site configurations such as fills and the beneficial effects of the pinning of piles. This prediction of lateral spreading can be made using either currently accepted simplified methods or site-specific analyses, as outlined in this report. As noted in the two cases studied, there can be a significant variation in the predicted displacements using the different methods, and this indicates that a designer must be aware that there can be a significant range in anticipated movements. Refined accuracy is not warranted. The beneficial resistance of the substructure should be included in the assessment of movements. The substructure is then assessed for the predicted movements, and if it can not tolerate the predicted displacements, then ground or structural remediation should be used.

It is important to recognize that the two case histories considered in this report are based on conditions whereby lateral spreading is parallel to the superstructure, which typically is one of the strong directions of the bridge. If the spreading effect is skewed with respect to the superstructure, then the skew must be accounted for in determining the likely plastic mechanism that will control.

The conclusions from this study of the effects of liquefaction when the design earthquake return period is increased from the existing AASHTO I-A 475-year return period (10% PE in 50-year ground motion) to 2,475-years (3% PE in 75-year ground motion) are summarized as follows.

- For both the Western (Washington State) and Mid-America (Missouri) examples there were no additional costs required to address the recommended liquefaction requirements when a bridge was designed for the current 475-year (10% PE in 50-year ground motion) earthquake and was then subjected to the 2,475-year (3% PE in 75-year ground motion) earthquake recommended in the LRFD provisions for the life-safety level of performance, despite significant increases in the PGA for the 2,475-year return period event.
- For the Western U.S. example, liquefaction occurred for the 475-year (10% PE in 50-year ground motion) event, and it was necessary to provide stone column mitigation measures in

the upper 30 feet or so. This would also most likely be necessary at both abutments (only one was studied in-depth in this effort). The cost for the stone columns at both abutments was estimated to be about 2.5% of the bridge cost. For the 2,475-year (3% PE in 75-year ground motion) event similar measures were required with the depth of the stone columns extended to 50 feet. The estimated cost of this remediation is of the order of 4% of the bridge cost.

- For the Mid-America example, liquefaction did not occur for the 475-year (10% PE in 50-year ground motion) event; however, the bridge was capable of meeting the liquefaction requirements for the recommended NCHRP 12-49 LRFD provisions for the 2,475-year (3% PE in 75-year ground motion) event, with liquefaction occurring at a depth of 20 to 40 feet, through pinning action of the piles. By allowing some inelastic deformations in the piles, no ground improvement was required.
- For the Mid-America and Western U.S. sites the higher operational level of performance can be achieved in the foundation system (i.e., piles remain in their elastic capacity) for the 2,475-year (3% PE in 75-year ground motion) event by improving the ground using stone columns. This improvement can be achieved for less than 5% additional cost in the case of the Western U.S. site and less than 10% additional cost in the case of the Mid-America site.

This study demonstrates the beneficial effects of considering the resistance that the substructure of the bridge offers to lateral movement of soil, 'pinning'. These effects can be significant and should be considered in predictions of lateral soil movements. The study also shows the benefit of allowing inelastic behavior in the foundation under the action of lateral ground movement. For many cases relatively large displacements of the ground may be accommodated by the structure without collapse.

There has been considerable advancement in the state of the art in assessing impacts of liquefaction since the current AASHTO *Specifications* (Division I-A provisions) were developed. These have been included in the recommended LRFD provisions and used in the two case studies. They are relatively easy to use, and they permit a much better understanding of the effects of liquefaction and lateral spreading. A summary of the new enhancements is as follows:

- A better ability to estimate the displacements that may occur as a result of lateral spreading. Currently, this is not always done in liquefaction studies.
- The ability to incorporate the beneficial effects of "pinning' of the piles and ground movement in resisting lateral flow movements.
- The new information available from USGS on the deaggregation of the ground shaking hazard into the contributions of different seismic sources, earthquake magnitude, and distances for a particular site.
- The ability to perform nonlinear stress analysis time-history studies using realistic acceleration histories of ground motion to better understand the sequence of events that occur during liquefaction and the modification in ground motions that occur as a result.

As discussed in Section A.6 there were two global options that were considered for the development of these recommended LRFD provisions. The one that was adopted was to design explicitly for ground motions for a larger event (3% PE in 75 years) but refine the provisions to reduce the conservatism and gain a better understanding of what occurs in a larger event while attempting to keep the costs about the same as the current provisions. Under this scenario, the degree of protection against larger earthquakes is quantified and based on scientific principles and engineering experience. The other option which is the basis of the current AASHTO Division 1-A provisions is to design for a moderate sized event and maintain the current conservative provisions as a measure of protection against larger events. In this scenario the degree of protection is unknown and depends on intuition and engineering judgment. These examples demonstrate the benefits of the designing for and understanding what occurs in a larger event.

The implications of the new LRFD recommendations in going to a 2,475-year return period (3% PE in 75-year ground motion) event is that there is a greater area that now requires more detailed seismic design, including a liquefaction assessment. The specific details of when liquefaction should be considered are covered in Section 3.10.5 of the provisions, but in general, liquefaction is considered for bridges classified as SDR 3

or greater for a site that has a mean magnitude earthquake from deaggregation greater than 6.4. If the mean magnitude is less than 6.0, then liquefaction is not required to be considered. Between a mean magnitude of 6.0 and 6.4, liquefaction may or may not be required to be considered depending on the combinations of soil type and acceleration levels. Although liquefaction must be assessed in certain designs, the Mid-America example has demonstrated that a bridge may meet the recommended performance requirements of the new provisions without any additional expenditure of funds. It is difficult to draw wider implications from this study without additional study.

It should be recognized that the approach recommended here for large, infrequent earthquakes is a departure from the traditional approach of preventing damage in the foundation. For ground movements on the order of those expected, it is felt that often either remediation is necessary or allowance of some inelastic action in foundation is necessary. It is recognized that only two specific examples were considered in this study, and that with time refinement will be possible as more structures are studied and designed. It is also recognized that the prediction of earthquake-induced ground movement is approximate at best, and much remains to be learned by the profession on how to produce more accurate predictions. Of all the issues, the greatest uncertainty lies in the methods of predicting ground displacements as seen in the variations of the simplified methods and the more precise nonlinear analyses. However, it is felt that the recommended approach is a reasonable beginning to rationally designing for such earthquake-induced hazards. The broader implications of these results deserve additional effort that was not part of this scope of work.

APPENDIX F

LOAD AND RESISTANCE FACTOR DESIGN SPECIFICATION FOR SINGLE-ANGLE MEMBERS

Load and Resistance Factor Design Specification for Single-Angle Members

November 10, 2000

Supersedes the *Specification for Load and Resistance Factor Design of Single-Angle Members* dated December 1, 1993

Prepared by the
American Institute of Steel Construction, Inc.
Under the Direction of the
AISC Committee on Specifications and approved by
the AISC Board of Directors

AMERICAN INSTITUTE OF STEEL CONSTRUCTION, INC.
One East Wacker Drive, Suite 3100
Chicago, IL 60601-2001

PREFACE

The intention of the AISC Specification is to cover the common everyday design criteria in routine design office usage. It is not feasible to also cover the many special and unique problems encountered within the full range of structural design practice. This separate Specification and Commentary addresses one such topic—single-angle members—to provide needed design guidance for this more complex structural shape under various load and support conditions.

The revised single-angle design criteria were developed through a consensus process by the AISC Task Committee 12 on Single Angles:

James M. Fisher, Chairman
Leroy A. Lutz, Vice-Chairman
Mohamed Elgaaly
Shu-Jin Fang
Theodore V. Galambos
Subhash Goel
Charlotte S. Harman
Todd Helwig
Donald W. White
Sergio Zoruba, Secretary

The full AISC Committee on Specifications has reviewed and approved this Specification.

A non-mandatory Commentary provides background for the Specification provisions and the user is encouraged to consult it.

The principal changes in this edition include:

Revisions to flexural design strength criteria

a. For the limit state of local buckling when the angle leg is in compression
b. For the limit state of yielding when the tip of an angle leg is in tension
c. For the limit state of lateral-torsional buckling
d. For bending about geometric axes

The reader is cautioned that professional judgment must be exercised when data or recommendations in this Specification are applied. The publication of the material contained herein is not intended as a representation or warranty on the part of the American Institute of Steel Construction, Inc.—or any other person named herein—that this information is suitable for general or particular use, or freedom from infringement of any patent or patents. Anyone making use of this information assumes all liability arising from such use. The design of structures is within the scope of expertise of a competent licensed structural engineer, architect, or other licensed professional for the application of principles to a particular structure.

Load and Resistance Factor Design Specification for Single-Angle Members

November 10, 2000

1. SCOPE

This document contains Load and Resistance Factor Design (LRFD) criteria for hot-rolled, single-angle members with equal and unequal legs in tension, shear, compression, flexure, and for combined forces. It is intended to be compatible with, and a supplement to, the 1999 AISC *Load and Resistance Factor Design Specification for Structural Steel Buildings* and repeats some common criteria for ease of reference. For design purposes, the conservative simplifications and approximations in the Specification provisions for single angles are permitted to be refined through a more precise analysis. As an alternative to this Specification, the 1989 AISC *Specification for Allowable Stress Design of Single-Angle Members* is permitted.

The Specification for single-angle design supersedes any comparable but more general requirements of the AISC LRFD. All other design, fabrication, and erection provisions not directly covered by this document shall be in compliance with the AISC LRFD. For design of slender, cold-formed steel angles, the AISI *LRFD Specification for the Design of Cold-Formed Steel Structural Members* referenced in Section A6 of the AISC LRFD is applicable.

2. TENSION

The tensile design strength $\phi_t P_n$ shall be the lower value obtained according to the limit states of yielding, $\phi_t = 0.9$, $P_n = F_y A_g$, and fracture, $\phi_t = 0.75$, $P_n = F_u A_e$.

a. For members connected by bolting, the net area and effective net area shall be determined from AISC LRFD Specification Sections B1 to B3 inclusive.

b. When the load is transmitted by longitudinal welds only or a combination of longitudinal and transverse welds through just one leg of the angle, the effective net area A_e shall be:

$$A_e = A_g U \qquad (2\text{-}1)$$

where

A_g = gross area of member
$U = \left(1 - \frac{\bar{x}}{l}\right) \leq 0.9$
$\bar{x}$ = connection eccentricity
l = length of connection in the direction of loading

c. When a load is transmitted by transverse weld through just one leg of the angle, A_e is the area of the connected leg and $U = 1$.

For members whose design is based on tension, the slenderness ratio l/r preferably should not exceed 300. Members in which the design is dictated by tension loading, but which may be subject to some compression under other load conditions, need not satisfy the compression slenderness limits.

3. SHEAR

For the limit state of yielding in shear, the shear stress, f_{uv}, due to flexure and torsion shall not exceed:

$$f_{uv} \leq \phi_v 0.6 F_y \qquad \phi_v = 0.9 \qquad (3\text{-}1)$$

4. COMPRESSION

The design strength of compression members shall be $\phi_c P_n$

where

$\phi_c = 0.90$
$P_n = A_g F_{cr}$

a. For $\lambda_c \sqrt{Q} \leq 1.5$

$$F_{cr} = Q(0.658^{Q\lambda_c^2}) F_y \qquad (4\text{-}1)$$

b. For $\lambda_c \sqrt{Q} > 1.5$

$$F_{cr} = \left[\frac{0.877}{\lambda_c^2}\right] F_y \qquad (4\text{-}2)$$

where

$\lambda_c = \frac{Kl}{r\pi}\sqrt{\frac{F_y}{E}}$
F_y = specified minimum yield stress of steel
Q = reduction factor for local buckling

The reduction factor Q shall be:

when $\frac{b}{t} \leq 0.446\sqrt{\frac{E}{F_y}}$:

$$Q = 1.0 \tag{4-3a}$$

when $0.446\sqrt{\frac{E}{F_y}} < \frac{b}{t} < 0.910\sqrt{\frac{E}{F_y}}$:

$$Q = 1.34 - 0.761\frac{b}{t}\sqrt{\frac{F_y}{E}} \tag{4-3b}$$

when $\frac{b}{t} \geq 0.910\sqrt{\frac{E}{F_y}}$:

$$Q = \frac{0.534E}{F_y\left(\frac{b}{t}\right)^2} \tag{4-3c}$$

where

b = full width of longest angle leg
t = thickness of angle

For members whose design is based on compressive force, the largest effective slenderness ratio preferably should not exceed 200.

5. FLEXURE

The flexure design strengths of Section 5.1 shall be used as indicated in Sections 5.2 and 5.3.

5.1. Flexural Design Strength

The flexural design strength shall be limited to the minimum value $\phi_b M_n$ determined from Sections 5.1.1, 5.1.2, and 5.1.3, as applicable, with $\phi_b = 0.9$.

5.1.1. For the limit state of local buckling when the tip of an angle leg is in compression:

when $\frac{b}{t} \leq 0.54\sqrt{\frac{E}{F_y}}$:

$$M_n = 1.5\,F_y S_c \tag{5-1a}$$

when $0.54\sqrt{\frac{E}{F_y}} < \frac{b}{t} \leq 0.91\sqrt{\frac{E}{F_y}}$:

$$M_n = F_y S_c \left[1.5 - 0.93\left(\frac{b/t}{0.54\sqrt{\frac{E}{F_y}}} - 1\right)\right] \qquad (5\text{-}1b)$$

when $\frac{b}{t} > 0.91\sqrt{\frac{E}{F_y}}$:

$$M_n = 1.34QF_yS_c \qquad (5\text{-}1c)$$

where

b = full width of angle leg with tip in compression
Q = reduction factor per Equation 4-3c
S_c = elastic section modulus to the tip in compression relative to axis of bending
E = modulus of elasticity

5.1.2. For the limit state of yielding when the tip of an angle leg is in tension

$$M_n = 1.5M_y \qquad (5\text{-}2)$$

where

M_y = yield moment about the axis of bending

5.1.3. For the limit state of lateral-torsional buckling:

when $M_{ob} \leq M_y$:

$$M_n = [0.92 - 0.17M_{ob}/M_y]M_{ob} \qquad (5\text{-}3a)$$

when $M_{ob} > M_y$:

$$M_n = [1.92 - 1.17\sqrt{M_y/M_{ob}}]M_y \leq 1.5M_y \qquad (5\text{-}3b)$$

where

M_{ob} = elastic lateral-torsional buckling moment, from Section 5.2 or 5.3 as applicable

5.2. Bending about Geometric Axes

5.2.1. a. Angle bending members with lateral-torsional restraint along the length shall be designed on the basis of geometric axis bending with the nominal flexural strength M_n limited to the provisions of Sections 5.1.1 and 5.1.2.

b. For equal-leg angles if the lateral-torsional restraint is only at the point of maximum moment, the required moment shall be limited to $\phi_b M_n$ per Section 5.1. M_y shall be computed using the geometric axis section modulus and M_{ob} shall be substituted by using 1.25 times M_{ob} computed from Equation 5-4.

5.2.2. Equal-leg angle members without lateral-torsional restraint subjected to flexure applied about one of the geometric axes are permitted to be designed considering only geometric axis bending provided:

a. The yield moment shall be based on use of 0.80 of the geometric axis section modulus.

b. With maximum compression of the angle-leg tips, the nominal flexural strength M_n shall be determined by the provisions in Section 5.1.1 and in Section 5.1.3,

where

$$M_{ob} = \frac{0.66Eb^4tC_b}{l^2}\left[\sqrt{1 + 0.78(lt/b^2)^2} - 1\right] \qquad (5\text{-}4)$$

l = unbraced length

$$C_b = \frac{12.5M_{\max}}{2.5M_{\max} + 3M_A + 4M_B + 3M_C} \leq 1.5$$

where

M_{max} = absolute value of maximum moment in the unbraced beam segment
M_A = absolute value of moment at quarter point of the unbraced beam segment
M_B = absolute value of moment at centerline of the unbraced beam segment
M_C = absolute value of moment at three-quarter point of the unbraced beam segment

c. With maximum tension at the angle-leg tips, the nominal flexural strength shall be determined according to Section 5.1.2 and in Section 5.1.3 using M_{ob} in Equation 5-4 with -1 being replaced by $+1$.

5.2.3. Unequal-leg angle members without lateral-torsional restraint subjected to bending about one of the geometric axes shall be designed using Section 5.3.

5.3. Bending about Principal Axes

Angles without lateral-torsional restraint shall be designed considering principal-axis bending, except for the alternative of Section 5.2.2, if appropriate. Bending about both of the principal axes shall be evaluated as required in Section 6.

5.3.1. Equal-leg angles:

a. Major-axis bending:

The nominal flexural strength M_n about the major principal axis shall be determined by the provisions in Section 5.1.1 and in Section 5.1.3,

where

$$M_{ob} = C_b \frac{0.46Eb^2t^2}{l} \qquad (5\text{-}5)$$

b. Minor-axis bending:

The nominal design strength M_n about the minor principal axis shall be determined by Section 5.1.1 when the leg tips are in compression, and by Section 5.1.2 when the leg tips are in tension.

5.3.2. Unequal-leg angles:

a. Major-axis bending:

The nominal flexural strength M_n about the major principal axis shall be determined by the provisions in Section 5.1.1 for the compression leg and in Section 5.1.3,

where

$$M_{ob} = 4.9E\frac{I_z}{l^2}C_b\left[\sqrt{\beta_w^2 + 0.052(lt/r_z)^2} + \beta_w\right] \qquad (5\text{-}6)$$

I_z = minor principal axis moment of inertia

r_z = radius of gyration for minor principal axis

$\beta_w = \left[\frac{1}{I_w}\int_A z_o(w^2 + z^2)dA\right] - 2z_o$, special section property for unequal-leg angles, positive for short leg in compression and negative for long leg in compression (see Commentary for values for common angle sizes). If the long leg is in compression anywhere along the unbraced length of the member, the negative value of β_w shall be used.

z_o = coordinate along z axis of the shear center with respect to centroid
I_w = moment of inertia for major principal axis

b. Minor-axis bending:

The nominal design strength M_n about the minor principal axis shall be determined by Section 5.1.1 when leg tips are in compression and by Section 5.1.2 when the leg tips are in tension.

6. COMBINED FORCES

The interaction equation shall be evaluated for the principal bending axes either by addition of all the maximum axial and flexural terms, or by considering the sense of the associated flexural stresses at the critical points of the cross section, the flexural terms are either added to or subtracted from the axial load term.

6.1. Members in Flexure and Axial Compression

6.1.1. The interaction of flexure and axial compression applicable to specific locations on the cross section shall be limited by Equations 6-1a and 6-1b:

For $\frac{P_u}{\phi P_n} \geq 0.2$

$$\left|\frac{P_u}{\phi P_n} + \frac{8}{9}\left(\frac{M_{uw}}{\phi_b M_{nw}} + \frac{M_{uz}}{\phi_b M_{nz}}\right)\right| \leq 1.0 \qquad (6\text{-}1a)$$

For $\frac{P_u}{\phi P_n} \leq 0.2$

$$\left|\frac{P_u}{2\phi P_n} + \left(\frac{M_{uw}}{\phi_b M_{nw}} + \frac{M_{uz}}{\phi_b M_{nz}}\right)\right| \leq 1.0 \qquad (6\text{-}1b)$$

where

P_u = required compressive strength
P_n = nominal compressive strength determined in accordance with Section 4
M_u = required flexural strength
M_n = nominal flexural strength for tension or compression in accordance with Section 5, as appropriate. Use section modulus for specific location in the cross section and consider the type of stress.
$\phi = \phi_c$ = resistance factor for compression = 0.90
ϕ_b = resistance factor for flexure = 0.90
w = subscript relating symbol to major-axis bending
z = subscript relating symbol to minor-axis bending

In Equations 6-1a and 6-1b when M_n represents the flexural strength of the compression side, the corresponding M_u shall be multiplied by B_1.

$$B_1 = \frac{C_m}{1 - \frac{P_u}{P_{e1}}} \geq 1.0 \qquad (6\text{-}2)$$

where

C_m = bending coefficient defined in AISC LRFD
P_{e1} = elastic buckling load for the braced frame defined in AISC LRFD

6.1.2. For members constrained to bend about a geometric axis with nominal flexural strength determined per Section 5.2.1, the radius of gyration r for P_{e1} shall be taken as the geometric axis value. The bending terms for the principal axes in Equations 6-1a and 6-1b shall be replaced by a single geometric axis term.

6.1.3. Alternatively, for equal-leg angles without lateral-torsional restraint along the length and with bending applied about one of the geometric axes, the provisions of Section 5.2.2 are permitted for the required and design bending strength. If Section 5.2.2 is used for M_n, the radius of gyration about the axis of bending r for P_{e1} shall be taken as the geometric axis value of r divided by 1.35 in the absence of a more detailed analysis. The bending terms for the principal axes in Equations 6-1a and 6-1b shall be replaced by a single geometric axis term.

6.2. Members in Flexure and Axial Tension

The interaction of flexure and axial tension shall be limited by Equations 6-1a and 6-1b where

P_u = required tensile strength
P_n = nominal tensile strength determined in accordance with Section 2
M_u = required flexural strength
M_n = nominal flexural strength for tension or compression in accordance with Section 5, as appropriate. Use section modulus for specific location in the cross section and consider the type of stress.
$\phi = \phi_t$ = resistance factor for tension = 0.90
ϕ_b = resistance factor for flexure = 0.90

For members subject to bending about a geometric axis, the required bending strength evaluation shall be in accordance with Sections 6.1.2 and 6.1.3. Second-order effects due to axial tension and bending interaction are permitted to be considered in the determination of M_u for use in Formulas 6-1a and 6-1b. In lieu of using Formulas 6-1a and 6-1b, a more detailed analysis of the interaction of flexure and tension is permitted.

COMMENTARY on the Load and Resistance Factor Design Specification for Single-Angle Members

November 10, 2000

INTRODUCTION

This Specification is intended to be complete for normal design usage in conjunction with the main 1999 AISC LRFD Specification and Commentary.

This Commentary furnishes background information and references for the benefit of the engineer seeking further understanding of the derivation and limits of the specification.

The Specification and Commentary are intended for use by design professionals with demonstrated engineering competence.

C2. TENSION

The criteria for the design of tension members in AISC LRFD Specification Section D1 have been adopted for angles with bolted connections. However, recognizing the effect of shear lag when the connection is welded, the criteria in Section B3 of the AISC LRFD Specification have been applied.

The advisory upper slenderness limits are not due to strength considerations but are based on professional judgment and practical considerations of economics, ease of handling, and transportability. The radius of gyration about the z axis will produce the maximum l/r and, except for very unusual support conditions, the maximum Kl/r. Since the advisory slenderness limit for compression members is less than for tension members, an accommodation has been made for members with $Kl/r > 200$ that are always in tension, except for unusual load conditions which produce a small compression force.

C3. SHEAR

Shear stress due to factored loads in a single-angle member are the result of the gradient in the bending moment along the length (flexural shear) and the torsional moment.

The maximum elastic stress due to flexural shear may be computed by

$$f_v = \frac{1.5V_b}{bt} \qquad \text{(C3-1)}$$

where

V_b = component of the shear force parallel to the angle leg with length b and thickness t, kips

The stress, which is constant through the thickness, should be determined for both legs to determine the maximum.

The 1.5 factor is the calculated elastic value for equal-leg angles loaded along one of the principal axes. For equal-leg angles loaded along one of the geometric axes (laterally braced or unbraced) the factor is 1.35. Constants between these limits may be calculated conservatively from V_bQ/It to determine the maximum stress at the neutral axis.

Alternatively, if only flexural shear is considered, a uniform flexural shear stress in the leg of V_b/bt may be used due to inelastic material behavior and stress redistribution.

If the angle is not laterally braced against twist, a torsional moment is produced equal to the applied transverse load times the perpendicular distance e to the shear center, which is at the heel of the angle cross section. Torsional moments are resisted by two types of shear behavior: pure torsion (St. Venant) and warping torsion (Seaburg and Carter, 1997). If the boundary conditions are such that the cross section is free to warp, the applied torsional moment M_T is resisted by pure shear stresses as shown in Figure C3.1a. Except near the ends of the legs, these stresses are constant along the length of the leg, and the maximum value can be approximated by

$$f_v = M_T t/J = \frac{3M_t}{At} \qquad \text{(C3-2)}$$

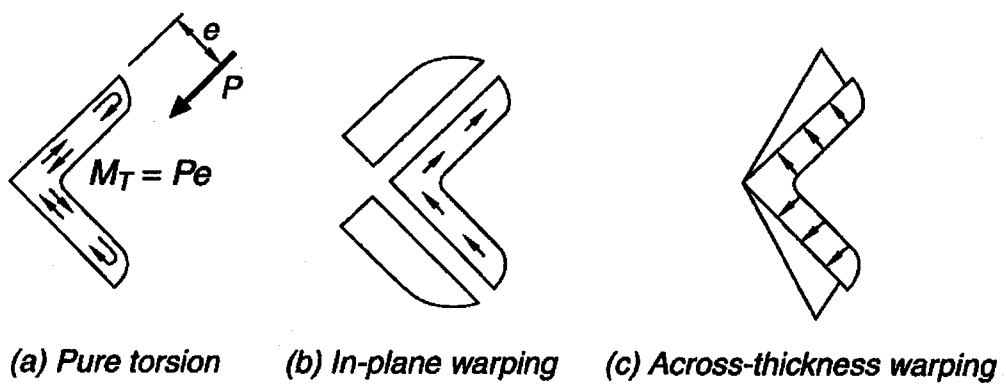

Fig. C.3.1. Shear stresses due to torsion.

where

J = torsional constant (approximated by $\Sigma bt^3/3$ when precomputed value is unavailable)
A = angle cross-sectional area

At a section where warping is restrained, the torsional moment is resisted by warping shear stresses of two types (Gjelsvik, 1981). One type is in-plane (contour) as shown in Figure C3.1b, which varies from zero at the toe to a maximum at the heel of the angle. The other type is across the thickness and is sometimes referred to as secondary warping shear. As indicated in Figure C3.1c, it varies from zero at the heel to a maximum at the toe.

In an angle with typical boundary conditions and an unrestrained load point, the torsional moment produces all three types of shear stresses (pure, in-plane warping, and secondary warping) in varying proportions along its length. The total applied moment is resisted by a combination of three types of internal moments that differ in relative proportions according to the distance from the boundary condition. Using typical angle dimensions, it can be shown that the two warping shears are approximately the same order of magnitude and are less than 20 percent of the pure shear stress for the same torsional moment. Therefore, it is conservative to compute the torsional shear stress using the pure shear equation and total applied torsional moment M_T as if no warping restraint were present. This stress is added directly to the flexural shear stress to produce a maximum surface shear stress near the mid-length of a leg. Since this sum is a local maximum that does not extend through the thickness, applying the limit of $\phi_v 0.6F_y$ adds another degree of conservatism relative to the design of other structural shapes.

In general, torsional moments from laterally unrestrained transverse loads also produce warping normal stresses that are superimposed on bending stresses. However, since the warping strength for a single angle is relatively small, this additional bending effect is negligible and often ignored in design practice.

C4. COMPRESSION

The provisions for the critical compression stress account for the three possible limit states that may occur in an angle column depending on its proportions: general column flexural buckling, local buckling of thin legs, and flexural-torsional buckling of the member. The Q-factor in the equation for critical stress accounts for the local buckling, and the expressions for Q are nondimensionalized from AISC LRFD Specification (AISC, 1999) Appendix B5. Flexural-torsional buckling is covered in Appendix E of the AISC LRFD Specification (AISC, 1999). This strength limit state is approximated by the Q-factor reduction for slender-angle legs. For non-slender sections where $Q = 1$, flexural-torsional buckling is relevant for relatively short columns, but it was shown by Galambos (1991) that the error of neglecting this effect is not significant. For this reason no explicit consideration of this effect is required in

these single-angle specifications. The provisions of Appendix E of AISC LRFD may be conservatively used to directly consider flexural-torsional buckling for single-angle members.

The effective length factors for angle columns may be determined by consulting the paper by Lutz (1992).

The resistance factor ϕ was increased from 0.85 in AISC LRFD for all cross sections to 0.90 for single angles only because it was shown that a ϕ of 0.90 provides an equivalent degree of reliability (Galambos, 1992).

C5. FLEXURE

Flexural strength limits are established for yielding, local buckling, and lateral-torsional buckling. In addition to addressing the general case of unequal-leg single angles, the equal-leg angle is treated as a special case. Furthermore, bending of equal-leg angles about a geometric axis, an axis parallel to one of the legs, is addressed separately as it is a very common situation.

The tips of an angle refer to the free edges of the two legs. In most cases of unrestrained bending, the flexural stresses at the two tips will have the same sign (tension or compression). For constrained bending about a geometric axis, the tip stresses will differ in sign. Criteria for both tension and compression at the tip should be checked as appropriate, but in most cases it will be evident which controls.

Appropriate serviceability limits for single-angle beams need also to be considered. In particular, for longer members subjected to unrestrained bending, deflections are likely to control rather than lateral-torsional or local buckling strength.

C5.1.1. These provisions follow the LRFD format for nominal flexural resistance. There is a region of full yielding, a linear transition to the yield moment, and a region of local buckling. The strength at full yielding is limited to a shape factor of 1.50 applied to the yield moment. This leads to a lower bound plastic moment for an angle that could be bent about any axis, inasmuch as these provisions are applicable to all flexural conditions. The 1.25 factor originally used was known to be a conservative value. Recent research work (Earls and Galambos, 1997) has indicated that the 1.50 factor represents a better lower bound value.

The *b/t* limits have been modified to be more representative of flexural limits rather than using those for single angles under uniform compression. Typically the flexural stresses will vary along the leg length permitting the use of the stress limits given. Even for the geometric axis flexure case which produces uniform compression along

one leg, use of these limits will provide a conservative value when compared to the results obtained by Earls and Galambos, 1997.

C5.1.2. Since the shape factor for angles is in excess of 1.50, the nominal design strength $M_n = 1.5M_y$ for compact members is justified provided that instability does not control.

C5.1.3. Lateral-torsional instability may limit the flexural strength of an unbraced single-angle beam. As illustrated in Figure C5.1, Equation 5-3a represents the elastic buckling portion with the nominal flexural strength, M_n, varying from 75 percent to 92 percent of the theoretical buckling moment, M_{ob}. Equation 5-3b represents the inelastic buckling transition expression between $0.75M_y$ and $1.5M_y$. Equation 5-3b has been modified to better reflect its use with the increased upper limit of $1.5\,M_y$. The maximum beam flexural strength $M_n = 1.5\,M_y$ will occur when the theoretical buckling moment M_{ob} reaches or exceeds $7.7M_y$ as illustrated in Figure C5.1. These equations are modifications of those developed from the results of Australian research on single angles in flexure and on an analytical model consisting of two rectangular elements of length equal to the actual angle leg width minus one-half the thickness (Leigh and Lay, 1984; Australian Institute of Steel Construction, 1975; Leigh and Lay, 1978; Madugula and Kennedy, 1985).

A more general C_b moment gradient formula consistent with the 1999 AISC LRFD Specification is used to correct lateral-torsional stability equations from the assumed most severe case of uniform moment throughout the unbraced length ($C_b = 1.0$). The equation for

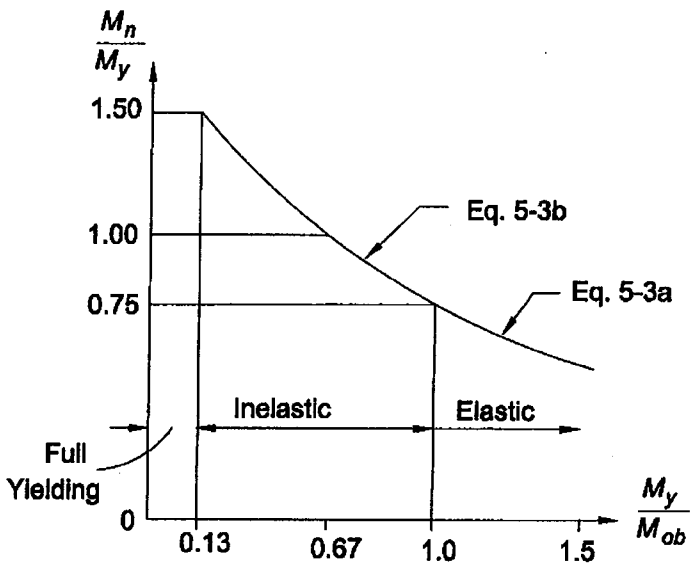

Fig. C5.1. Lateral-torsional buckling limits of a single-angle beam.

C_b used in the ASD version is applicable only to moment diagrams that are straight lines between brace points. In lieu of a more detailed analysis, the reduced maximum limit of 1.5 is imposed for single-angle beams to represent conservatively the lower envelope of this cross section's non-uniform bending response.

C5.2.1. An angle beam loaded parallel to one leg will deflect and bend about that leg only if the angle is restrained laterally along the length. In this case simple bending occurs without any torsional rotation or lateral deflection and the geometric axis section properties should be used in the evaluation of the flexural design strength and deflection. If only the point of maximum moment is laterally braced, lateral-torsional buckling of the unbraced length under simple bending must also be checked, as outlined in Section 5.2.1b.

C5.2.2. When bending is applied about one leg of a laterally unrestrained single angle, it will deflect laterally as well as in the bending direction. Its behavior can be evaluated by resolving the load and/or moments into principal axis components and determining the sum of these principal axis flexural effects. Section 5.2.2 is provided to simplify and expedite the design calculations for this common situation with equal-leg angles.

For such unrestrained bending of an equal-leg angle, the resulting maximum normal stress at the angle tip (in the direction of bending) will be approximately 25 percent greater than calculated using the geometric axis section modulus. The value of M_{ob} in Equation 5-4 and the evaluation of M_y using 0.80 of the geometric axis section modulus reflect bending about the inclined axis shown in Figure C5.2.

The deflection calculated using the geometric axis moment of inertia has to be increased 82 percent to approximate the total deflection. Deflection has two components, a vertical component (in the direction of applied load) 1.56 times the calculated value and a horizontal component of 0.94 of the calculated value. The resultant total deflection is in the general direction of the weak principal axis bending of the angle (see Figure C5.2). These unrestrained bending deflections should be considered in evaluating serviceability and will often control the design over lateral-torsional buckling.

The horizontal component of deflection being approximately 60 percent of the vertical deflection means that the lateral restraining force required to achieve purely vertical deflection (Section 5.2.1) must be 60 percent of the applied load value (or produce a moment 60 percent of the applied value) which is very significant.

Lateral-torsional buckling is limited by M_{ob} (Leigh and Lay, 1984 and 1978) in Equation 5-4, which is based on

$$M_{cr} = \frac{2.33Eb^4t}{(1 + 3\cos^2\theta)(Kl)^2} \times \left[\sqrt{\sin^2\theta + \frac{0.156(1 + 3\cos^2\theta)(Kl)^2t^2}{b^4}} + \sin\theta\right] \quad \text{(C5-1)}$$

(the general expression for the critical moment of an equal-leg angle) with $\theta = -45°$ for the condition where the angle tip stress is compression (see Figure C5.3). Lateral-torsional buckling can also limit the moment capacity of the cross section when the maximum angle tip stress is tension from geometric axis flexure, especially with use of the new flexural capacity limits in Section 5.1. Using $\theta = 45°$ in Equation C5-1, the resulting expression is Equation 5-4 with a $+1$ instead of -1 as the last term.

Stress at the tip of the angle leg parallel to the applied bending axis is of the same sign as the maximum stress at the tip of the other leg when the single angle is unrestrained. For an equal-leg angle this stress is about one-third of the maximum stress. It is only necessary to check the nominal bending strength based on the tip of the angle leg with the maximum stress when evaluating such an angle. Since this maximum moment per Section 5.2.2 represents combined principal axis moments and Equation 5-4 represents the design limit for these combined flexural moments, only a single flexural term needs to be considered when evaluating combined flexural and axial effects.

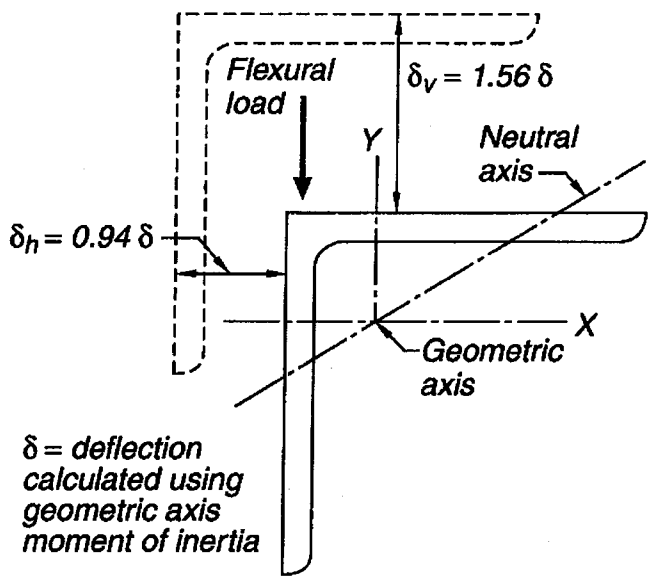

Fig. C5.2. Geometric axis bending of laterally unrestrained equal-leg angles.

C5.2.3. For unequal-leg angles without lateral-torsional restraint the applied load or moment must be resolved into components along the two principal axes in all cases and designed for biaxial bending using the interaction equation.

C5.3.1. Under major axis bending of equal-leg angles Equation 5-5 in combination with 5-3a or 5-3b controls the nominal design moment against overall lateral-torsional buckling of the angle. This is based on M_{cr}, given earlier with $\theta = 0$.

Lateral-torsional buckling for this case will reduce the stress below $1.5M_y$ only for $l/t \geq 7350C_b/F_y$ ($M_{ob} = 7.7M_y$). If the lt/b^2 parameter is small (less than approximately $0.87C_b$ for this case), local buckling will control the nominal design moment and M_n based on lateral-torsional buckling need not be evaluated. Local buckling must be checked using Section 5.1.1.

C5.3.2. Lateral-torsional buckling about the major principal W axis of an unequal-leg angle is controlled by M_{ob} in Equation 5-6. Section property β_w reflects the location of the shear center relative to the principal axis of the section and the bending direction under uniform bending. Positive β_w and maximum M_{ob} occurs when the shear center is in flexural compression while negative β_w and minimum M_{ob} occurs when the shear center is in flexural tension (see Figure C5.4). This β_w effect is consistent with behavior of singly symmetric I-shaped beams which are more stable when the compression flange is larger than the tension flange. For principal W-axis bending of equal-leg angles, β_w is equal to zero due to symmetry and Equation 5-6 reduces to Equation 5-5 for this special case.

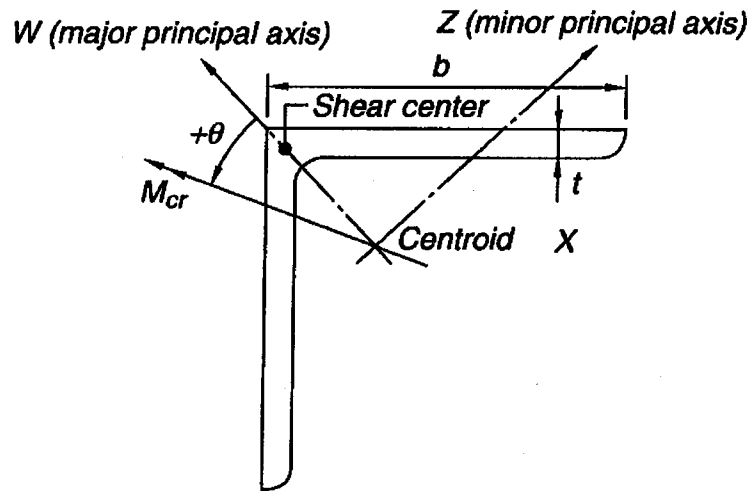

Fig. C5.3. Equal-leg angle with general moment loading.

TABLE C5.1
β_w Values for Angles

Angle Size (in.)	β_w (in.)*
9 × 4	6.54
8 × 6 8 × 4	3.31 5.48
7 × 4	4.37
6 × 4 6 × 3.5	3.14 3.69
5 × 3.5 5 × 3	2.40 2.99
4 × 3.5 4 × 3	0.87 1.65
3.5 × 3 3.5 × 2.5	0.87 1.62
3 x 2.5 3 x 2	0.86 1.56
2.5 x 2	0.85
Equal legs	0.00

* Has positive or negative value depending on direction of bending (see Figure C5.4).

For reverse curvature bending, part of the unbraced length has positive β_w, while the remainder has negative β_w and conservatively, the negative value is assigned for that entire unbraced segment.

β_w is essentially independent of angle thickness (less than one percent variation from mean value) and is primarily a function of the leg widths. The average values shown in Table C5.1 may be used for design.

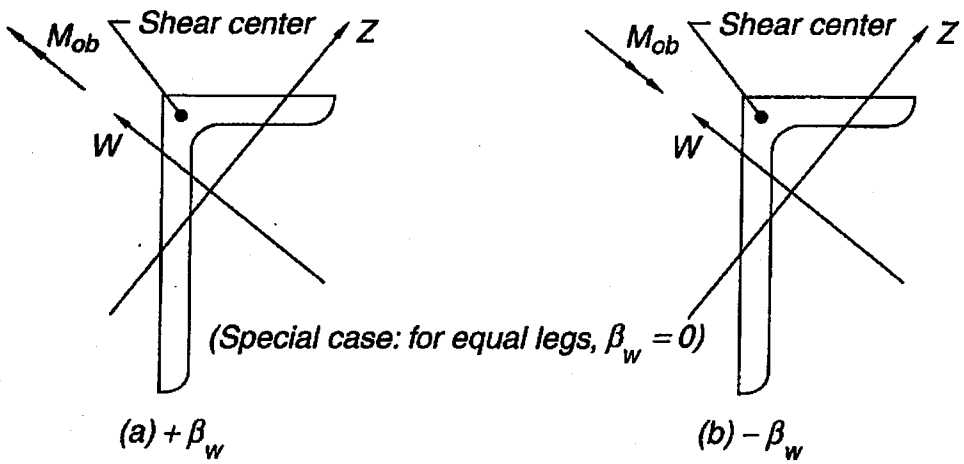

Fig. C5.4. Unequal-leg angle in bending.

C6. COMBINED STRESSES

The stability and strength interaction equations of AISC LRFD Specification Chapter H have been adopted with modifications to account for various conditions of bending that may be encountered. Bending will usually accompany axial loading in a single-angle member since the axial load and connection along the legs are eccentric to the centroid of the cross section. Unless the situation conforms to Section 5.2.1 or 5.2.2 in that Section 6.1.2 or 6.1.3 may be used, the applied moment should be resolved about the principal axes for the interaction check.

For the non-symmetric and singly symmetric single angles, the interaction expression related to stresses at a particular location on the cross section is the most accurate due to lack of double symmetry. At a particular location, it is possible to have stresses of different sign from the various components such that a combination of tensile and compressive stress will represent a critical condition. The absolute value of the combined terms must be checked at the angle-leg tips and heel and compared with 1.0.

When using the combined force expressions for single angles, M_{uw} and M_{uz} are positive as customary. The evaluation of M_n in Section 5.1 is dependent on the location on the cross section being examined by using the appropriate value of section modulus, S. Since the sign of the stress is important in using Equations 6-1a and 6-1b, M_n is considered either positive or negative by assigning a sign to S to reflect the stress condition as adding to, or subtracting from, the axial load effect. A designer may choose to use any consistent sign convention.

It is conservative to ignore this refinement and simply use positive critical M_n values in the bending terms and add the absolute values of all terms (Elgaaly, Davids, and Dagher, 1992 and Adluri and Madugula, 1992).

Alternative special interaction equations for single angles have been published (Adluri and Madugula, 1992).

C6.1.3. When the total maximum flexural stress is evaluated for a laterally unrestrained length of angle per Section 5.2, the bending axis is the inclined axis shown in Figure C5.2. The radius of gyration modification for the moment amplification about this axis is equal to $\sqrt{1.82} = 1.35$ to account for the increased unrestrained bending deflection relative to that about the geometric axis for the laterally unrestrained length. The 1.35 factor is retained for angles braced only at the point of maximum moment to maintain a conservative calculation for this case. If the brace exhibits any flexibility permitting lateral movement of the angle, use of $r = r_x$ would not be conservative.

List of References

Alduri, S. M. and Madugula, M. K. S. (1992), "Eccentrically Loaded Steel Single-Angle Struts," *Engineering Journal,* AISC, 2nd Quarter.

American Institute of Steel Construction, Inc. (1999), *Load and Resistance Factor Design Specification for Structural Steel Buildings,* Chicago, IL.

American Institute of Steel Construction, Inc. (1989), *Specification for Allowable Stress Design of Single-Angle Members,* Chicago, IL.

Australian Institute of Steel Construction (1975), *Australian Standard AS1250,* 1975.

Earls, C. J., and Galambos, T.V. (1997), "Design Recommendations for Equal Leg Single Angle Flexural Members," *Journal of Constructional Steel Research,* Vol. 43, Nos. 1-3, pp. 65–85.

Elgaaly, M., Davids, W. and Dagher, H. (1992), "Non-Slender Single-Angle Struts," *Engineering Journal,* AISC, 2nd Quarter.

Galambos, T. V. (1991), "Stability of Axially Loaded Compressed Angles," Structural Stability Research Council, *Annual Technical Session Proceedings,* Apr. 15–17, Chicago, IL.

Gjelsvik, A. (1981), *The Theory of Thin-walled Bars,* John Wiley and Sons, New York.

Leigh, J. M. and Lay, M. G. (1978), "Laterally Unsupported Angles with Equal and Unequal Legs," Report MRL 22/2 July 1978, Melbourne Research Laboratories, Clayton.

Leigh, J. M. and Lay, M. G. (1984), "The Design of Laterally Unsupported Angles," in *Steel Design Current Practice,* Section 2, Bending Members, AISC, January.

Lutz, L. A. (1992), "Critical Slenderness of Compression Members with Effective Lengths About Nonprincipal Axes," Structural Stability Research Council, Annual Technical Session Proceedings, Apr. 6–7, Pittsburgh, PA.

Madugula, M. K. S. and Kennedy, J. B. (1985), *Single and Compound Angle Members,* Elsevier Applied Science, New York.

Seaburg, P. A., and Carter, C. J. (1997), *Torsional Analysis of Structural Steel Members,* Steel Design Guide Series No. 9, AISC, Chicago, IL.

NOTES

American Institute of Steel Construction, Inc.
One East Wacker Drive, Suite 3100
Chicago, IL 60601-2001

Pub No. S351L (3M201)